Doctoral School on Industrial Engineering
Università Politecnica delle Marche

# Effect of some inhibitors on the passivation of galvanized rebars embedded in concrete

*Curriculum: Materials Engineering*

Ph.D. Dissertation of:

Daria Timofeeva

Supervisors:

Dr. Tiziano Bellezze

Prof. Gabriella Roventi

Coordinator:

Prof. Ferruccio Mandorli

XV Cycles – New series

## Acknowledgements

I wish to express my sincere appreciation to those who have contributed to this thesis and supported me in one way or the other during this amazing journey.

First of all, I am extremely grateful to my supervisors, Dr. Tiziano Bellezze and Prof. Gabriella Roventi, for always giving necessary suggestions to perform this study. In spite of the encountered difficulties, they guided me to the goal and now it is finally achieved.

My sincere gratitude is reserved for Professor Romeo Fratesi for his advice and providing numerous sources of information on corrosion and protection of materials. It has always been friendly upbeat working atmosphere in the team due to him. His cheerful disposition is legendary among students and colleagues, and no corrosion conference is complete without someone remember an interesting phrase once said by him.

I would also like to take this opportunity to thank Dr. Giampaolo Giuliani for invaluable technical assistance. I owe him every single piece of steel galvanized and every single hole drilled in the sample. He is the most indispensable man in the laboratory.

Very special thanks to Dr. Sergey Saltykov, the Head of the Department of Chemistry at the Lipetsk State Technical University, for his commitment and devotion to science that inspire students to follow his footsteps.

Heartfelt thanks to all my friends whom I was lucky enough to have met in Italy, in particular to Evgenia, Emanuele, Inna, Katarina and Anna. They have always come to my rescue in any time I needed, helping me by word and deed. I am very grateful for all the care they have taken of me.

Finally, I would like to acknowledge my parents for all the attention and love, they gave me and for the trust, they always had in me. I would not be here if it not for them. They are the most important people in my world and I dedicate this thesis to them.

## Abstract

The use of hot-dip galvanized steel reinforcements is one of the most common methods used to prevent deterioration of reinforced concrete structures. Zinc active corrosion, which occurs just after the embedding of galvanized steel in concrete, is accompanied by gaseous hydrogen evolution, which causes the loss of adhesion between the zinc coating and the cement paste still not hardened.

Chromium VI compounds are strong oxidants naturally present in the cements and reduce the passivation time and the amount of hydrogen developed. The EU Directive 2003/53/EC obliges to keep the content of soluble chromium VI in cement below 2 ppm on the total dry weight of the cement due to its toxicity and carcinogenic properties.

The objectives of this research project were to find a replacement for chromium VI compounds through study of galvanized steel passivation mechanism in concrete in presence of chromates and comparison of several inhibitors by their effectiveness as on zinc corrosion. The oxygen effect on the process of zinc passivation was also studied. The investigation was performed both in concrete and in saturated solution of calcium hydroxide, by means of corrosion potential and impedance measurements. To study the changes in the passivating layer, scanning electron microscopy, energy-dispersive X-ray spectroscopy and X-ray diffraction analysis were utilized.

The results obtained indicate that the passivation of galvanized steel in concrete containing chromates occurs in several steps with different mechanisms and that dissolved oxygen plays an important role on the beginning of the passivation process. Among inhibitors studied in present work, nitrite seems to be the most promising, both in concrete and in $Ca(OH)_2$ saturated solution. The future development of this research could be a depth study of the nitrite impact and a further search for alternative environmentally friendly corrosion inhibitors of galvanized steel.

## Riassunto

L'uso di barre d'acciaio zincate a caldo è uno dei metodi più comuni per prevenire il deterioramento delle strutture in calcestruzzo armato. La corrosione attiva dello zinco, che avviene subito dopo l'immersione dell'acciaio galvanizzato nel calcestruzzo, è accompagnata dallo sviluppo di idrogeno, che causa la perdita di adesione tra il rivestimento di zinco e la pasta di cemento non ancora indurita.

I composti di cromo VI sono forti ossidanti naturalmente presenti nei cementi che riducono il tempo della passivazione e la quantità d'idrogeno sviluppato. La Direttiva 2003/53/ CE obbliga a mantenere il contenuto di cromo VI idrosolubile nel cemento al di sotto di 2 ppm sul peso totale a secco del cemento.

Gli obiettivi di questo lavoro sono stati: trovare un sostituto per i composti di cromo VI attraverso lo studio del meccanismo di passivazione dell'acciaio zincato nel calcestruzzo in presenza di cromo VI e confrontare diversi inibitori per la loro efficacia sulla corrosione dello zinco. E' stato inoltre studiato l'effetto dell'ossigeno sulla passivazione dello zinco. L'indagine è stata effettuata nel calcestruzzo e in soluzione satura di idrossido di calcio, mediante misure del potenziale di corrosione e prove di impedenza. Per studiare gli strati di passivazione sono state utilizzate la microscopia SEM-EDX e la diffrattometria a raggi X.

I risultati ottenuti indicano che la passivazione dell'acciaio zincato nel calcestruzzo in presenza di cromati avviene in più fasi con meccanismi diversi e che la presenza di ossigeno disciolto è importante per accelerare la passivazione. Tra gli inibitori studiati, il nitrito sembra quello più promettente, sia nel calcestruzzo che in soluzione satura di idrossido di calcio. Gli sviluppi futuri di questa ricerca potrebbero essere l'approfondimento dello studio dell'effetto dei nitriti e l'ulteriore ricerca di inibitori di corrosione a basso impatto ambientale.

## List of Figures

## List of Tables

## Contents

## Introduction

Reinforced concrete is well known as strong and durable construction material. However, in the presence of certain deleterious factors and agents, such as high humidity, contents of salts and diffusion of oxygen and carbon dioxide the steel can corrode, that may eventually result in splitting of the concrete by the force of the corrosion products. Corrosion-induced damage to reinforced concrete often necessitates early repair and occasionally complete replacement of the structure or element well before its design life is reached. Since the cost of repairing reinforced concrete structures is generally high, concrete technology is continuously developing methods to prevent the onset of deterioration in reinforced concrete structures.

The application of hot-dip galvanized coating to steel reinforcement is one of the most common and widespread methods for providing corrosion protection in many types of concrete construction. The corrosion protection afforded by galvanizing is due to several beneficial effects. Zinc-coated steel has the substantially higher chloride threshold compared with uncoated steel [1, 2]. It is resistant to the effects of carbonation of the concrete mass [3]. Furthermore, the zinc coating not only delays the initiation of the corrosion process and acts as a barrier against corrosive agents, but it also provides cathodic protection of exposed steel when the coating is already damaged, working as a sacrificial anode [1,4].

Just embedded in concrete, the galvanized steel actively corrodes with the formation of gaseous hydrogen, which causes the loss of adhesion between the zinc coating and the cement paste still not hardened [4-6]. After this stage, the pure zinc $\eta$-phase, present on the rebar surface, passivates and forms a protective layer of calcium hydroxyzincate [4]. Some components of the cement matrix reduce the time of zinc active corrosion and, thus, the amount of hydrogen developed during the initial set of concrete [11, 12]. Depending on the origin of the raw materials used and the clinker production conditions, cement may contain up to 30 ppm hexavalent chromium [13]. The soluble chromates, naturally present in the cements in small amounts, determine an inhibition of the zinc active corrosion for a certain period [14, 15].

However, chromium VI compounds are reported to be genotoxic carcinogens [16]. When dissolved, chromium VI can penetrate unprotected skin and cause an allergic reaction known as chromate dermatitis, depending on the intensity and duration of exposure. Therefore, during recent years several countries have introduced measures to limit the amount of chromium VI in cement products. In 2003 the European Commission introduced new legislation to restrict the marketing and use throughout the European Union of cement products containing soluble chromium VI at a concentration of more than 0.0002 wt% (2 ppm) on the total dry weight of the cement. According to EU Directive 2003/53/EC, reducing agents, such as ferrous sulphate or antimony salts, should be added into the cements, originally containing chromium VI, to keep its content below the allowed limit of 2 ppm during the mixing.

In connection with the recent European Union policy for toxic materials and due to the interest of Construction and Building Materials industry, in the last decade numerous studies were devoted to the search for environmentally friendly chromium-free methods of corrosion protection applied on hot-dip galvanized steel reinforcement [16, 17]. Some of these studies are dedicated to the application of conversion chromium-free pre-treatments on galvanized rebars with the most commonly used phosphates [7-10]. Another part of papers provides the data on the efficiency of different cement inhibiting admixtures on the corrosion protection of steel in concretes and mortars [18-28]. Some researchers investigated the

effect of various inhibitors on galvanized steel, zinc and zinc alloys in acid, neutral and slightly alkaline environments other than highly alkaline concrete pore solution [29-32]. Yet there are small number of works considering synergic effect of simultaneous application of hot-dip galvanized coating on rebars and of inhibitor admixtures in the cement matrix [12, 17, 35-38]. Most of these works are dedicated to the use of nitrites [12, 37, 38]. The results presented by different researchers are quite contradictory and depend largely on the choice of materials and the experimental conditions.

According to the existing state-of-the-art in the field of corrosion in concrete, following goals and objectives of the present research project were established:

- Study the passivation mechanism of galvanized rebars embedded in concrete in presence of hexavalent chromium;
- Study the oxygen effect on the process of zinc and galvanized steel passivation;
- Study the relation between the passivation process and oxygen/oxidant amount in the medium;
- Compare the power and effectiveness of different inhibitors as "passivating promoters" of zinc;
- Find an appropriate replacement for chromium inhibitor of galvanized steel corrosion in concrete.

In the present work, the efficiency of several generic oxidants and non-oxidizing inhibitors, namely chromate, nitrite, oxygen peroxide, molybdate and diethanolamine, was studied. All of them were examined both in concrete and in calcium hydroxide saturated solution. Concrete samples were manufactured with ordinary Portland cements with different initial content of soluble chromium VI in the cement, in order to evaluate oxidants' influence on the galvanized steel passivation in concrete mixes containing chromates or chromium-free. $Ca(OH)_2$ saturated solution was used because it simulates the alkaline pore solution of concrete. During experiments both galvanized steel and pure zinc samples discs were used as pure zinc replicates the $\eta$-phase present on the upper layer of galvanized steel.

The study on the oxygen effect on the passivation process was carried out with a series of additional experiments in aerated and deaerated $Ca(OH)_2$ saturated solutions with pure zinc and galvanized steel samples in the presence of chromate as oxidant.

All tests included potential monitoring performed by means of the Agilent acquisition system mod. 34970A (multiplexer mod. 34901). The experiments in $Ca(OH)_2$ saturated solutions also comprised electrochemical impedance measurements, by means of Gamry Instruments Reference 600 potentiostat. To study the changes in the passivating layer scanning electron microscopy (SEM), energy-dispersive X-ray spectroscopy (EDX) and X-ray diffraction analysis (XRD) were utilized by means of a Zeiss Supra 40 microscope, Bruker's Quantax series 5000 L device and Philips PW 1730 diffractometer with Cu K$\alpha$ radiation ($\lambda$=0.154 nm), respectively.

The first part of the thesis contains theoretical considerations about the research and consists of three chapters. The first chapter describes the current situation on the market of building materials, concrete mix-designs and their constituents, as well as the description of modern cements, their origin and production, chemical and physical properties. The focus of this chapter is on the chromium content and on the methods of its reduction in cementitious materials. The second chapter contains information on the principles and mechanisms of iron, zinc and galvanized steel corrosion in alkaline media. The third chapter illustrates methods of corrosion protection for galvanized steel and zinc in alkaline environment, gives

the information on typology of inhibitors and mechanisms of their impact on the metals and provides detailed literature review in the field of corrosion protection in concrete.

The second part of the thesis contains complete description of research experimental design. It includes information on materials used for sample preparations, specifications of manufactured specimens, inhibitor concentration calculations, experimental conditions, electrochemical techniques and methods of visual and instrumental observations. Results obtained in experiments are given in the Chapter 7 of the thesis, which includes electrochemical diagrams, digital photo images, SEM observation, X-ray diffractograms and data tables with detailed description of received information. The conclusive chapter of the thesis provides a qualitative and quantitative critical evaluation of the results achieved and those that eventually could not be reached and indicates possible future developments and promising research directions.

# PART I

# Theoretic

# 1 Concrete as a building material

Concrete is the world's most versatile and most widely produced material. As of 2015, more than 10 billion cubic meters of concrete are manufactured each year, more than one cubic meter for every person on the planet [39]. The reasons for the popularity of concrete are multiple. First, the components are available in almost every comer of the world, enabling concrete to be produced worldwide for the local market and, thus, avoiding the transport costs necessary for most other materials. Second, the cost of production is low, compared with other engineered construction materials. Moreover, in recent years, additional "raw" materials in the form of waste products have been added to concrete, that further has reduced production costs. A third advantage of concrete is that it can be cast, at ambient temperature, to produce complex shapes with adequate strength. Its versatility is such that essentially the same material is used in engineering constructions such as a highway bridge or an offshore oil platform. Finally, a major factor in its universal usage is that concrete, unlike most other structural materials, exhibits excellent resistance to water, making it an ideal material for transportation and control of water, e.g., in pipelines and dams.

According to a standard definition concrete is a composite material that consists essentially of a binding medium within which are embedded particles or fragments of aggregate; in hydraulic-cement concrete, the binder is formed from a mixture of hydraulic cement and water [40]. A wide variety of different types of concrete exists, created by changing the proportions of the main ingredients. In this manner or by substitution for the cementitious and aggregate phases, the finished product can be fitted to its application with various density, strength, thermal resistance and chemical properties.

## 1.1 Cement paste

Among all the components of concrete, the cement paste phase is the most important as it determines the durability and the long-term performance of concrete. The properties of cement paste depend on the choice of cement type and on the water/cement ratio.

The historical development of building materials led to appearance of variant of hydraulic cements. Many of these cements are used only for certain, limited purposes, others such as Portland cement or Portland cement blends have a wider application. The European standard EN 197-1 defines and gives the specifications of common cements, which are intended for use in any plain and reinforced concrete [41]. The standard divides common cements on five main types according to their composition:

- CEM I Portland cement, with at least 95 % of clinker (by total binder mass);
- CEM II Portland-composite cement, with addition of up to 35 % single constituent;
- CEM III Blastfurnace cement, with addition of 36-95 % blast furnace slag;
- CEM IV Pozzolanic cement, with addition of 11-55 % pozzolanic materials;
- CEM V Composite cement, with simultaneous addition of slag and pozzolana.

The second classification of common cements given in the standard is based on the strength performance at 28 days. The classification includes three classes of standard strength: class 32,5, class 42,5 and class 52,5 (the number corresponds to a minimum compressive strength at 28 days).

Table 1-1. Strength classes of common cements according to EN 197-1 [41]

| Strength class | Compressive strength MPa | | | |
|---|---|---|---|---|
| | Early strength | | Standard strength | |
| | 2 days | 7 days | 28 days | |
| 32,5 N | - | ≥ 16 | ≥ 32,5 | ≤ 52,5 |
| 32,5 R | ≥ 10 | - | ≥ 32,5 | ≤ 52,5 |
| 42,5 N | ≥ 10 | - | ≥ 42,5 | ≤ 62,5 |
| 42,5 R | ≥ 20 | - | ≥ 42,5 | ≤ 62,5 |
| 52,5 N | ≥ 20 | - | ≥ 52,5 | - |
| 52,5 R | ≥ 30 | - | ≥ 52,5 | - |

Each class of standard strength includes two classes of early strength: a class with ordinary early strength, indicated by N, and a class with high early strength, indicated by R (Tab. 1-1).

Among cements not listed in EN 197-1, should be mentioned high alumina, geopolymer cements and gypsum plasters [42-45].

High alumina cement (HAC) is obtained by heating until molten a suitable mixture of limestone and bauxite (mostly consisting of alumina) at about 1600 ºC. Its primary component is $CaO \cdot Al_2O_3$. It is characterized by a very rapid rate of development of strength and approaches closely to its final strength in 24 hours after gauging. HAC concrete has a high resistance against acids and high temperatures. The problem with this material can occur during the hydration, which in some cases accompanied by development of high porosity and thus a decrease in strength and resistance against attacks of aggressive agents.

Gypsum plasters are produced by heating finely ground gypsum $CaSO_4 \cdot 2H_2O$ at different temperatures to obtain dehydrated or semi-hydrated forms of gypsum. On heating to 150 °C, hemihydrate $CaSO_4 \cdot ½H_2O$ is produced, known as ordinary plaster of Paris; by increasing heating temperature up to 180 °C, the nearly water-free form called γ-anhydrite can be obtained. The hydration of plasters relies on the reaction between water and partially hydrated $CaSO_4$. The setting of hemihydrate plasters is characterized by overall expansion of the mass, caused by the manner of crystal growth. Thus, gypsum plasters require specific additions, when the low setting expansion of material is desirable.

Over last decade numerous studies have been devoted to geopolymer cements [45-51]. Geopolymer cements consist of inorganic alumina-silicate polymers, synthesized from materials of geological origin or by-product materials such as fly ash which is rich in silicon and aluminum, and are considered environmentally friendly as their production consumes less energy and do not increase $CO_2$ emission to the atmosphere comparatively to Portland cements. Despite many advantages, geopolymer building materials have certain drawbacks such as high scale porosity that decreased corrosion protection properties due to the high risk of aggressive species penetration in the bulk of the material, or mechanical properties that can be comparable to those of Portland concretes or lower depending on the choice of geopolymer. Moreover, the geopolymerization process involves alkaline activation of aluminosilicate and thus requires the use of high alkaline corrosive user-hostile products [52].

### *1.1.1 Portland cement*

The Portland cement production consists in the mixing of limestone and clay, or other raw materials of similar bulk composition and sufficient reactivity, the burning of the mix at a fusion temperature of about 1450 ºC to form a clinker, and the grinding of the clinker with a few per cent of gypsum or other forms of calcium sulfate to fine powder. The calcium sulfate quantity determines the rate of set and the rate of strength development [53].

The Portland cement clinker normally contains about 67 % CaO, 22 % $SiO_2$, 5 % $Al_2O_3$, 3 % FeO and 3 % other components and consists of four major phases: tricalcium silicate, dicalcium silicate, tricalcium aluminate and tetracalcium aluminoferrite [53]. Table 1-2 shows the typical ranges of percentages by mass of these phases in Portland cement. Other components, such as alkali sulfates and oxides, are present in minor amounts.

Table 1-2. Content of Portland cement main phases [42]

| Phase* | Compound name | Actual formula | CCN** | Content % mass. |
|---|---|---|---|---|
| Alite | Tricalcium silicate | $3CaO{\cdot}SiO_2$ | $C_3S$ | 45 – 60 |
| Belite | Dicalcium silicate | $2CaO{\cdot}\ SiO_2$ | $C_2S$ | 5 – 30 |
| Celite | Tricalcium aluminate | $3CaO{\cdot}Al_2O_3$ | $C_3A$ | 6 – 15 |
| Felite | Tetracalcium aluminoferrite | $4CaO{\cdot}Al_2O_3{\cdot}Fe_2O_3$ | $C_4AF$ | 6 – 8 |

* According to Törnebohm's classification

** Cement chemist notation

The hydration of cement can be thought of as a two-step process. In the first step, called dissolution, the cement dissolves, releasing ions into the mix water. The mix water is thus no longer pure $H_2O$, but an aqueous solution containing a variety of ionic species, called the pore solution. The gypsum and the cement minerals $C_3S$ and $C_3A$ are all highly soluble, meaning that they dissolve quickly. Therefore, the concentrations of ionic species in the pore solution increase rapidly as soon as the cement and water are combined. Eventually the concentrations increase to the point that the pore solution is supersaturated, meaning that it is energetically favourable for some of the ions to combine into new solid phases rather than remain dissolved. This second step of the hydration process is called precipitation. A key point, of course, is that these new precipitated solid phases, called hydration products, are different from the starting cement minerals. Precipitation relieves the supersaturation of the pore solution and allows dissolution of the cement minerals to continue. Thus, cement hydration is a continuous process by which the cement minerals are replaced by new hydration products, with the pore solution acting as a necessary transition zone between the two solid states [54].

As noted above, some of the cement minerals and constituents are very soluble, and thus when cement and water are first combined there is a short period of fast reaction and heat output as the cement dissolves, lasting for less than one minute (Stage 1). Stage 1 is brief because of the rapid formation of an amorphous layer of hydration product around the cement particles, which separates them from the pore solution and prevents further rapid dissolution. This is followed by the induction period, during which almost no reaction occurs (Stage 2). The precise nature of the induction period, and in particular the reason for its end,

is not fully known, or perhaps it should be stated that it is not fully agreed upon, as there are strongly held but differing opinions among cement chemists.

During Stage 3, the rapid reaction period, the rate of reaction increases rapidly, reaching a maximum at a time that is usually less than 24 hours after initial mixing, and then decreases rapidly again to less than half of its maximum value. This behaviour is due almost entirely to the hydration of the $C_3S$, and the rate of hydration is controlled by the rate at which the hydration products nucleate and grow. Both the maximum reaction rate and the time at which it occurs depend strongly on the temperature and on the average particle size of the cement. This reaction period is sometimes divided into two stages (before and after the maximum rate) but as the rate-controlling, mechanism is the same throughout (nucleation and growth); it is preferable to treat this as single stage.

At the end of Stage 3 about 30% of the initial cement has hydrated, and the paste has undergone both initial and final set. Stage 3 is characterized by a continuous and relatively rapid deposition of hydration products (primarily C-S-H gel and CH) into the capillary porosity, which is the space originally occupied by the mix water. This causes a large decrease in the total pore volume and a concurrent increase in strength. The microstructure of the paste at this point consists of unreacted cores of the cement particles surrounded by a continuous layer of hydration product, which has a very fine internal porosity filled with pore solution, and larger pores called capillary pores [62].

In order for further hydration to take place, the dissolved ions from the cement must diffuse outward and precipitate into the capillary pores, or water must diffuse inward to reach the unreacted cement cores. These diffusion processes become slower and slower as the layer of hydration product around the cement particles becomes thicker and thicker. This final period (Stage 4) is called the diffusion-limited reaction period.

### *1.1.2 Water/cement ratio*

The water to cement ratio, or w/c ratio, largely determines the strength and durability of the concrete when it is cured properly. The w/c ratio refers to the ratio of the weights of water and cement used in the concrete mix. A w/c ratio of 0.4 means that for every 100 kg of cement used in the concrete, 40 L of water is added [63].

For ordinary concrete, a w/c ratio of 0.6 to 0.7 is considered normal. A lower w/c ratio of 0.4 is generally specified if a higher quality concrete is desired. The practical range of the w/c ratio is from about 0.3 to over 0.8. A ratio of 0.3 is very stiff (unless superplasticizers are used), and a ratio of 0.8 makes a wet and fairly weak concrete. For reference, a 0.4 w/c ratio is generally expected to make a concrete with a compressive strength of about 385 bar when it is properly cured. On the other hand, a ratio of 0.8 will make a weak concrete of only about 140 bar.

The simplest way to think about the w/c ratio is to think that the greater the amount of water in a concrete mix, the more dilute the cement paste will be. This not only affects the compressive strength, it also affects the tensile and flexural strengths, the porosity, the shrinkage and the colour.

The more the w/c ratio is increased (that is, the more water that is added for a fixed amount of cement), the more the strength of the resulting concrete is reduced. This is mostly because adding more water creates a diluted paste that is weaker and more susceptible to cracking and shrinkage. Shrinkage leads to micro-cracks, which are zones of weakness. Once the fresh concrete is placed, excess water is squeezed out of the paste by the weight of the

aggregate and the cement paste itself. When there is a large excess of water, that water bleeds out onto the surface. The micro channels and passages that were created inside the concrete to allow that water to flow become weak zones and micro-cracks.

Using a low w/c ratio is the usual way to achieve a high strength and high quality concrete, but it does not guarantee that the resulting concrete is always appropriate for countertops. Unless the aggregate gradation and proportion are balanced with the correct amount of cement paste, excessive shrinkage, cracking and curling can result.

### *1.1.3 Hexavalent chromium content*

The content of trace elements in cement is of great importance as well, in accordance with the relevant European policy on environmental protection and human health and safety. Ordinary Portland cements contain trace amounts of several heavy metals such as lead, zinc, arsenic and chromium [53]. The final composition of a certain Portland cement equally depends on the origin of raw materials, their physical and chemical properties, and the clinkering process conditions, i.e. temperature and period of burning, since the burning consists of series of reactions between finely divided solids.

The chromium content of cement usually applies to compounds containing chromium. An important factor is the oxidation state of chromium in these compounds. The most often discussed forms in the building materials industry are Cr III and Cr VI. Cr III because it is the major form of chromium in cement, and Cr VI because it has taken the most attention regarding health issues. Chromium has also been detected in the form of Cr IV and Cr V although during cement hydration, these forms disproportionate to Cr III and Cr VI [13].

Trivalent chromium compounds comprise chromic oxide, chromic sulfate, chromic chloride, and chromic potassium sulfate and can be characterized as stable, stable, having low solubility and low reactivity. Their influence on the environment and living creatures is low.

Hexavalent chromium compounds comprise chromium trioxide, chromic acid, ammonium dichromate, barium chromate, calcium chromate, lead chromate, potassium dichromate, sodium chromate, sodium dichromate, strontium chromate, and zinc chromate. They can be characterized as unstable and strong oxidants. It's solubility in water is connected with stated health risks. When dissolved, Cr VI can penetrate unprotected skin and is transformed into Cr III that reacts with epidermal proteins forming the allergen that causes sensitivity to certain people [56].

The amount of hexavalent chromium in cement can derive from: oxidation of total chromium from the raw materials; fuel piercing the system during the burning of clinker; magnesia-chrome kiln refractory brick; wear metal from crushers and raw mill grinding process; and additions of gypsum, pozzolanic materials, slag and other mineral components. The process of cement production, particularly the kiln, can influence how much hexavalent chromium will develop.

All raw materials for cement production comprise small or trace amounts of total chromium. Total chromium from the primary raw materials varies with the type and origin. Limestone contains from 2 ppm to 20 ppm of total chromium, clay contains from 50 ppm to 200 ppm, fly ash contains from 200 ppm to 250 ppm of total Cr [13]. From the total amount of chromium in raw materials most accounts for trivalent chromium. Most raw materials does not contain water soluble hexavalent chromium. The content of hexavalent chromium reported for fly ashes is in the range of about 0.5 ppm.

The formation of soluble hexavalent chromium in the kiln system depends mostly on the oxygen concentration and alkalinity. The source of chromium input in the kiln feed is primarily as Cr III, which in high-alkaline environment can be oxidized to Cr VI. The amount of Cr VI compounds formed is connected with level of oxygen and pressure of the system.

The data on the amount of total and water soluble chromium in final products, i. e. clinker and cement, reported in papers differs a lot, depending from the area of manufacturing and the method chosen for the study. S. W. Chang et al. state 20.58 ± 1.53 mg/kg of total chromium for grey Portland cement and 7.78 ± 0.54 mg/kg of total chromium for white Portland cement [53]. Inductively coupled plasma atomic emission spectroscopy (ICP-AES) was used for quantification of matter. Both tested cements had Korean origin of production.
M. Schembri et al. with the use of atomic absorption spectroscopy determined following amount of acid soluble chromium in cements: 169.32 mg/kg in grey Portland cement (Italy) and 90.20 mg/kg in white Portland cement (Denmark) [57]. The water soluble chromium content in Portland cements usually ranges from 1 ppm to 30 ppm [13].

The use of materials to reduce the level of hexavalent chromium formation is prevalent in the cement industry due to the 2003 European Directive which declares that cement and cement-containing preparations may not be used or placed on the market, if they contain, when hydrated, more than 0.0002% (2 ppm) soluble chromium VI of the total dry weight of the cement. Cement companies are adding reducing agents to comply with this directive. Several substances are used for that purpose, among them are ferrous sulphate, stannous sulphate, manganese sulphate, stannous chloride and zinc salts.

Two form of ferrous sulphate are mostly used nowadays in cement manufacturing industry: heptahydrate ($FeSO_4 \cdot 7H_20$) and monohydrate ($FeSO_4 \cdot H_20$). By adding a reducing agent, such as ferrous sulphate, the water-soluble Cr VI can be converted into a hardly soluble Cr III form that is not capable to penetrate the unprotected skin:

$$CrO_4^{2-} + 3Fe^{2+} + 4OH^- + 4H_2O \rightarrow Cr(OH)_3 + 3Fe(OH)_3 \qquad (1.1)$$

The chemical reaction does not start until immediately after the mixing of water. Due to the highly alkaline environment, the iron is exposed to competing reactions, such as hydrolysis and oxidation by dissolved atmospheric oxygen. Ferrous sulphate has shown its worth as a reliable chromate reducer in terms of practical application. However, ferrous sulphate addition may effect cement quality. Excess sulphate may be followed by decrease in concrete strength, expansion, and possible internal sulphate attack. At high dosages, there can be concerns of risen water demand, long setting time, and possible concrete staining or mottling.

Stannous sulphate can withstand relatively high temperatures without degradation, enabling addition to finish mill. It is more effective at low concentrations compared to ferrous sulphate [58]. Although low storage stability of the cement with the addition of stannous sulphates as chromate reducers can be observed as a result of chemical transformations taking place in the cement matrix. Oxygen, humidity, and high content of free lime can accelerate the loss of reducing agent activity [59].

Antimony (III) compounds ($Sb_2O_3$, $H_3SbO_3$) are more resistant at high moisture, temperature, high free lime content and they have high reducing efficiency (0.02 to 0.04% required to reduce 30 ppm Cr VI totally) than ferrous sulphate and stannous sulphate [60]. Beside these advantages, antimony salts have toxicological effect, which is suspected of being carcinogenic [61].

## 1.2 Aggregates

Aggregates are inert granular materials such as sand, gravel, or crushed stone that, along with water and Portland cement, are an essential ingredient in concrete.

For a good concrete mix, aggregates need to be clean, hard, strong particles free of absorbed chemicals or coatings of clay and other fine materials that could cause the deterioration of concrete. Aggregates, which account for 60 to 75 percent of the total volume of concrete, are divided into two distinct categories--fine and coarse. Fine aggregates generally consist of natural sand or crushed stone with most particles passing through a 1 cm sieve. Coarse aggregates are any particles greater than 0.5 cm, but generally range between 1 and 4 cm in diameter. Gravels constitute the majority of coarse aggregate used in concrete with crushed stone making up most of the remainder [64].

Natural gravel and sand are usually dug or dredged from a pit, river, lake, or seabed. Crushed aggregate is produced by crushing quarry rock, boulders, cobbles, or large-size gravel. Recycled concrete is a viable source of aggregate and has been satisfactorily used in granular subbases, soil-cement, and in new concrete.

After harvesting, aggregate is processed: crushed, screened, and washed to obtain proper cleanliness and gradation. If necessary, a benefaction process such as jigging or heavy media separation can be used to upgrade the quality. Once processed, the aggregates are handled and stored to minimize segregation and degradation and prevent contamination.

Aggregates strongly influence concrete's freshly mixed and hardened properties, mixture proportions, and economy. Consequently, selection of aggregates is an important process.

Grading refers to the determination of the particle-size distribution for aggregate. Grading limits and maximum aggregate size are specified because these properties affect the amount of aggregate used as well as cement and water requirements, workability, pump ability, and durability of concrete. In general, if the water-cement ratio is chosen correctly, a wide range in grading can be used without a major effect on strength. When gap-graded aggregate are specified, certain particle sizes of aggregate are omitted from the size continuum. Gap-graded aggregate are used to obtain uniform textures in exposed aggregate concrete. Close control of mix proportions is necessary to avoid segregation.

Particle shape and surface texture influence the properties of freshly mixed concrete more than the properties of hardened concrete. Rough-textured, angular, and elongated particles require more water to produce workable concrete than smooth, rounded compact aggregate. Consequently, the cement content must also be increased to maintain the water-cement ratio. Generally, flat and elongated particles are avoided or are limited to about 15 percent by weight of the total aggregate. Unit-weight measures the volume that graded aggregate and the voids between them will occupy in concrete.

The void content between particles affects the amount of cement paste required for the mix. Angular aggregates increase the void content. Larger sizes of well-graded aggregate and improved grading decrease the void content. Absorption and surface moisture of aggregate are measured when selecting aggregate because the internal structure of aggregate is made up of solid material and voids that may or may not contain water. The amount of water in the concrete mixture must be adjusted to include the moisture conditions of the aggregate.

Abrasion and skid resistance of an aggregate are essential when the aggregate is to be used in concrete constantly subject to abrasion as in heavy-duty floors or pavements. Different minerals taken together wear and polish at different rates. Harder aggregate can be selected in highly abrasive conditions to minimize wear.

## 1.3 Porosity and pore solution in concrete

A typical pore size distribution for hardened cement encompasses a large range, extending from about 0.5 nm or less in diameter. The larger pores, ranging from 1 to 10 nm, are the residual unfilled spaces between cement grains, earlier defined as capillary pores. The finest pores, ranging from approximately 10 nm to 0.5 nm, are called gel pores since they constitute the internal porosity of the C-S-H gel phase. While this is certainly a useful distinction, it should be kept in mind that the sizes of capillary and gel pores overlap, and the spectrum of pore sizes in a cement paste is continuous. Internal features with dimensions of 0.5 nm or smaller are formed by the interlayer spaces of C-S-H gel. Water located in these features is not in the liquid, so these are not true pores as defined for cement paste. Voids greater than 10 nm often exist in concrete, either from the unintentional entrapment of air during the mixing procedure, or from intentional air-entrainment, which purposefully disperses air voids of approximately 50 nm in diameter throughout the paste to relieve pressures induced from the freezing of water in pores [65].

The process of hydration can be thought of as the progressive conversion of free (liquid) water in the capillary pores into bound water in the solid hydration products. The binding of water ensures that the hydration products occupy a greater volume than the solid reactants (i.e. the cement minerals) that they replace. The greater the volume fraction of the paste occupied by solid phases, the stronger and stiffer the cement paste or concrete.

If all of the hydration products were in the form of relatively large crystals, then to a good approximation the water could simply be divided into bulk liquid water and structural (chemically bound) water. However, the case for cement paste is much more complicated. While all of the hydration products do contain chemically bound water, the C-S-H gel phase also contains significant amounts of free and adsorbed water in its gel pores, and holds more tightly bound water within its interlayer or interparticle spaces. The water in cement paste that is not bound into the solid phases is an important phase in its own right that is involved in important properties such as ionic transport, drying shrinkage, and creep.

The water within a few molecular distances of a pore surface has very different properties than bulk liquid water. The first layer of molecules is physically adsorbed on the surface, while the next few layers are aligned in a non-random way due to the polar nature of the water molecule. In the larger capillary pores the fraction of this "surface water" is negligible and on average the water maintains the properties of the bulk liquid. As the pore size decreases to the order of nanometres (as with gel pores), the surface water becomes a significant fraction of the total water content. As a result, the average physical properties of gel water such as density, viscosity, dielectric constant and conductivity often differ from those of bulk water. Perhaps most importantly, the rate of diffusion of surface water is significantly lower than that of bulk water. This reduced mobility has been postulated to play important roles in the mechanisms of creep and of drying shrinkage at low humidity. The reduced mobility of the surface water in a paste can be measured directly using nuclear magnetic resonance (NMR), and this can be used to infer the fine pore size distribution and surface area.

The C-S-H gel contains a certain fraction of water that is more tightly bound than adsorbed water on a gel pore surface, but which is still in the form of an $H_2O$ molecule rather than a chemically bound hydroxyl ($OH^-$) group. To fully specify the physical location of this water requires a description of the nanometre-level structure of C-S-H gel, but this structure is not completely agreed on at present. Traditional view of the C-S-H gel is based on a layered structure at the scale of tens of nanometres, because crystalline C-S-H minerals with

compositions similar to C-S-H gel have a layered structure. The spaces between these layers can hold significant numbers of "interlayer" water molecules. More recent analysis of C-S-H gel has indicated that the structure is actually based on very small particles about 5 nm in size that are randomly agglomerated into larger structures. Models based on these observations consider interlayers to be present within these particles but not at larger scales. However, "interparticle" water held between closely packed 5 nm C-S-H particles would have the same physical characteristics as interlayer water. Regardless of the details of the C-S-H structure, it is difficult to draw a sharp physical distinction between interlayer/interparticle water and water that is adsorbed on the smallest gel pores, because there is an overlap in the RH at which they will be removed.

## 2 Durability of reinforced concrete structures

The exceptional durability of Portland cement concrete is a major reason why it is the world's most widely used construction material. However, material limitations, design and construction practices, and severe exposure conditions can cause concrete to deteriorate, which may result in aesthetic, functional, or structural problems. Concrete can deteriorate for a variety of reasons, and concrete damage is often the result of a combination of factors.

### 2.1 Deterioration due to chemical attack

Concrete performs well when exposed to various atmospheric conditions, water, soil, and many other chemical exposures. However, some chemical environments can deteriorate even high-quality concrete. Solid dry chemicals rarely attack concrete. To produce significant attack on concrete, aggressive chemicals must be in solution and above some minimum concentration.

Acids react with the calcium hydroxide of the hydrated Portland cement. In most cases, the chemical reaction forms water-soluble calcium compounds, which are then leached away by aqueous solutions. The products of combustion of many fuels contain sulphurous gases, which combine with moisture to form sulfuric acid. In addition, certain bacteria convert sewage into sulfuric acid. Sulfuric acid is particularly aggressive to concrete because the calcium sulphate formed from the acid reaction will also deteriorate concrete via sulphate attack. In addition to individual organic and mineral acids which may attack concrete, acid-containing or acid-producing substances, such as acidic industrial wastes, silage, fruit juices, and sour milk, will also cause damage. Animal wastes contain substances which may oxidize in air to form acids which attack concrete. The saponification reaction between animal fats and the hydration products of Portland cement consumes these hydration products, producing salts and alcohols, in a reaction analogous to that of acids. Acid rain, which often has a pH of 4 to 4.5, can slightly etch concrete, usually without affecting the performance of the exposed surface [66].

The chlorides and nitrates of ammonium, magnesium, aluminium, and iron all cause concrete deterioration, with those of ammonium producing the most damage. Most ammonium salts are destructive because, in the alkaline environment of concrete, they release ammonia gas and hydrogen ions. These are replaced by dissolving calcium hydroxide from the concrete. The result is a leaching action, much like acid attack.

### 2.2 Alkali-aggregate reactivity

In most concrete, aggregates are more or less chemically inert. However, some aggregates react with the alkali hydroxides in concrete, causing expansion and cracking over a period of years. This alkali-aggregate reactivity has two forms—alkali-silica reaction (ASR) and alkali-carbonate reaction (ACR). ASR is of more concern than ACR because aggregates containing reactive silica materials are more common [67].

Aggregates containing certain forms of silica will react with alkali hydroxide in concrete to form a gel that swells as it draws water from the surrounding cement paste or the environment.

Reactions observed with certain dolomitic rocks are associated with alkali-carbonate reaction (ACR). Dedolomitization, or the breaking down of dolomite, is normally associated with expansive alkali-carbonate reactivity. This reaction and subsequent crystallization of brucite may cause considerable expansion. The deterioration caused by alkali-carbonate reaction is similar to that caused by alkali-silica reaction; however, alkalicarbonate reaction is relatively rare because aggregates susceptible to this reaction are less common and are usually unsuitable for use in concrete for other reasons, such as strength potential.

## 2.3 Erosion of concrete

Abrasion damage occurs when the surface of concrete is unable to resist wear caused by rubbing and friction. As the outer paste of concrete wears, the fine and coarse aggregate are exposed and abrasion and impact will cause additional degradation that is related to aggregate-to-paste bond strength and hardness of the aggregate. Although wind-borne particles can cause abrasion of concrete, the two most damaging forms of abrasion occur on vehicular traffic surfaces and in hydraulic structures, such as dams, spillways, and tunnels.

In some areas, abrasive materials such as sand are applied to pavements to improve traction, but experience has shown that this causes little wear if the concrete is of good quality and the aggregates are wear resistant. Compressive strength is the most important factor controlling the abrasion resistance of concrete, with abrasion resistance increasing with increase in compressive strength. The service life of some concrete, such as warehouse floors subjected to abrasion by steel or hard rubber wheels, may be greatly increased by the use of specially hard or tough aggregate.

## 2.4 Corrosion of embedded metals

### *2.4.1 Corrosion of steel reinforcement in concrete*

Corrosion of reinforcing steel and other embedded metals is the leading cause of deterioration in concrete. When steel corrodes, the resulting rust occupies a greater volume than the steel. This expansion creates tensile stresses in the concrete, which can eventually cause cracking, delamination, and spalling (Figs. 2-1).

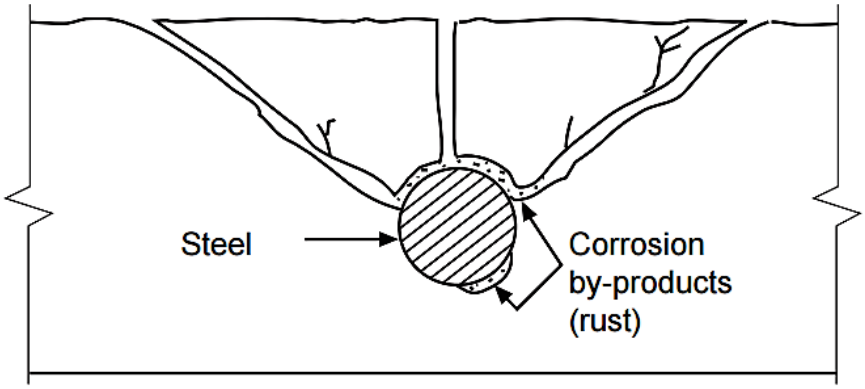


Figure 2-1. The expansion of corroding steel, causing formation of cracks, delamination, and spalling.

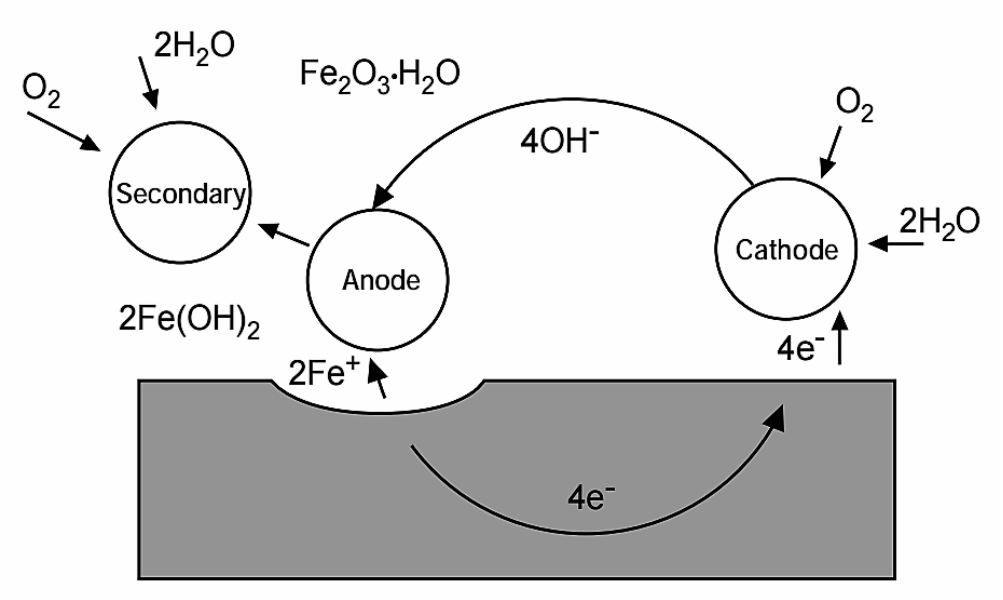


Figure 2-2. Scheme of the corrosion of reinforcing steel bar in concrete

Steel corrodes because it is not a naturally occurring material. Rather, iron ore is smelted and refined to produce steel. The production steps that transform iron ore into steel add energy to the metal. Steel, like most metals except gold and platinum, is thermodynamically unstable under normal atmospheric conditions and will release energy and revert back to its natural state—iron oxide, or rust. For corrosion to occur, four elements must be present: there must be at least two metals (or two locations on a single metal) at different energy levels, an electrolyte, and a metallic connection. In reinforced concrete, the rebar may have many separate areas at different energy levels. Concrete acts as the electrolyte, and the metallic connection is provided by wire ties, chair supports, or the rebar itself [68].
Figure 2-2 shows a corroding steel bar embedded in concrete. At active sites on the bar, called anodes, iron atoms lose electrons and move into the surrounding concrete as ferrous ions. This process is called a half-cell oxidation reaction, or the anodic reaction, and is represented as:

$$2Fe \rightarrow 2Fe^{2+} + 4e^{-} \tag{2.1}$$

The electrons remain in the bar and flow to sites called cathodes, where they combine with water and oxygen in the concrete. The reaction at the cathode is called a reduction reaction. A common reduction reaction is:

$$2H_2O + O_2 + 4e^{-} \rightarrow 4OH^{-} \tag{2.2}$$

To maintain electrical neutrality, the ferrous ions migrate through the concrete pore water to these cathodic sites where they combine to form iron hydroxides, or rust:

$$2Fe^{2+} + 4OH^{-} \rightarrow 2Fe(OH)_2 \tag{2.3}$$

This initial precipitated hydroxide tends to react further with oxygen to form higher oxides. The increases in volume as the reaction products react further with dissolved oxygen leads

to internal stress within the concrete that may be sufficient to cause cracking and spalling of the concrete cover.

### *2.4.2 Corrosion thermodynamics*

Corrosion measurements are quantified by constructing a corrosion cell (an electrochemical cell, in which the oxidation and reduction reactions generally take place at separate electrodes in the cell, which develop an electrical potential difference between them. The (open circuit) cell potential is a measure of the tendency of a metal to corrode. When the two electrodes are in electrical contact, an electrical circuit is formed in which electron current flows through the electrical connection between the electrodes and a corresponding ion current flows through the electrolyte between the electrodes. The current flow is a measure of the corrosion, taking place at the anode [69].

One can assert the tendency of a metal to corrode from thermodynamic considerations. The change $\Delta G$ in Gibbs free energy for the corrosion reaction predicts whether a corrosion reaction occurs spontaneously; it does so spontaneously if $\Delta G < 0$. The change in free energy can be calculated from a measurement of the cell potential E. The maximum amount of electrical energy (or work done) that can be delivered by an electrochemical cell in a given state is nFE, which is equivalent to the change in Gibbs free energy:

$$\Delta G = -nFE \qquad (2.4)$$

where n is the number of moles of electrons exchanged in an electrochemical reaction, F is Faraday's constant (96,485 C /mol), and E is the cell potential (in volts) for the cell in a given state. For cell conditions in a standard state:

$$\Delta G^0 = -nFE^0 \qquad (2.5)$$

where $E^0$ represents the standard-state electrochemical cell potential, and $\Delta G^0$ represents the Gibbs free energy change for constituents in their standard states. The standard Electromotive Force (emf) registers values for $E^0$.

How the cell potential varies with cell conditions is established by the Nernst equation. The Nernst equation codifies the fundamental relationship in electrochemical reactions that expresses the electrochemical cell potential in terms of reactants and products of the reaction. It can be derived based on Gibbs free energy criterion for chemical reactions. For a general chemical reaction, the change in Gibbs free energy is related to the activities of the reactants and products of reaction, as follows:

$$\Delta G - \Delta G^0 = RT \ln (a_{products} / a_{reactants}) \text{ or} \qquad (2.6)$$

$$\Delta G - \Delta G^0 = 2.303\, RT \log_{10} (a_{products} / a_{reactants}) \qquad (2.7)$$

where $\Delta G$ and $\Delta G^0$ represent changes in the free energy of products and reactants in non-standard and standard states, respectively; R is the gas constant (8.314 J/mol•K), T is the temperature in Kelvins, and the quantities $a_{products}$ and $a_{reactants}$ are the activities (roughly related to concentration) of products and reactants, respectively. Eqns (2.6) and (2.7) establish the Nernst equation (2.8, 2.9), which relates the cell potential, in any state, to the cell potential in a standard state and to the products and reactants of the electrochemical reaction.

$$E - E^0 = -(2.303\, RT/nF) \log_{10} (a_{products} / a_{reactants}), \text{ or} \qquad (2.8)$$

$$E = E^0 - (2.303\ RT/nF)\ \log_{10}\ (a_{products} / a_{reactants}) \qquad (2.9)$$

Though the thermodynamic aspect is useful in determining the relative tendencies of metal reactivity (or corrosion), in practical situations the kinetics of a corrosion reaction are important in governing the extent to which a metal corrodes, that is, the rate of corrosion. The corrosion rate is proportional to corrosion current. Thus, a definite way of knowing if a metal in a given environment is corroding is to make a current measurement.

### *2.4.3 Corrosion rate*

The corrosion rate depends on the kinetics of both anodic (oxidation) and cathodic (reduction) reactions. According to Faraday's law, there is a linear relationship between the metal dissolution rate or corrosion rate, $R_M$, and the corrosion current $i_{corr}$:

$$R_M = \frac{M}{nF\rho} i_{corr} \qquad 2.10$$

where $M$ is the atomic weight of the metal, $\rho$ is the density, n is the charge number which indicates the number of electrons exchanged in the dissolution reaction and F is the Faraday constant, (96.485 C/mol). The ratio M/n is also sometime referred to as equivalent weight [68].

Calculation of corrosion rates requires the determination of corrosion currents. When reaction mechanisms for the corrosion reaction are known, the corrosion currents can be calculated using Tafel Slope Analysis. The relationship between current density and potential of anodic and cathodic electrode reactions under charge transfer control is given by the Butler-Volmer equation:

$$i = i_{corr}\left(e^{2.303\frac{\eta}{b_a}} - e^{2.303\frac{\eta}{b_c}}\right) \qquad 2.11$$

$$\eta = E - E_{corr} \qquad 2.12$$

In the above equation E is the applied potential and i the measured current density. The overpotential,$\eta$, is defined as the difference between applied potential and the corrosion potential $E_{corr.}$ The corrosion potential, $E_{corr}$ is the open circuit potential of a corroding metal. The corrosion current, $i_{corr}$, and the Tafel constants $b_a$, and $b_c$ can be measured from the experimental data.

For large anodic overpotentials ($\eta/b_a >> 1$) the Butler-Volmer equation simplifies to the Tafel equation for the anodic reaction:

$$\eta = log(i_{corr}) + b_a \cdot log(i) \qquad 2.13$$

Analogously, for large cathodic overpotentials ($\eta/b_a$ << -1) the Tafel equation for the cathodic reaction is given by:

$$\eta = log(i_{corr}) - b_c \cdot log|i| \qquad 2.14$$

The Tafel equations predict a straight line for the variation of the logarithm of current density with potential. Therefore, currents are often shown in semilogarithmic plots known as Tafel plots. This type of analysis is referred to as Tafel Slope Analysis.

### *2.4.4 Pourbaix diagrams*

Pourbaix Diagrams plot electrochemical stability for different redox states of an element as a function of pH. These diagrams are essentially phase diagrams that plot the map the conditions of potential and pH (most typically in aqueous solutions) where different redox species are stable. Typically, the water redox reactions are plotted as dotted lines on these more complicated diagrams for other elements. The lines in Pourbaix diagrams represent redox and acid-base reactions, and are the parts of the diagram where two species can exist in equilibrium. Pourbaix diagrams are usually plotted for lower ion concentrations (often 1 mM) that are more relevant to corrosion and electrochemical experiments [69].

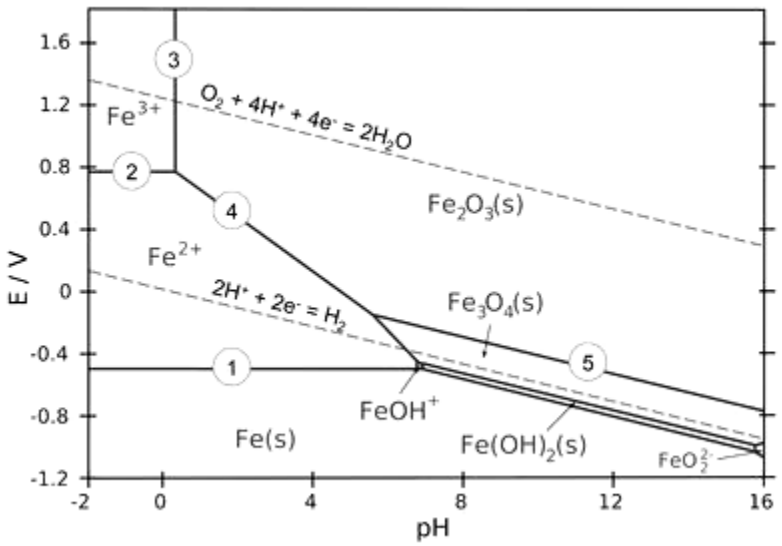


Figure 2-3. Pourbaix diagram for iron at ionic concentrations of 1.0 mM

Areas in the Pourbaix diagram mark regions where a single species ($Fe^{2+}$(aq), $Fe_3O_4$(s), etc.) is stable. More stable species tend to occupy larger areas. Lines mark places where two species exist in equilibrium. Pure redox reactions are horizontal lines - these reactions are not pH-dependent. Pure acid-base reactions are vertical lines - these do not depend on potential. Reactions that are both acid-base and redox have a slope of -0.0592 V/pH x H+/e-)

Examples of equilibria in the iron Pourbaix diagram (numbered on the plot):

1. $Fe^{2+}+2e^- \rightarrow Fe(s)$ (pure redox reaction - no pH dependence)

2. $Fe^{3+}+e-\rightarrow Fe^{2+}$ (pure redox reaction - no pH dependence)
3. $2Fe^{3+}+3H_2O\rightarrow Fe_2O_3(s)+6H^+$ (pure acid-base, no redox)
4. $2Fe^{2+}+3H2O\rightarrow Fe_2O_3(s)+6H^++2e^-$ (slope = -59.2 x 6/2 = -178 mV/pH)
5. $2Fe_3O_4(s)+H2O\rightarrow 3Fe_2O_3(s)+2H^++2e^-$ (slope = -59.2 x 2/2 = -59.2 mV/pH)

The water redox lines have special significance on a Pourbaix diagram for an element such as iron. Recall that liquid water is stable only in the region between the dotted lines. Below the $H_2$ line, water is unstable relative to hydrogen gas, and above the $O_2$ line, water is unstable with respect to oxygen. For active metals such as Fe, the region where the pure element is stable is typically below the $H_2$ line. This means that iron metal is unstable in contact with water, undergoing reactions:

$Fe(s)+2H^+\rightarrow Fe^{2+}(aq)+H2$ (in acid)

$Fe(s)+2H_2O\rightarrow Fe(OH)_2(s)+H_2$ (in base)

Iron (and most other metals) are also thermodynamically unstable in air-saturated water, where the potential of the solution is close to the $O_2$ line in the Pourbaix diagram. Here the spontaneous reactions are:

$4Fe(s)+3O_2+12H+\rightarrow 4Fe^{3+}+6H_2O$ (in acid)

$4Fe(s)+3O_2\rightarrow 2Fe_2O_3(s)$ (in base)

Unstable in water, no matter what the pH or potential. Given enough time, it will all turn into rust. However, iron (and other active metals) can corrode, or can be stabilized against corrosion, depending on the conditions.

The corrosion of iron (and other active metals) is rapid in parts of the Pourbaix diagram where the element is oxidized to a soluble, ionic product such as $Fe^{3+}(aq)$. However, solids such as $Fe_2O_3$,, form a protective coating on the metal that greatly impedes the corrosion reaction. This phenomenon is called passivation.

At slightly acidic pH, iron is quite unstable with respect to corrosion by the reaction:

$Fe(s)+2H^+\rightarrow Fe^{2+}(aq)+H_2$

but only in water that contains relatively little oxygen, i.e., in solutions where the potential is near the $H_2$ line. Saturating the water with air or oxygen moves the system closer to the $O_2$ line, where the most stable species is $Fe_2O_3$ and the corrosion reaction is:

$4Fe(s)+3O_2\rightarrow 2Fe_2O_3(s)$

This oxidation reaction is orders of magnitude slower because the oxide that is formed passivates the surface. Therefore, iron corrodes much more slowly in oxygenated

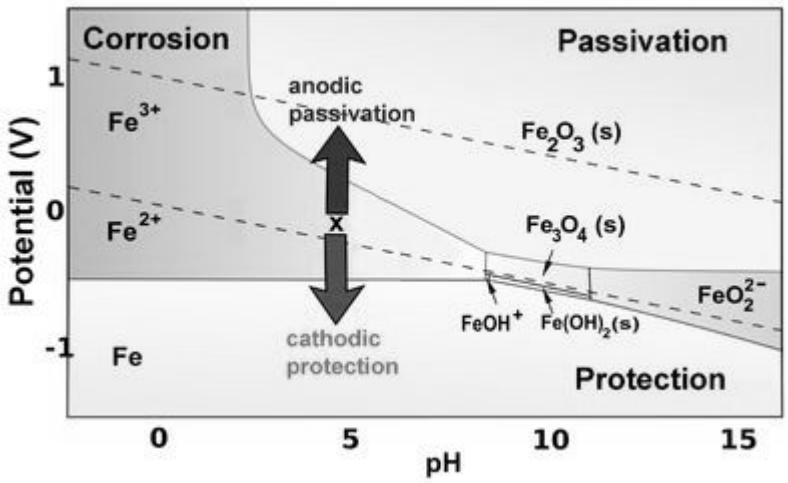


Figure 2-4. Pourbaix diagram for iron: areas of corrosion, passivation and protection

solutions. More generally, iron (and other active metals) are passivated whenever they oxidize to produce a solid product, and corrode whenever the product is ionic and soluble. This behaviour can be summed up on the color-coded Pourbaix diagram on Figure 2-4.

The "Protection" part of the diagram, an active metal such as iron can be protected by a second mechanism, which is to bias it so that its potential is below the oxidation potential of the metal. This cathodic protection strategy is most frequently carried out by connecting a more active metal such as Mg or Zn (Fig. 2-5) to the iron or steel object (e.g., the hull of a ship, or an underground gas pipeline) that is being protected. The active metal (which must be higher than Fe in the activity series) is also in contact with the solution and slowly corrodes, so it must eventually be replaced. In some cases a battery - the anode of which oxidizes water to oxygen in the solution - is used instead to apply a negative bias.

Another common mode of corrosion of iron and carbon steel is differential aeration**.** In this case, part of the iron object - e.g., the base of a bridge, or the drill in an oilrig - is under water or in an anoxic environment such as mud or soil. The potential of the solution is close to the $H_2$ line in the Pourbaix diagram, where Fe can corrode to $Fe^{2+}$ (aq). Another part of the iron object is in the air, or near the surface where water is well oxygenated. At that surface oxygen can be reduced to water, $O_2 + 4H^+ + 4e^- = 2H_2O$. The conductive iron object completes the circuit, carrying electrons from the anode (where Fe is oxidized) to the cathode (where $O_2$ is reduced). Corrosion by differential aeration can be rapid because soluble ions

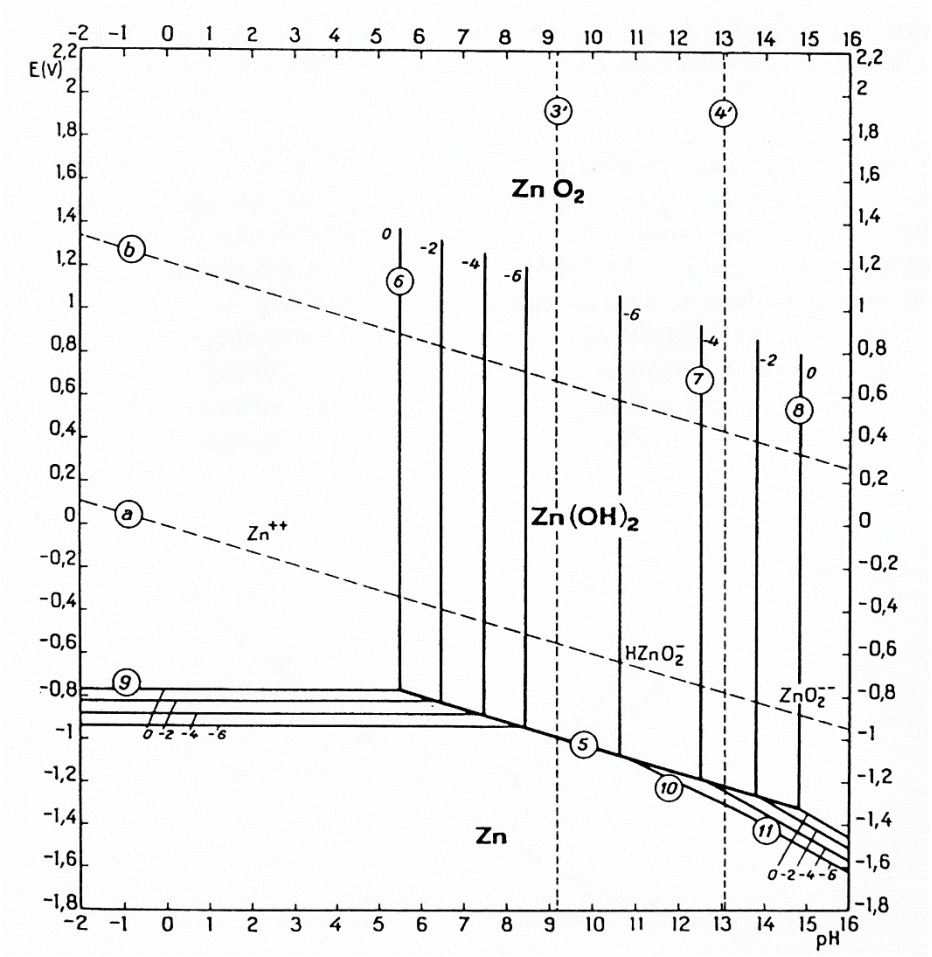


Figure 2-5. Pourbaix diagram for zinc at 25° C

are produced, and the reaction has a driving force of over 1 V.

Differential aeration is involved in the formation of a rust ring around wet areas of cast iron, e.g., an iron frying pan left partially submerged in water for a day or more. Under the water, Fe is oxidized to soluble $Fe^{2+}$, and at the water line $O_2$ is reduced to $H_2O$. As $Fe^{2+}$ ions diffuse towards the water surface, they encounter oxygen molecules and are oxidized to $Fe^{3+}$. However $Fe^{3+}$ is insoluble at neutral pH and deposits as rust, typically just below the water line, forming the rust ring. Table 2-1 demonstrates reactions typical for zinc in aqueous solutions.

Table 2-1. Reactions of zinc in aqueous solutions and equilibrium conditions

| Reaction | Equilibrium | Standard potential or equilibrium condition |
|---|---|---|
| *Two dissolved substances* | | |
| 1 | $Zn^{2+} + H_2O = ZnOH^+ + H^+$ | $\log (ZnOH^+)/(Zn^{2+}) = -9.67 + pH$ |
| 2 | $ZnOH^+ + H_2O = HZnO_2^- + 2H^+$ | $\log (HZnO_2^-)/(ZnOH^+) = -17.97 + 2pH$ |
| 3 | $Zn^{2+} + 2H_2O = HZnO_2^- + 3H^+$ | $\log (HZnO_2^-)/(Zn^{2+}) = -27.63 + 3pH$ |
| 4 | $HZnO_2^- = ZnO_2^{2-} + H^+$ | $\log (ZnO_2^{2-})/(HZnO_2^-) = -13.17 + pH$ |
| *Two solid substances* | | |
| 5 | $Zn + H_2O = ZnO + 2H^+ + 2e^-$ | $E_0 = -0.439 - 0.0591\ pH$ |
| *One solid and one dissolved substance* | | |
| 6 | $Zn^{2+} + H_2O = ZnO + 2H^+$ | $\log(Zn^{2+}) = 10.96 - 2pH$ |
| 7 | $ZnO + H_2O = HZnO_2^- + H^+$ | $\log(HZnO_2^-) = -16.68 + pH$ |
| 8 | $ZnO + H_2O = ZnO_2^{2-} + 2H^+$ | $\log(ZnO_2^{2-}) = -29.78 + 2pH$ |
| 9 | $Zn = Zn^{2+} + 2e^-$ | $E_0 = -0.763 + 0.0295 \log(Zn^{2+})$ |
| 10 | $Zn + 2H_2O = HZnO_2^- + 3H^+ + 2e^-$ | $E_0 = 0.054 - 0.0886pH + 0.0295 \log(HZnO_2^-)$ |
| 11 | $Zn + 2H_2O = ZnO_2^{2-} + 4H^+ + 2e^-$ | $E_0 = 0.441 - 0.1182\ pH + 0.0295 \log(ZnO_2^{2-})$ |
| *Stability of water* | | |
| (a) | $H_2 = 2H^+ + 2e^-$ | $E_0 = 0.000 - 0.0591\ pH$ |
| (b) | $2H_2O = O_2 + 4H^+ + 4e^-$ | $E_0 = 1.228 - 0.0591\ pH$ |

### *2.4.5 Concrete and the passivating layer*

Although steel's natural tendency is to undergo corrosion reactions, the alkaline environment of concrete (pH of 12 to 13) provides steel with corrosion protection. At the high pH, a thin oxide layer forms on the steel and prevents metal atoms from dissolving. This passive film does not actually stop corrosion; it reduces the corrosion rate to an insignificant level. For steel in concrete, the passive corrosion rate is typically 0.1 μm per year. Without the passive film, the steel would corrode at rates at least 1,000 times higher. Because of concrete's inherent protection, reinforcing steel does not corrode in the majority of concrete elements and structures. Corrosion can occur when the passivating layer is destroyed. The destruction of the passivating layer occurs when the alkalinity of the concrete is reduced or when the chloride concentration in concrete is increased to a certain level.

### *2.4.6 The role of chloride ions*

Exposure of reinforced concrete to chloride ions is the primary cause of premature corrosion of steel reinforcement. The intrusion of chloride ions, present in de-icing salts and seawater,

into reinforced concrete can cause steel corrosion if oxygen and moisture are also available to sustain the reaction. Chlorides dissolved in water can permeate through sound concrete or reach the steel through cracks. Chloride-containing admixtures can also cause corrosion. No other contaminant is documented as extensively in the literature as a cause of corrosion of metals in concrete than chloride ions. The mechanism by which chlorides promote corrosion is not entirely understood, but the most popular theory is that chloride ions penetrate the protective oxide film easier than do other ions, leaving the steel vulnerable to corrosion. The risk of corrosion increases as the chloride content of concrete increases. When the chloride content at the surface of the steel exceeds a certain limit, called the threshold value, corrosion will occur if water and oxygen are also available. However, only water-soluble chlorides promote corrosion; some acid-soluble chlorides may be bound within aggregates and, therefore, unavailable to promote corrosion. Although chlorides are directly responsible for the initiation of corrosion, they appear to play only an indirect role in the rate of corrosion after initiation. The primary rate-controlling factors are the availability of oxygen, the electrical resistivity and relative humidity of the concrete, and the pH and temperature.

### *2.4.7 The role of the carbonation process*

Carbonation occurs when carbon dioxide from the air penetrates the concrete and reacts with hydroxides, such as calcium hydroxide, to form carbonates. This reaction reduces the pH of the pore solution to as low as 8.5, at which level the passive film on the steel be not stable. Carbonation is generally a slow process. In high-quality concrete, it has been estimated that carbonation will proceed at a rate up to 1.0 mm per year. The amount of carbonation is significantly increased in concrete with a high water/cement ratio, low cement content, short curing period, low strength, and highly permeable or porous paste. Carbonation is highly dependent on the relative humidity of the concrete. The highest rates of carbonation occur when the relative humidity is maintained between 50% and 75%. Below 25% relative humidity, the degree of carbonation that takes place is considered insignificant. Carbonation-induced corrosion often occurs on areas of building facades that are exposed to rainfall, shaded from sunlight, and have low concrete cover over the reinforcing steel.

# 3 Prevention of corrosion in concrete

Corrosion-induced damage to reinforced concrete often necessitates early repair and occasionally complete replacement of the structure or element well before its design life is reached. Since the cost of repairing reinforced concrete structures is generally high, concrete technology is continuously developing methods to prevent the onset of deterioration in reinforced concrete structures. These methods include:

— The impregnation of concrete body with hydrophobic materials, e.g. silanes or silicates, intended to reduce its permeability

— The application of waterproofing concrete surface coatings such as the acrylic based, epoxy resin, polyurethane, cementitious based, etc. The addition of organic or inorganic corrosion inhibitors to concrete

— The use of corrosion-resisting materials, e. g. stainless steel, as replacement for conventional steel reinforcement

— Cathodic protection of the reinforcement

— The application of metallic (e.g. zinc, copper, stainless steel, etc.) and non-metallic (e. g. epoxy, silicate polymer-based, etc.) coatings to the reinforcement

All of the above methods may be used separately or in conjunction. Among them, the use of coated steel reinforcement in particular has been widely accepted as an economical and convenient means of providing corrosion protection in many types of concrete construction.

## 3.1 Coatings of reinforcement

### *3.1.1 Metallic coatings*

Metallic coating serves two functions: it acts as a barrier to the environment, with greater corrosion resistance than the substrate metal and it provides cathodic protection at breaks of the coating due to galvanic corrosion as the coating is usually selected with a more-active corrosion potential than the substrate. Metal coatings are applied by immersion, electroplating, cladding, flame-spraying, chemical deposition, and vapour deposition [70]. For metal-coated steel reinforcement, numerous coating systems, containing aluminium, nickel, zinc, copper, and stainless steel have been used in concrete.

Practically the most important application of metallic coatings is zinc-coated steel. Single construction elements are zinc-coated by electroplating or by dipping in molten zinc. Larger object, such as whole constructions may be zinc-coated by spraying with molten zinc or by painting with zinc-rich paint. The last mentioned two methods are considerably more expensive than the first two [71].

Hot-dip galvanizing is known as the major method used to apply zinc-based coating on steel in order to provide sacrificial protection against corrosion. According to the Fe–Zn phase diagram, when iron is immersed in molten zinc at the typical galvanizing temperature

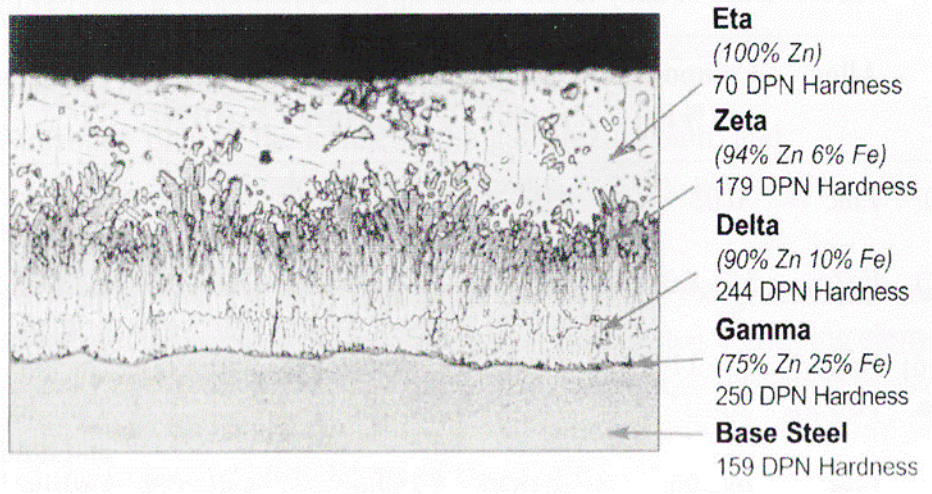


Figure 3-1. Microstructure of galvanized coating on steel (200 x) [1]

(450–490 °C), the following layers should form: zinc saturated α-iron, γ phase layer, δ phase layer, ζ phase layer and η phase layer (Fig. 3-1). However, the sequential nucleation of the Fe–Zn phases occurs at the interface beginning with ζ phase layer, followed by δ phase layer, then the γ phase layer after some incubation time [72].

In order to these intermetallic layer to form properly, the steel must be prepared and processed in a specific way. The galvanizing process comprises three basic stages: surface preparation, fluxing and galvanizing.

Surface preparation is usually performed in a sequence of alkane cleaning, water rinsing, acid pickling and water rinsing. The alkaline cleaner is used to clean the metal of organic contaminants such as oil, grease or paints, which are not readily removed by acid pickling. Surface preparation can be also accomplished using abrasive cleaning.

The method of applying the flux to the steel depends upon whether the wet or dry galvanizing process is used. Dry galvanizing requires that the steel be dipped in an aqueous zinc ammonium chloride solution and then thoroughly dried. This pre-fluxing prevents oxides from forming on metal prior to the actual galvanizing stage. In the wet galvanizing process, a layer of liquid zinc ammonium chloride is floated on the top of the bath of molten zinc. The final cleaning occurs as the element being galvanized passes through this flux layer before entering the galvanizing bath.

The element to be coated is immersed in a bath of molten zinc maintained at a temperature of 435-460 ºC. Typical bath chemistry used in hot-dip galvanizing contains a minimum 98 % pure zinc along with a variety trace elements or alloy additions. These additions could include tin, aluminium, lead, nickel, and bismuth, can be made to the bath to enhance the appearance of the final product. The time of immersion in the bath varies depending on the thickness and the chemical composition of the steel being coated.

The presence of silicon at certain levels (0.1 - 0.4 wt%) in steel ("reactive" steels) can result in rapid alloy layer growth, producing a coating of excessive thickness. For the 0.06 wt. % Si steel, the coating is characterized by a thick and discontinuous ζ -phases for this reactive steel is similar to that which occurs in silicon-free steel that has been hot dipped at about 500 ºC in the regime of rapid reaction with zinc. This rapid growth also results in a dull coating appearance because the intermetallic phases reach the coating surface after withdrawal from the zinc melt. For the 0.38 wt% Si steel, the coating is also characterized by the thick and

discontinuous ζ layer and a layer consisting of η and δ phases. Like galvanizing of 0.1 wt. % Si steel, the discontinuity of the alloy layer is the basic cause for the rapid growth [73].

The addition of aluminium to molten zinc reduces the reactivity of steels containing silicon. In the early stages of dipping, a thin layer of 01 is formed but grows very slowly. After a certain time, outbursts of δ phase are formed; these later coalesce into a continuous layer. It can therefore be assumed that the delay in the formation of the ζ phase is responsible for the lower reaction rate when steel containing silicon is dipped in the Polygalva process. However, dipping time must be controlled very carefully, as the required coating thickness may not be obtained after normal dipping times. The addition of 0.06 wt. % Al also adds complexity to the galvanizing process because it causes the conventional zinc ammonium chloride flux to lose effectiveness.

Bonding between reinforcing bars and concrete is essential for reliable performance of concrete structures. The bond strengths for reinforcements in concrete are usually examined by either a pull-out test or a bending test [71]. Many factors, such as concrete mix and additives, curing conditions, and age, may affect the bonding between the galvanized steel and concrete. The bond strength of galvanized steel is similar to that of black steel. Particularly, for deformed rebars the bond strength for black steel and galvanized steel is essentially the same because the strength is mainly provided by the mechanical interlocking between the ridges of the deformed bars and the concrete. It has been noted that hydrogen evolution may occur during curing, resulting in a more porous interface between the galvanized steel and the concrete; this may affect the bond strength.

### *3.1.2 Organic and duplex coatings*

Coating of metal surface with organic materials is by far one of important methods for corrosion prevention. Organic coatings are conveniently applied as a liquid, primarily by brushing, rolling and spraying. The liquid consists of solvent, resin, and pigment. Organic coatings are classified according to the resin binder, which controls protectiveness and resistance to degradation.

The lifetime of organic coatings usually depends on the ability of the protective film to reduce the transport of corrosive species through it. During an organic coatings lifetime, the protective ability of the coating diminishes in the process known as aging. The protective coating then becomes permeable to water, and some ions. This enables corrosion reactions at the metal-coating interface. The rate of corrosion depends on the transport of corrosive species through the coating: water diffusion through the film and, its accumulation on the coating/metal-phase boundary (water uptake), ion diffusion and conduction through the protective film and finally through the nature of corrosion reactions. The main causes for the protective properties of organic coatings are the result of a barrier (reduction of the corrosive species transport through the film) and chemical (coating influence on the mechanism of corrosion reaction on the steel-coating interface) mechanism. The commercial qualities of protective coating systems often incorporate both mechanisms to achieve optimal protection of steel surfaces. The most important factors, which contribute to the barrier properties of the protective coating, are the type of resin (chemical composition of film), and the dry film thickness. The barrier properties of the coating can be improved by the use of leafy barrier pigments, such as aluminium or micaceous iron oxide, which lengthen the paths of the corrosive species through the film. The chemical influence of organic coatings, to the mechanism of the corrosion reaction, is the result of using active anticorrosive pigments [74].

Nowadays is huge number of studies are devoted to the use of anticorrosive systems. An anticorrosive coating system usually consists of multiple layers of different coatings with different properties and purposes. Depending on the required properties of the coating system, the individual coats can be metallic, inorganic, or organic. A typical anticorrosive system for highly corrosive marine environments usually consists of a primer, one or several intermediate coats, and a topcoat. The function of the primer is to protect the substrate from corrosion and ensure good adhesion to the substrate. For this reason, metallic zinc or inhibitive pigments are often formulated into coatings applied as primers for structures situated in the splash zone or in an atmospheric environment. The function of the intermediate coat is generally to build up the thickness of the coating system and impede transport of aggressive species to the substrate surface. The intermediate coat must also ensure good adhesion between the primer and the topcoat. The topcoat is exposed to the external environment and must provide the surface with the required colour and gloss [75].

The use of anticorrosive, e.g. duplex metallic/epoxy, systems has several advantages. The epoxy coating is able to provide a good barrier protection to rebar in concrete, but only if there is no obvious mechanical damages in the organic coating. Once the epoxy coating is damaged, the corrosion of steel rebar become seriously. The galvanized coating is able to provide cathodic protection to rebar, but it is too active in very strong alkaline environment to remain a long-term protection. While epoxy/zinc duplex coating provides the major protection for a construction in corrosive environment. Galvanized coating is able to supply an effective protection when the epoxy coating is suffered any mechanical damage, and the epoxy coating is helpful to last the galvanic protection of galvanized coating for steel [76-78].

Nevertheless, duplex systems have disadvantages and difficulties in operation marked by other authors, such as swelling, blistering and peeling of the epoxy layer as a result of roughness and irregularities of galvanized coating surface or not carefully carried out the zinc surface preparation prior to applying the epoxy layer [79-81].

## 3.2 Reinforcement surface treatments

Surface treatments are applied to new structures as a preventive measure, to existing structures where the need of future protection is anticipated.

To protect the galvanized steel reinforcement against corrosion during transportation and storage, a passivation treatment is generally adopted, such as hexavalent chromium-base passivation treatment. Several non-chromate passivation treatments have been developed such as phosphate-based, cerium-based, molybdate-based, and tungstate-based treatments. Unlike hexavalent chromium, they are less harmful to the environment and is an effective corrosion inhibitor for zinc [82]. Phosphate conversion coatings are used by industries as a surface pre-treatment of metals before painting, promoting the paint adherence and protecting the substrate against corrosion. This type of coating can be applied on steel, galvanized steel, iron, as well as on other metal materials [83].

Conversion coatings are protective surface layers on a metal that is produced in chemical reaction between the metal and a chemical solution. Examples of conversion coatings are phosphate, chromate, and black oxide. A conversion coating is growing into the part as it is designed but is also of bigger volume than the original element.

Conversion coating may be produced by several methods, which can be categorized mainly into two types, immersion and electroplating. The former comprises direct immersion, spraying, rolling, whilst the latter requires the use of impressed currents.

Chromate conversion coatings have received wide spread and have been used extensively. After immersion, different films have been considered to develop, including $Al_2O_3$ and $Cr_2O_3$; with the additional presence of $PO_4^{3-}$ species in the coating bath, $CrPO_4$ also develops. This type of immersion treatment, operating at temperatures up to 70º C, produces markedly different films from the variously hydrated aluminas formed in the first category.

In order to reduce contact of chromium compounds with environment, alternative conversion coating have been developed, such as zirconium or titanium conversion coating. The final corrosion resistance of the coatings is not considered to be equal to that of chromate coatings, limiting their widespread use. The most used chromate-free pre-treatments of galvanized steel in concrete are phosphate-containing and organic pre-treatments [18].

## 3.3 Corrosion inhibitors in concrete

Inhibitors are substances that react with, or precipitate at, the metal surface, thus significantly reducing the corrosion rate of metal. An ideal corrosion inhibitor not only prevents corrosion of reinforcing bars, but also has no adverse effect on the properties of concrete. The factors that could be affected by the inhibitor are: the rate of ingress of chlorides from the environment; the degree to which these chlorides are chemically bound or physically trapped in the concrete cover; the rate of ingress of dissolved oxygen to sustain the cathodic half-cell reaction; the electrical resistance of the concrete; and the chemical composition of the electrolyte (i.e., the cement paste pore solution) [84].

Some inhibitors act with precipitation of almost insoluble compounds at the metal surface (adsorption inhibitors). Other inhibitors act to passivate the surface of metal due to production of dense and adherent protective layers as a result of some corrosion of the metal surface. In this case corrosion can occur quite rapidly, but the rate of corrosion diminishes to very low levels once the passivating film has developed [1].

### *3.3.1 Anodic inhibitors*

Anodic inhibitors usually act by forming a protective oxide film on the surface of the metal causing a large anodic shift of the corrosion potential. This shift forces the metallic surface into the passivation region. They are also sometimes referred to as passivating agents. Chromates, nitrates, nitrites, molybdates are some examples of anodic inhibitors.

Chromates are oxidizing inhibitors whose action partly consists in an oxidation of corrosion products to less soluble form. In addition, these inhibitors form a constituent part of the passivating films, which contain chromates as well as chromium oxides. In aqueous solution, chromate and dichromate anions exist in a chemical equilibrium.

$$2\ CrO_4^{2-} + 2\ H^+ \Leftrightarrow Cr_2O_7^{2-} + H_2O \qquad (3.1)$$

The equilibrium depends on pH and the concentration of chromium. The chromate ion is the prevalent species in alkaline solutions, but dichromate can become the prevalent ion in acidic solutions.

Chromates are very effective inhibitors which afford good protection to many metals including steel and zinc [85]. However, due to its toxicity, its application is trying to cut and replaced by other environmentally friendly inhibitors. The inhibiting effect of chromate depends on the pH. Studies of chromium VI in acidic solution showed that passivating layer development on zinc in an acidic solution containing Cr VI was achieved by relatively fast impedance measurements in the pre-stationary state of the system [86].

Sodium molybdate, $Na_2MoO_4$, is a non-toxic, environment-friendly corrosion inhibitor. Like chromate, molybdate is classified as an anodic inhibitor. Inhibition by molybdate requires the presence of a definite concentration, depending on environment. However, dissimilar from chromate, the molybdate ion is non-oxidizing; its effective use requires the needs the presence of oxygen or other oxidizing agent.

Aramaki explored the inhibiting effect of molybdate on zinc in an aerated 0.5 M NaCl with $10^{-2} – 3 \cdot 10^{-2}$ M of sodium molybdate by means of polarization measurements. Molybdate ion was not markedly efficient inhibitor for zinc corrosion [31]. According to Panagopoulos et al. study the use of $Na_2MoO_4 \cdot 2H_2O$ as corrosion inhibitor significantly improved the corrosion resistance of zinc, as the absorption of $MoO_4^{2-}$ ions and subsequent formation of a molybdenum oxide film onto the surface of zinc hindered the corrosion process. Inhibition efficiencies above 90% can be obtained for sodium molybdate concentrations equal or higher than 0.05 M. Though the use of molybdate in the 0.01 M NaCl solution did not improve the corrosive behaviour of zinc, possibly due to the low adhesion of absorbed molybdenum oxide film onto the surface of zinc [33].

The study of Verbruggen et al. for steel in simulated pore concrete solution showed that molybdate concentration $10^{-4}$ M is not enough for complete counteract with the metal surface, nevertheless sodium molybdate is still able to inhibit partly — and does not increase corrosion — when it is present in low concentration. Inhibitor mechanism of molybdate observed in that study is that molybdate adsorbs on the already formed porous oxide layer and stabilizes it [29]. Shkirskiy et al. studied the effect of molybdate $10^{-2}$ M on hot-dip galvanized steel in 0.5 M NaCl at pH 4–13. In strong alkaline electrolyte (pH 13) no film was formed which on galvanized steel that correlates with low oxidizing capacity of Mo VI at this pH. In acid solutions (pH 4 and lower), the formed films were rich in Mo IV and their inhibition efficiencies were less than 30% [87]. To summarize, molybdate as a soluble inhibitor was reported to have a performance comparable to Cr VI on Al and Fe based substrates while its performance on Zn based substrates in neutral and acid electrolytes was lower than the performance of Cr VI. The mechanism of molybdate action at neutral and acid pH included the formation of Mo-rich protective film. The films with good performance were formed in the presence of phosphates which are known to affect the reactivity of Zn themselves.

Nitrite is one of the most commonly used anodic inhibitors and has, when applied according to the specifications together with high-quality concrete and sufficient cover, a long and proven protective effect. Calcium nitrite first saw use in Japan, where it was used at comparatively small doses to counter the salt present in sea sand used in construction of reinforced concrete. Sodium nitrite had been used for corrosion inhibition in non-concrete applications before, but the addition of such an alkali salt was not advantageous in concrete. In the presence of an alkali-metal salt admixture alkali-aggregate reactions become more prominent.

The first study of commercial calcium nitrite to be published detailed its ability to increase 28-day strength by over 6% for each per cent of calcium nitrite added (by weight of cement), starting with a large increase at the 24 h test. Its acceleration of initial set was more than 2 h at 2% addition, and final set was accelerated by more than 3 h.

Sodium nitrite ($NaNO_2$) is classified as an anodic inhibitor and requires a critical concentration for the protection of steel. At low concentrations, the nitrite may create imperfect passivity and subsequently the corrosion will be increased. The chloride concentration is equally important since when the chloride/nitrite ratio is high, the passivity effect is lost.

Calcium nitrite ($Ca(NO_2)_2$) acts as a moderate set accelerator of concrete and normally requires the additional use of water reducing and retarding admixtures.

Nitrite acts as passivator due to its oxidizing properties. The passive film formed in presence of nitrite is very thin and typically $2 \cdot 10^{-3}$ μm, and it is possibly formed through the adsorption of the nitrite ions followed by an oxidation step. All investigations reported in the literature revealed a critical concentration ratio (threshold value) between nitrite and chloride of about 0.6 (with some variations from 0.5 to 1) in order to prevent the onset of corrosion. This indicates that nitrite has to be in sufficiently high concentration in order to be effective. The delay in time to corrosion initiation is distributed around a mean value and depends on the inhibitor dosage. However, nitrite is not allowed to use in reinforced concrete structures permanently immersed in water for environmental and health reasons [41].

Fayala et al. studied the effect of sodium nitrite n the corrosion of galvanized steel and on mortar properties. The study showed that the corrosion was accelerated in mortar with 2 % sodium nitrite [17]. According to Ngala et al., nitrite causes partial reduction in the corrosion rate of moderately pre-corroding steel in non-carbonated concrete with modest levels of chloride contamination and in carbonated concrete without chloride. In the case of non-carbonated concrete with higher levels of chloride contamination and the inhibitor was ineffective [89]. In neutral and acid solutions $NaNO_2$ shows a limited inhibiting effect on the corrosion of steels in the propagation period when the chloride and proton concentrations is not very high; in case when the corrosion process is very developed, with high chloride and proton concentrations, $NaNO_2$ cannot reduce the corrosion levels [90]. In fact, the effect of nitrite in concrete depends on pH. The study of Garces et al. demonstrated that the presence of nitrites in quantities up to 0.1 M effects an important decrease in the corrosion rate of steels in solutions from pH 11 to 7. These solutions could be related to beginning of the corrosion process, when chlorides are increasing their concentration at the steel surface and therefore, the passive layer is becoming weaker, although pits are not yet developed. Increasing of concentration of nitrites up to 0.5 M provides a similar decrease in the corrosion rate of steels to that observed for nitrite concentration of 0.1 M in solutions with pH ranging from 11 to 9. For solution of pH 7, high concentration of nitrite causes increase of corrosion rate [91]. Okeniyi et al. make comparative study for nitrite and chromate in concrete exposed to sulphate and saline media, where $NaNO_2$ admixtures performed poorly inhibiting effect on steel-rebar corrosion in the acidic medium [92].

A major advantage to the use of calcium nitrite corrosion inhibitor is that the engineer can use rational procedures based on chloride exposure, concrete quality, and quantity of calcium nitrite to design for service life on the basis of expected chloride-to-nitrite ratios [25].

### *3.3.2 Adsorption inhibitors*

The most common adsorption inhibitors are the silicates and the phosphates. Protection efficiency of adsorption inhibitors strongly correlates with pH. Phosphates also need oxygen for effective inhibition. Silicates and phosphates do not afford the level of protection provided by chromates and nitrites, however, they are very useful in situations where eco-friendly admixtures are required. Sodium silicates act partly as alkalizers, partly as anodic inhibitors. Their inhibitor effect seems to be connected with colloidal anions, formed by hydrolysis. This anions probably migrate electrophoretically towards anode surfaces. As with phosphates, good protective films are formed only with given content of soluble calcium salts in solution.

Phosphates are one such alternative and are usually classified as non-oxidising anodic inhibitors effective only in the presence of oxygen or other oxidant. However, under certain conditions, phosphates may also act as cathodic inhibitors. The phosphate ions in solution react with metal ions released due to corrosion and precipitate a surface film. The quality of such a film defines the inhibition efficiency. Phosphates are classified as non-oxidising anodic inhibitors for zinc, although their action as cathodic inhibitors has also been reported. The mechanism by which phosphate acts is not totally understood but it is generally accepted that phosphate ions in solution react with metal cations released from the surface and precipitate a film with barrier properties at anodic areas. Enhanced cathodic inhibition may occur in the presence of $Ca^{2+}$ or $Zn^{2+}$ ions in solution, due to precipitation of calcium phosphate on the alkaline cathodic areas [93]. The addition of orthophosphates to solution raises alkalinity but also contributes in the formation of protective films, especially in presence of calcium-ions. These protective films seem to consist mainly of metal oxides and only a small proportion of phosphates.

Monofluorophosphate (MFP) has been used as a corrosion inhibitor for concrete reinforcements over the last 20 years. It is applied at the concrete surface in the form of an aqueous solution with a mass percentage ranging between 10% and 20%. The effectiveness of MFP, applied to the surface of a concrete structure, is based on both its diffusion into the concrete pore network and its action on steel reinforcement surface. Accordingly, the fundamental stage herein is the ease of access of MFP to the reinforcements. In early-age concrete, the penetration of an aqueous MFP solution is insufficient or impossible and, as a consequence, the $PO_3F^{2-}$ ions, which actually perform the inhibiting action, are not present in sufficient quantities within the interstitial solution to successfully inhibit corrosion. By forming apatites with Ca-containing compounds when the concrete has not been carbonated, $PO_3F^{2-}$ ions are trapped but reaction products may accumulate in some parts of the porous network, thus blocking the penetration of aggressive species. In a carbonated concrete, aqueous MFP solutions are better able to penetrate. MFP penetration should occur by means of a pure diffusion process whenever the concrete is saturated. Other types of penetrations could also arise depending on the amount of water in the concrete pore network [94]. Though the study of Ngala et al. showed low effectiveness of MFP on the corrosion protection of steel in both non-carbonated and carbonated concretes under the conditions studied [95]. Other authors declare good inhibiting effect of monofluorophosphate [41]. Laboratory studies of steel in mortar showed that by applying several intense flushing before ingress of chlorides, the onset of corrosion during the test duration of 90 days could be prevented ceevn at chloride concentrations about 2 % to the weight of cement. A critical concentration ratio MFP/chloride greater than 1 had to be achieved, otherwise the reduction in corrosion rate was not significant. The inhibition mechanism of the MFP is not clear, it may be anodic, cathodic or mixed. $Na_2PO_3F$ hydrolyses in aqueous and neutral media to form orthophosphate and fluoride. The inhibiting action of $Na_2PO_3F$ may be attributed to the formation of phosphates, and so the anodic formation of a passive layer of $Fe_3O_4$, $\gamma Fe_2O_3$ and $FePO_4 \cdot H_2O$. However, as $PO_3F^{2-}$ , $PO_4^{3-}$ and $OH^-$ are all potential corrosion inhibitors, it is difficult to say which, if any, of these ions may be responsible for corrosion inhibition effects induced by MFP [96].

### *3.3.3 Organic inhibitor*

Organic compounds used as inhibitors, occasionally, they act as cathodic, anodic or together, as cathodic and anodic inhibitors, nevertheless, as a general rule, act through a process of surface adsorption, designated as a film-forming. Naturally, the occurrence of molecules exhibiting a strong affinity for metal surfaces compounds showing good inhibition efficiency and low environmental risk. These inhibitors build up a protective hydrophobic film adsorbed molecules on the metal surface, which provides a barrier to the dissolution of the metal in the electrolyte. They must be soluble or dispersible in the medium surrounding the metal [97].

The efficiency of an organic inhibitor depends of the:

- chemical structure, like the size of the organic molecule;
- aromaticity and/or conjugated bonding, as the carbon chain length;
- type and number of bonding atoms or groups in the molecule (either π or σ);
- nature and the charges of the metal surface of adsorption mode like bonding strength to metal substrate;
- ability for a layer to become compact or cross-linked,
- capability to form a complex with the atom as a solid within the metal lattice;
- type of the electrolyte solution like adequate solubility in the environment.

The efficiency of these organic corrosion inhibitors is related to the presence of polar functional groups with S, O or N atoms in the molecule, heterocyclic compounds and pi electrons, generally have hydrophilic or hydrophobic parts ionisable. The polar function is usually regarded as the reaction centre for the establishment of the adsorption process. The organic acid inhibitor that contains oxygen, nitrogen and/or sulphur is adsorbed on the metallic surface blocking the active corrosion sites. Although the most effective and efficient organic inhibitors are compounds that have π-bonds, it present biological toxicity and environmental harmful characteristics. Due to the metal surface covered is proportional to the inhibitor concentrates, the concentrations of the inhibitor in the medium is critical. Some examples are amines, urea, mercaptobenzothiazole (MBT), benzotriazole e toliotriazol, aldehydes, heterocyclic nitrogen compounds, sulphur-containing compounds and acetylenic compounds and also ascorbic acid, succinic acid, tryptamine, caffeine and extracts of natural substances.

Since about 25 years a group of organic molecules, especially alkanolamines and amines and their salts with organic and inorganic acids are used as components in corrosion inhibitor blends. Several studies indicate the the blends are effective in solutions whereas pure solvents as dimethylethanolamine are not [41]. The adsorption of amines depends on the strength of the bond amine-metal and on the solubility of amine. The strength of the amine-metal bond is due to the high density of electrons of the nitrogen atom and the capacity of these electrons to form coordinate bonds.

Inhibitors containing sulphur are usually more effective than nitrogen compounds since sulphur is a still better electron donor than nitrogen, thus it has a greater tendency to form coordinate bonds, leading to adsorption.

Aminoalcohols such as ethanolamine and dimethylethanolamine control corrosion by attacking cathodic activity, blocking sites where oxygen picks up electrons and is reduced to hydroxyl ion. They may adsorb at anodic sites as well. N,N-dimethylethanolamine (DMEA) is used to protect rebar in concrete in commercial corrosion inhibitors. X-ray photoelectron spectroscopy was used to examine steel surfaces which were first cut, polished and oxidized

and then immersed in solutions of sodium chloride and DMEA. Electrons ejected from the *1s* levels of carbon, nitrogen and oxygen, and from the *2p* levels of iron and chlorine, were analysed to estimate surface concentrations of these species. Below 1 M (about 9% by weight), DMEA adsorbed on the steel oxide surface in slightly more than monolayer thickness (between 0.75 and 0.9 nm). Higher concentrations (>2 M) cause more adsorption, but only up to a bilayer thickness. DMEA is strongly and irreversibly adsorbed and cannot be completely rinsed off the iron oxide surface. Immersion of steel in solutions containing both DMEA and NaCl for 5 min was sufficient to reach equilibrium; DMEA was found to partially displace chloride from the iron oxide surface. These observations suggest that inhibition of corrosion occurs through a mechanism whereby DMEA displaces chloride ion and forms a durable passivating film. In this view, although the aminoalcohols adsorb on non-corroding sites which may seem more cathodic than anodic, they can just as easily be said to adsorb on potentially anodic sites [88].

Diethanolamine (DEA) improves the corrosion resistance of galvanized rebars in concrete, decrease of the total porosity of concrete according to results obtained by Fayala et al. [17].

Benzoic acid in the form of sodium benzoate has proved to be one of the most suitable organic acid for corrosion inhibition. Benzoate is not an oxidizer. In accordance with its character of anion, it is usually classed among the anodic inhibitors. Despite this, it is not considered as dangerous, since too small concentration has detrimental effect. However, relatively high concentrations of this inhibitor are necessary to obtain substantial effect.

The effects of sodium benzoate (NaBz), sodium N-dodecanoylsarcosinate (NaDS), sodium S-octyl-3-thiopropionate (NaOTP), 8-quinolinol (8-QOH) and 1,2,3-benzotriazole (BTAH) on corrosion of zinc in an aerated 0.5 M NaCl solution were investigated by Aramaki. These inhibitors formed precipitate films of zinc (II) salts or complexes on the zinc surface together with zinc hydroxide and oxide to prevent corrosion in the solution. High inhibition efficiencies of NaOTP were acquired at concentrations $c = 1 \cdot 10^{-6}$ - $3 \cdot 10^{-5}$ M, BTAH at $c = 1 \cdot 10^{-4}$ - $1 \cdot 10^{-3}$ M, 8-QOH at $c = 1 \cdot 10^{-3}$ - $3 \cdot 10^{-3}$ M and NaBz at $c = 3 \cdot 10^{-3} \pm 1 \cdot 10^{-2}$ M. NaOTP formed a protective film composed of zinc hydroxide and oxide and a small quantity of the $Zn^{2+}$ chelate compound with $OTP^-$, $[Zn(OTP)_2]$. BTAH formed a film of the complex polymer, $[Zn(BTA)_2]_n$ on the zinc surface, and showed high inhibition efficiencies. 8-QOH was also effective on zinc corrosion in 0.5 M NaCl by forming a film of yellow chelate, $[Zn(8\text{-}QO)_2] \cdot 2H_2O$ on the zinc surface. NaBz formed a thick film of zinc hydroxide and salt or complex of $Bz^-$ on the surface. NaDS did not markedly suppress zinc corrosion in 0.5 M NaCl [98].

Benzotriazole (BTAH) showed his efficiency on zinc and copper-zinc alloy in chloride solution. The surface layers formed on alloys in BTAH-inhibited solution comprised both polymer and oxide components, namely Cu(I)BTA and Zn(II)BTA polymers and $Cu_2O$ and ZnO oxides [99]. The inhibiting effect of BTAH was also proved for corrosion protection of galvanized steel cut edges in sodium chloride solution. The inhibition involves a change of rate control, from cathodic diffusion control to activation control at both metals, due to the formation of a surface film on both steel and zinc, which causes anodic polarization on both materials, particularly on zinc. The film, which grows very fast on zinc in the cut edge, undergoes local dissolution and re-healing events [100].

Polyethylene glycol (PEG), with a molecular weight of 600, and polyoxyethylen alkyl phosphate ester acid form (GAFAC RA600) were studied as inhibitors of zinc in strong alkaline solutions. The optimal concentrations of the organic inhibitors studies were found to be in

the range of 2000 ppm. The electrochemical studies point out that the inhibition properties of PEG, in the strong alkaline solution, are by far much more efficient than the inhibition capability of GAFAC RA600 [101].

Volatile Corrosion Inhibitors (VCI), also called Vapour Phase Inhibitors (VPI), are compounds transported in a closed environment to the site of corrosion by volatilization from a source. In boilers, volatile basic compounds, such as morpholine or hydrazine, are transported with steam to prevent corrosion in the condenser tubes by neutralizing acidic carbon dioxide or by shifting surface pH towards less acidic and corrosive values. In closed vapor spaces, such as shipping containers, volatile solids such as salts of dicyclo-hexylamine, cyclohexylamine and hexamethyleneamine are used. When these inhibitors are exposed to the metal surface, the vapour of these salts condenses and is hydrolysed by any moisture to liberate protective ions. It is desirable, for an efficient VCI, to provide inhibition rapidly while lasting for long periods. Both qualities depend on the volatility of these compounds; fast action wanting high volatility while enduring protection requires low volatility.

Various organic inhibitors have been studied for inhibition of zinc and galvanized steel corrosion in neutral, weak acid and alkaline solutions. They are, for example, 2-quinolinecarboxylic acid, 8-quinolinol (8-QOH), salicyl alcohol, mercaptobenzothiazole, mercaptobenzoxazole, benzotriazole, 3-amino-5-heptyl-1,2,4-triazole, polythioglycolates and 2-hydrazone-3-bornane-methylenedithiol. Most of these inhibitors suppress zinc corrosion by covering the surface with layers of their complex or chelate precipitates with $Zn^{2+}$. Most of these compounds are mildly or moderately toxic, being considered to be environmentally acceptable in uses for surface treatments.

# PART II

# Experimental

# 4 General description of experimental design

The second part of the thesis contains full description of experimental design developed for the present study.

The study was performed in two different environments: concrete and saturated solution of calcium hydroxide. Comparison of the corrosion behaviour of galvanized steel in concrete prepared with different types of Portland cement: white and grey, was made in the presence of several inhibitors. Potential monitoring was performed for galvanized steel bars embedded in concrete cubic specimens, while galvanized steel sheets were applied for specimens of the same structure when potential monitoring was followed by EDX-analysis and SEM-observation.

For a clear understanding of the passivation mechanism a series of experiments was carried out in $Ca(OH)_2$ saturated solution simulating the alkaline pore fluid of concrete. Both galvanized steel sheets and pure zinc discs were used as samples because pure zinc replicates the $\eta$ phase present on the upper layer of galvanized steel. Potential monitoring was performed in all tests; electrochemical impedance measurements were made if a tested inhibitor showed good results and relative efficiency. Certain samples were also analysed with SEM and EDX techniques.

The research was logically divided into two parts in terms of selection and evaluation of corrosion inhibitors. The first part was devoted to thorough investigation of inhibiting effect of chromate and identification of passivation mechanism of galvanized steel in concrete in presence of chromium VI, followed by the clarifying tests in $Ca(OH)_2$ saturated solution. The second part contained approbation of other inhibitors - whether inorganic or organic – and consisted of preliminary experiments in $Ca(OH)_2$ saturated solution and the main experiment in concrete environment. For the second part the following substances were chosen for the experiments in $Ca(OH)_2$ saturated solution on the base of literature review: chromate, nitrite, molybdate and diethanolamine (see Chapter 3).

The study on the oxygen effect on the passivation process was carried out with a series of additional experiments in $Ca(OH)_2$ saturated solution with pure zinc and galvanized steel samples in the presence of chromate or permanganate as the oxidant. Potential monitoring, EIS analysis were performed before and after continuous bubbling of nitrogen gas through electrochemical cell solution in order to relate corrosion behaviour to the degree of aeration.

Detailed description of the sample preparation procedure, materials and methods used for the experimentation are given below in the following chapters

.

# 5 Tests performed in concrete

## 5.1 Preparation of the concrete specimens

For the tests performed in concrete, cubic specimens with an edge length of 100 mm were manufactured with the concrete mix-design given in Table 5-1. Three different types of cement were used for concrete preparation:

– CEM I 52.5 R, grey ordinary Portland cement (OPC) without reducing agents;
– CEM I 52.5 R, grey ordinary Portland cement (OPC) with $FeSO_4$ admixture;
– CEM I 52.5 R, white ordinary Portland cement (WOPC).

The chemical composition of cements used is reported in Table 5-2, components' appearance is shown in Figure 5-1.

Table 5-1. Concrete mix-design

| Material | Type | Content* kg/m³ |
|---|---|---|
| Cement | OPC/WOPC | 420 |
| Water | Tap | 230 |
| Sand | $D_{max}$ = 6 mm | 920 |
| Medium aggregate | $D_{max}$ = 12 mm | 640 |

* Saturated surface dry condition, w/c = 0.6

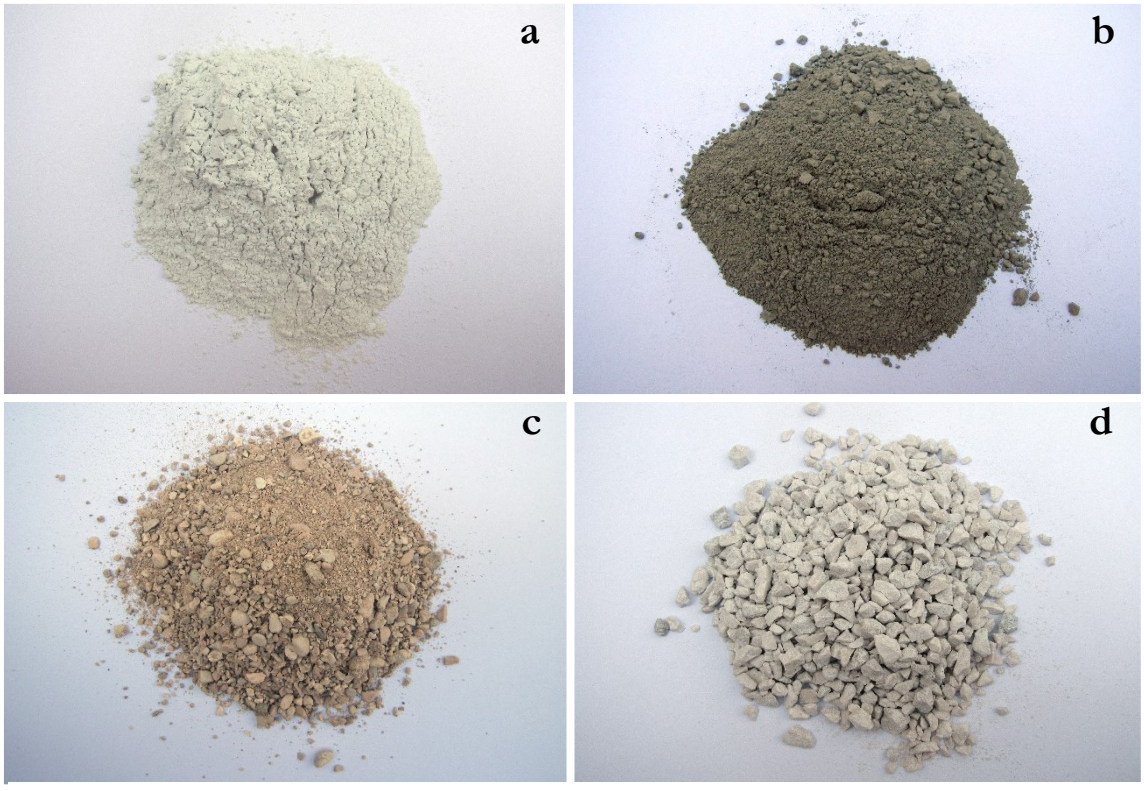


Figure 5-1. Concrete mix components: *a* – WOPC, *b* – OPC, *c* – sand, *d* – medium aggregate

Table 5-2. Chemical composition of cements*

| Type | LOI % | $SiO_2$ % | $Al_2O_3$ % | $Fe_2O_3$ % | CaO % | MgO % | $SO_3$ % | $Na_2O$ % | $K_2O$ % | IR % | Cr VI ppm** | pH |
|---|---|---|---|---|---|---|---|---|---|---|---|---|
| WOPC | 2.4 | 22.2 | 3.2 | 0.2 | 65.7 | 1.0 | 3.7 | 0.14 | 0.87 | 0.3 | <2 | 13.03 |
| OPC | 1.8 | 21.9 | 3.3 | 5.1 | 62.5 | 2.7 | 2.1 | 0.30 | 0.40 | 0.9 | 11 | 13.17 |

* LOI – loss on ignition, IR – insoluble residue

** Water-soluble hexavalent chromium content on the total dry weight of the cement

Note – Cr VI amount indicated for OPC is total: reduced and unreduced

Each specimen was reinforced with two or three galvanized steel bars, 130 mm long and 8 mm in diameter, positioned in order to have a concrete cover of 15 mm (Fig. 5-2). Several concrete specimens were also provided with galvanized steel sheets 100 x 25 x 1 mm for the post exposure characterization of the passivating layer by means of X-ray diffractometry.

Before galvanizing bars and sheets were degreased by immersion in 15% solution of NaOH for 30 minutes and pickled by immersion in 15 % solution of HCl for another 30 minutes. Then a flux of zinc ammonium chloride was applied to them, followed by drying in an oven at 120 °C for 10 minutes. After pre-treatment bars were hot-dip galvanized in a pure zinc bath at 444 ± 1 °C for 5 minutes. The thickness of the coating obtained on bars was 240 ± 10 μm with the external η-layer of pure zinc about 75 μm thick, the coating obtained on sheets was 55 ± 5 μm with the external η-layer of pure zinc about 10 μm thick. Figures 5-3 and 5-4 show the microstructure of the coating obtained on the surface of steel bars and steel sheets, respectively. The ends of rebars were covered with bicomponent epoxy resin (Fig. 5-5). The reference electrode was placed in fresh concrete equidistant from the embedded bars at the centre of the top of each specimen.

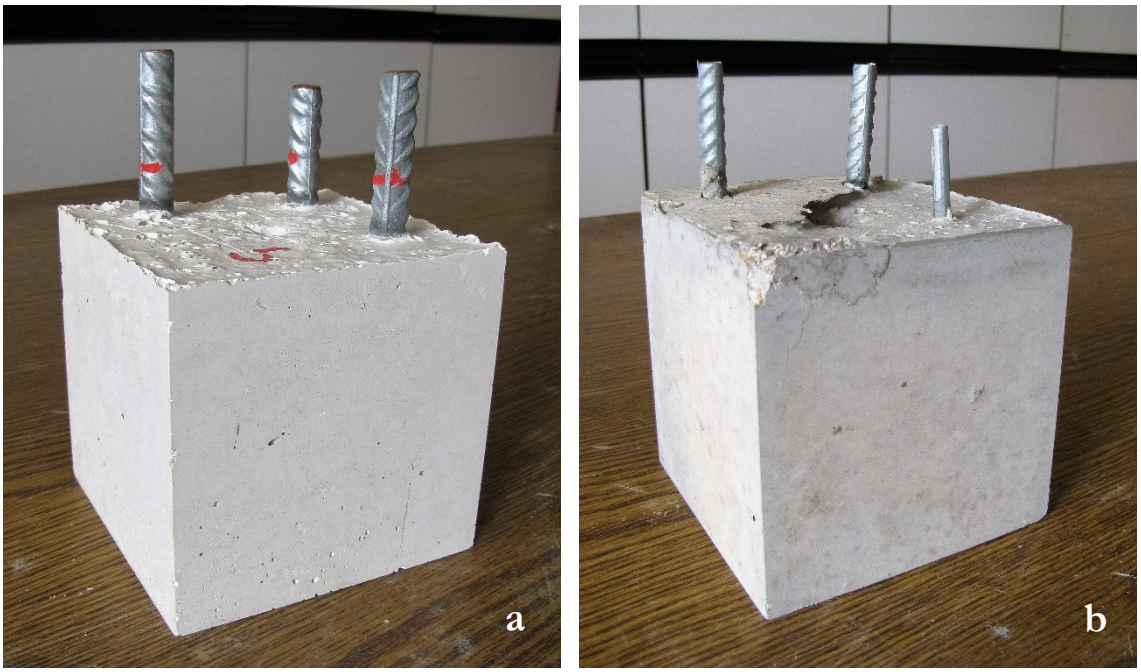


Figure 5-2. Concrete specimens produced from white (*a*) and grey (*b*) cement, withdrawn from molds

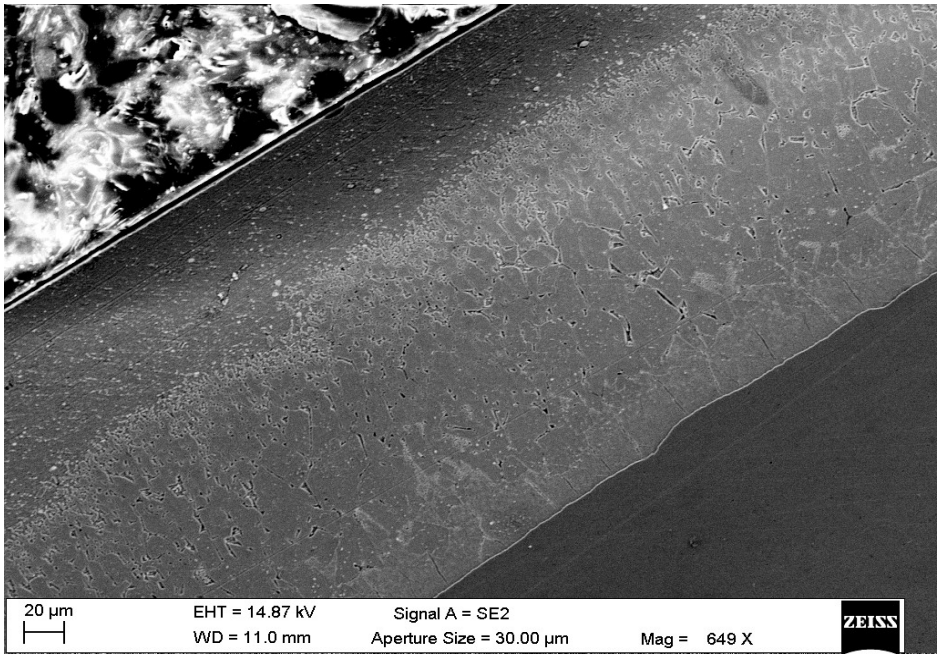


Figure 5-3. SEM image of cross-sectional area of the hot-dip galvanized coating on the steel bar

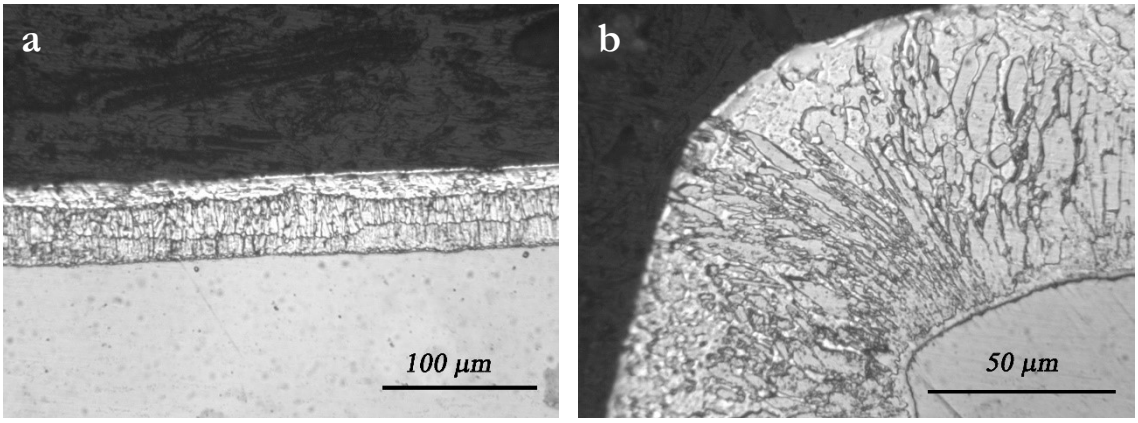


Figure 5-4. Microstructure of the galvanized coating on the steel sheet: working surface, original magnification x 20 (*a*) and corner protection, original magnification x 50 (*b*)

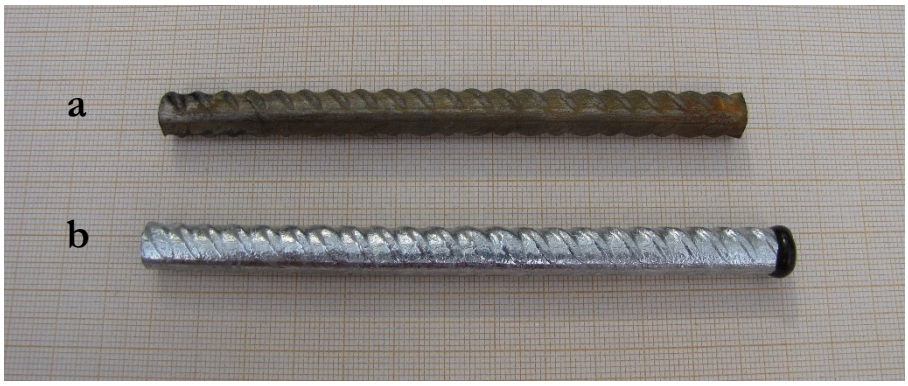


Figure 5-5. Steel bar samples: before (*a*) and after (*b*) galvanization

## 5.2 Addition of inhibitors to the concrete specimens

First preliminary tests with galvanized bars in concrete specimens produced with three different types of cement were performed without additions of inhibitors. Then several series of experiments in concrete with additions of inhibitors were made.

### *5.2.1 Addition of chromium VI*

For the study of relation between corrosion behaviour of galvanized steel and amount of Cr VI in concrete mix, six cubic specimens with white cement were produced as described above. Different amount of $K_2Cr_2O_7$ was added to each specimen to obtain concentrations of Cr VI from 0 to 15 ppm on the total dry weight of the cement. Table 5-3 contains information on the amounts of $K_2Cr_2O_7$ used in each concrete mix.

In order to study changes induced by the immersion in concrete on the coating surface some experiments were performed using galvanized sheets instead of the bars. For that, three concrete specimens were produced with white Portland cement as described above. Certain amount of $K_2Cr_2O_7$ was added to concrete mix to obtain concentration of Cr VI 15 ppm on the total dry weight of the cement (Tab. 5-3). Two galvanized steel sheets were embedded in each concrete specimen. Steel sheets were used instead of steel bars in this experiment for the convenience of further observations by SEM, EDX and RDX analysis. Immediately after embedding of galvanized steel sheets in concrete, potential monitoring started. Then, after a certain time one of the specimens was demolished and the two sheets were removed for SEM, EDX and RDX analysis. For the other samples potential monitoring continued until the next time point. The first specimen was destroyed after 3 hours, the second – after 12 hours, and the last – after 25 hours.

Table 5-3. $K_2Cr_2O_7$ mass needed to produce 1 $m^3$ of concrete with given concentration of Cr VI

| Cr VI ppm on the total dry weight of cement | 0 | 3 | 6 | 9 | 12 | 15 |
|---|---|---|---|---|---|---|
| $K_2Cr_2O_7$ g/$m^3$ of concrete | 0 | 3.57 | 7.13 | 10.70 | 14.26 | 17.83 |

### *5.2.2 Additions of peroxide and nitrite*

Concrete specimens were produced with white Portland cement and grey Portland cement with $FeSO_4$ additive using the above mix design (Tab. 5-1) Certain amount of $H_2O_2$ and $NaNO_2$ was added to a concrete mix to obtain the concentration indicated in the Table 5-4. Each specimen was reinforced with two galvanized steel bars and one rod of pure zinc. The appropriateness of replacing one of three galvanized bars in the specimen with a zinc rod consisted in the need to compare corrosion behaviour of galvanized steel and pure zinc in concrete. Theoretically, pure zinc simulates η-phase present on the upper layer of galvanized steel. Thus, comparability of results, along with the previous microscope observation (Fig. 5-3), could revalidate the quality of galvanized coating and, thereby, allow to use pure zinc samples instead of galvanized steel ones in further tests with $Ca(OH)_2$ saturated solution.

Steel bars were pre-treated and galvanized according the procedure described above, the characteristics of the coating obtained were similar to the ones previously stated.

In order to study changes induced by the immersion in concrete on the coating surface another experiment was performed using galvanized sheets instead of the bars. For that, two

concrete specimens were produced with grey Portland cement with $FeSO_4$ additive as described above. Certain amount of $NaNO_2$ was added to concrete mix to obtain concentration of 3% and 6 % of nitrite on the total dry weight of the cement. One galvanized steel sheet was embedded in each concrete specimen. As for the experiments described previously, steel sheets were used instead of the bars for the convenience of further observations by SEM, EDX and RDX analysis. Immediately after embedding of galvanized steel sheets in concrete, potential monitoring started. Specimens were demolished and sheets were removed after 1 week from the concrete pouring.

Table 5-4. Additions of oxidants in concrete specimens tested

| Oxidant | Concentration by the total dry weight of cement | | |
|---|---|---|---|
| $NaNO_2$ | 3 % | 6 % | 10 % |
| $H_2O_2$ | 1,2 % | 2,4 % | - |

### *5.2.3 Additions of diethanolamine and molybdate*

Concrete specimens were produced with white Portland cement and grey Portland cement with $FeSO_4$ additive using the above mix design (Tab. 5-1). Certain amounts of diethanolamine and sodium molybdate were added to a concrete mix to obtain the concentration indicated in the Table 5-5. Specimens manufactured with white concrete were reinforced with two galvanized steel bars, specimens manufactured with grey concrete were reinforced with two galvanized steel bars and one galvanized steel sheet. Sheets were used in the experiment for the convenience of further observations by SEM, EDX and RDX analysis.

Immediately after embedding of galvanized steel samples in concrete, potential monitoring started. After 1 week from the concrete pouring, the concrete specimens were broken mechanically at the metal–cement paste interface and the galvanized steel sheets were submitted to SEM, EDX and RDX analysis.

Table 5-5. Concrete specimens with additions of inhibitors

| Specimen type | Sample label* | Concentration on the dry weight of cement |
|---|---|---|
| *Specimens with white concrete* | | |
| Specimen with DEA | BB(T1, T2) | 8.3 mL/kg |
| *Specimens with grey concrete* | | |
| Control specimen | G(T1, T2, L) | - |
| Specimen with DEA | GB(T1, T2, L) | 8.3 mL/kg |
| Specimen with $MoO_4^{2-}$ | BC(T1, T2, L) | 0.1 mM |

* T – galvanized steel bar, L – galvanized steel sheet

## 5.3 Methods and techniques of experimental investigation in concrete

Immediately after immersion of galvanized steel samples, bars and sheets, potential monitoring started for each concrete specimen (Fig.5-6). Corrosion potential of the galvanized steel samples was measured continuously, using the Agilent acquisition system mod. 34970A (multiplexer mod. 34901). Silver-silver chloride electrode (E = +0.197 vs. NHE) and copper-copper sulphate electrode (E = +0.316 vs. NHE) were used as reference. For the convenience of presentation, all data were recalculated respect to saturated calomel electrode (E = +0.241 vs. NHE).

Visual observation of demolished specimens and removed bars was made to reveal the surface changes and gaseous hydrogen evolution marks on the concrete/bar interface. To study the changes in the passivating layer on the surface of galvanized steel sheets scanning electron microscopic, energy-dispersive X-ray spectroscopic and X-ray diffraction analysis were utilized. SEM observations, EDX and XRD analysis were performed by means of a Zeiss Supra 40 microscope, Bruker's Quantax series 5000 L device and Philips PW 1730 diffractometer with Cu Kα radiation (λ=0.154 nm), respectively.

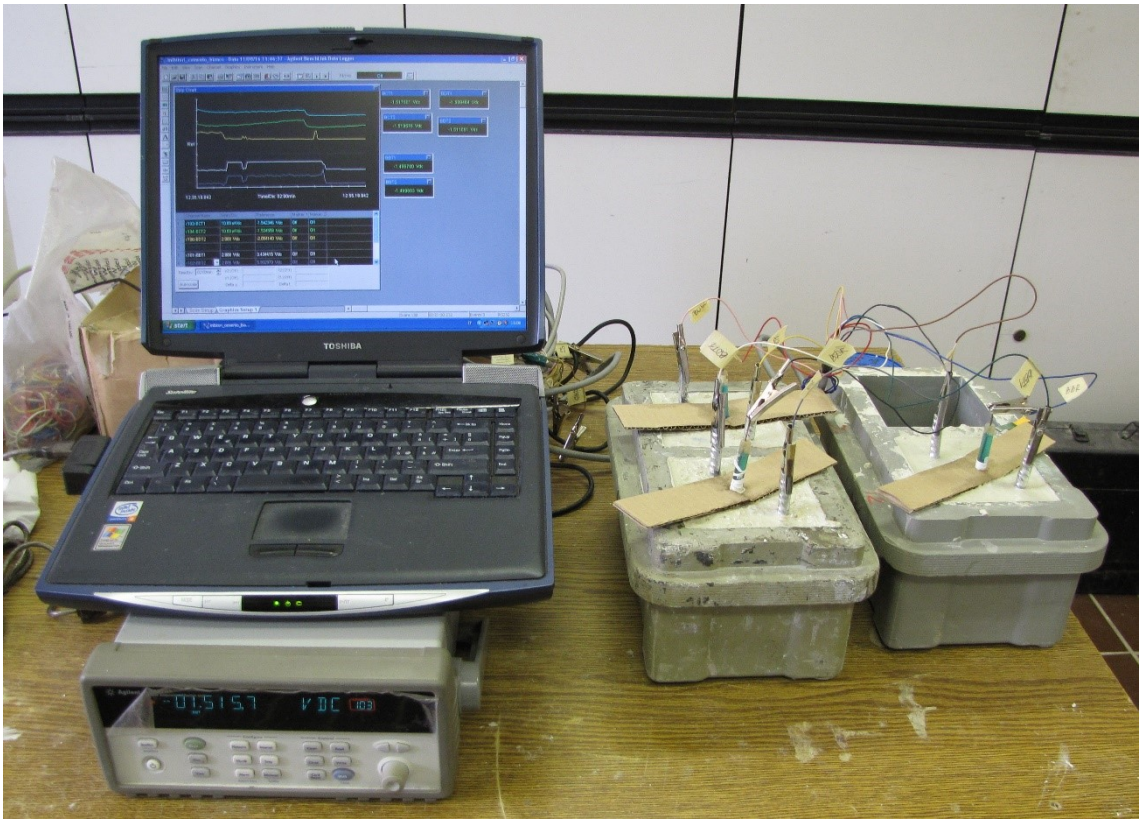


Figure 5-6. Potential monitoring of galvanized steel samples embedded in concrete by means of Agilent acquisition system

# 6 Tests performed in simulated concrete pore solution

## 6.1 Preparation of samples and solutions

To simulate concrete pore solution the saturated calcium hydroxide solution was prepared by stirring calcium hydroxide 2 g $Ca(OH)_2$ in 1 L of distilled water. Two types of samples were used in the series of experiments in solution:

- Commercial grade (pure, 98%) zinc plates (30 mm diameter, 1 mm thick) were inserted inside hard-rock type epoxy resin curable at room temperature to form a sample. After resin solidification samples were polished with emery paper by decreasing the grade to 1200 mesh. The border between zinc plate and epoxy resin was shielded with bicomponent epoxy resin glue. Then samples were used working electrodes with a surface of about 3.80 $cm^2$ exposed to the test solution (Fig. 6-1a);
- Galvanized steel sheets were shielded with epoxy resin to obtain a working exposed surface of about 3.50 $cm^2$. The electric contact was obtained by tin soldering a conductive wire with the sheet; this contact was masked by an epoxy resin. Before the explosion to the test solution, samples were degreased with acetone and rinsed with distilled water (Fig. 6-1b).

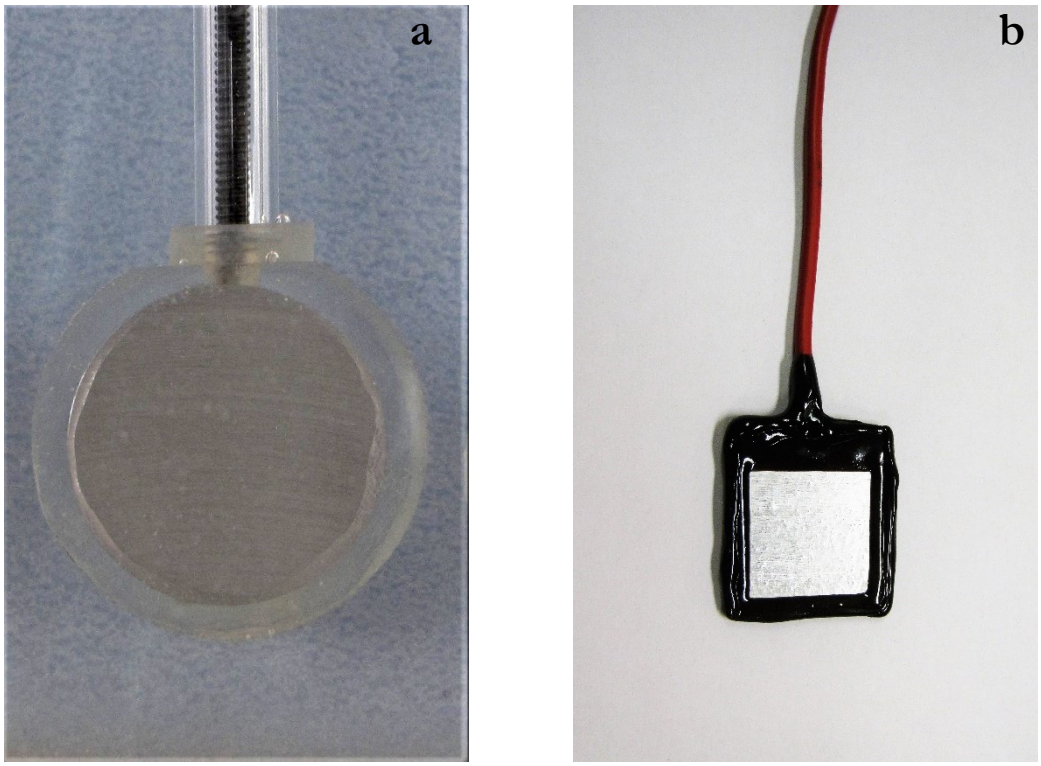


Figure 6-1. Pure zinc (a) and galvanized steel (b) samples for tests in solution

## 6.2 Additions of inhibitors in solution

First preliminary tests with galvanized steel sheets and pure zinc plates in saturated calcium hydroxide solution without additions of inhibitors were performed. Then several series of experiments in $Ca(OH)_2$ saturated solution with additions of inhibitors were carried out.

### *6.2.1 Additions of chromium VI*

*Test 1: Preliminary.* Initial test in saturated calcium hydroxide solution with addition of chromium VI consisted in potential monitoring of zinc samples in $Ca(OH)_2$ saturated solution by using a three electrode cell. After one hour of immersion of sample in solution, 70 μl of 0.05M $K_2Cr_2O_7$ solution were added to the solution every 5 minutes until the passivation of zinc occurred. The test was repeated several times to calculated an average amount of additions of 0.05M $K_2Cr_2O_7$ solution needed to obtain the zinc passivation.

*Test 2: Influence of oxidant concentration.* The second test included potential monitoring of zinc samples immersed in $Ca(OH)_2$ saturated solutions with different concentration of chromium VI. Different amount of $K_2Cr_2O_7$ was added to the solution to obtain concentrations of Cr VI from 0 to 6.2 ppm. After potential monitoring some samples from the series were analyzed by means of SEM-EDX analyses.

*Test 3: Passive layer formation.* A series of experiments in $Ca(OH)_2$ saturated solution was made to investigate the mechanism of zinc passivation. For the experiment 3 samples of pure zinc, SCE reference electrode and Pt counter electrode were used. The program of the experiments included continuous potential monitoring and EIS measurements after 30 min, 3 h, 7.5 h and 24 h from the instant of zinc immersion in the solution. These experiments were repeated in solutions without addition of Cr VI and with different Cr VI additions (1.6 ppm, 2.3 ppm, 3.1 ppm and 6.2 ppm).

*Test 4: Effect of dilution.* In another experiment corrosion potential of galvanized steel was measured in $Ca(OH)_2$ saturated solution on changing Cr VI concentration. Corrosion potential was registered continuously, whereas impedance and potentiodynamic polarization measurements were carried out at regular intervals. Galvanized steel sample was immersed in Cr VI free solution; then 6.2 ppm Cr VI was added and then concentration of Cr VI was decreasing by dilution of working solution with $Ca(OH)_2$ saturated solution until it reached 0.6 ppm.

*Test 5: Oxygen effect on the passivation process.* The study on the oxygen effect on the passivation process was carried out with a series of additional experiments in $Ca(OH)_2$ saturated solution by using pure zinc and galvanized steel samples in the presence of chromate as oxidant. Experiment included two types of test. During the test of first type, the calcium saturated solution was bubbled with nitrogen gas for one hour to deaerate it. After bubbling a portion of 0.05 M $K_2Cr_2O_7$ solution was added to obtain 6.2 ppm Cr VI concentration; then a sample was immersed in the deaerated solution with chromium VI addition and potential monitoring started. During the test of second type, a sample was immersed in the $Ca(OH)_2$ saturated solution; then the addition of Cr VI was made and deaeration with $N_2$ bubbling initiated. Impedance and potentiodynamic polarization measurements were carried out for several samples in this series of experiments.

### *6.2.2 Addition of other inhibitors*

Experiments in Ca(OH)2 saturated solution with addition of inhibitors other than hexavalent chromium were performed with the use of galvanized steel samples (Fig. 6-1b) Initially each the sample was immersed in beaker with calcium hydroxide saturates solution. After activation of galvanized steel sample occurred, it was moved to another vessel containing Ca(OH)2 saturated solution with admixture of a certain inhibitor. Immediately after immersion potential monitoring started. After 30 minutes the first impedance measurement was done and was repeated every 2 hours alternating with potential monitoring.

Three substances were studied in the present experiment: sodium nitrite, sodium molybdate and diethanolamine. Table 6-1 contains the concentrations of inhibitors used in Ca(OH)2 saturated solution.

Table 6-1. Concentration of inhibitors in $Ca(OH)_2$ saturated solution

| Inhibitor | Concentration |
|---|---|
| Nitrite $NO_2^-$ | 3 wt% |
| Molybdate $MoO_4^{2-}$ | 0.01 M |
| Diethanolamine DEA | 3.5 L/m$^3$ |

## 6.3 Methods and techniques of experimental investigation in solution

Corrosion potential of the galvanized steel sheet, with an exposed area of 3.5 cm$^2$, or pure zinc plate, with an exposed area of 3.8 cm$^2$, acting as working electrode was measured continuously, using the Agilent acquisition system mod. 34970A (multiplexer mod. 34901) with a saturated calomel electrode (E = +0.241 vs. NHE) as reference and a platinum electrode as a counter.

Electrochemical impedance (EIS) measurements were performed by means of a Gamry Instruments Reference 600 potentiostat. The tests were performed at 25±1 °C using a three-electrode-cell (Fig. 6-2). Impedance measurements were performed in potentiostatic configuration. The amplitude and the frequency range for AC signal were respectively 5 mV rms and 100kHz-10mHz. For this range, 5 measurements per decade were done.

The analysis of the corrosion products was performed on samples removed from the solution after different immersion time, washed accurately with bi-distilled water and dried with cold air to avoid the signal of the compounds formed in the solution.

XRD analysis was performed by means of a Philips PW 1730 X-Ray diffractometer, using Cu Kα (λ=0.154 nm) radiation. Scanning electron microscopy (SEM) observations were performed using a Zeiss Supra 40 microscope and EDX analysis were obtained by means of a Bruker's Quantax series 5000 L device.

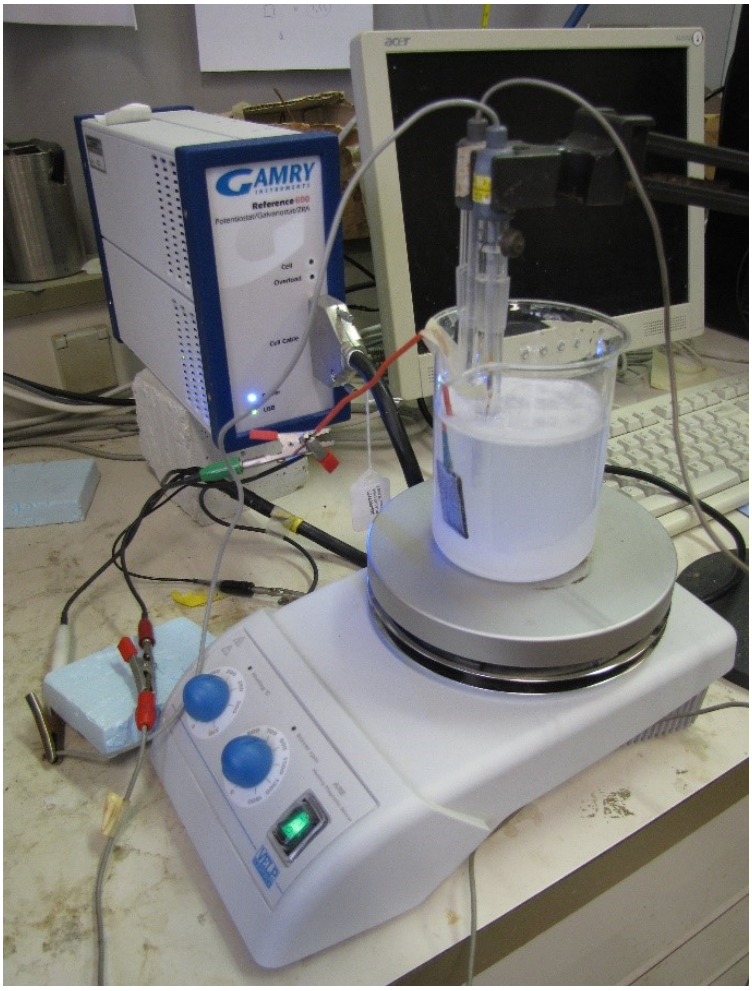


Figure 6-2. Three-electrode electrochemical cell used for the EIS measurements

# 7 Results and Discussions

## 7.1 Tests with additions of chromium VI

### *7.1.1 Potential monitoring of galvanized rebars in concrete specimens*

As a preliminary test the study of galvanized steel corrosion behaviour in different types of cement was performed. Figure 7-1 shows corrosion potential change in time of three groups of three different galvanized bars embedded in concrete specimens produced from three types of cements containing no additional inhibitors except for those naturally present.

Corrosion potential of the galvanized steel just immersed in concrete mix made with grey cement, naturally containing 11 ppm of Cr VI, is about -800 mV vs SCE and it stays relatively stable even after 24 hours of measurement (Fig. 7-1a). On the contrary, galvanized bars embedded in white concrete and grey concrete with an admixture of reducing agent corrode actively in the beginning of immersion, but after several hours of corrosion potential quickly rises above -700 mV vs SCE indicating the passivation of zinc (Fig. 7-1b and 7-1c).

The test demonstrates that Cr VI naturally present in grey cement causes immediate passivation of galvanized steel. The small amount of Cr VI, present in two other types of cement, does not affect the passivation of embedded bars. The reducing effect of iron sulphate in grey concrete last over time and allows to maintain the low level of soluble chromium VI during the casting stage.

At the end of potential monitoring concrete specimens were demolished and bars were removed for visual observation. A strong development of pores was observed on the surface of grey concrete with original and reduced amount of Cr VI. This reveals evolution of hydrogen on the bar-concrete interface during the initial set, when concrete is not yet hardened. Withal, hydrogen evolution effect was not detected in the OPC concrete specimen, which agrees with the fact that potential of the embedded bars remained constantly above -900 mV vs SCE. Thus, the presence of Cr VI in the concrete mix promotes the passivation of galvanized steel and suppresses undesirable development of hydrogen.

Figures 7-2 and 7-3 demonstrate the results of scanning electron microscopy and x-ray microanalysis of the galvanized steel sheet removed from the concrete specimen, made with grey cement with reduced chromium VI, after one week of immersion. SEM image of the sheet shows a surface covered with grey crystals. EDX indicates the presence of about 3.8 wt% of Ca, thus the passivation of galvanized steel is correlated to the formation of calcium hydroxyzincate layer.

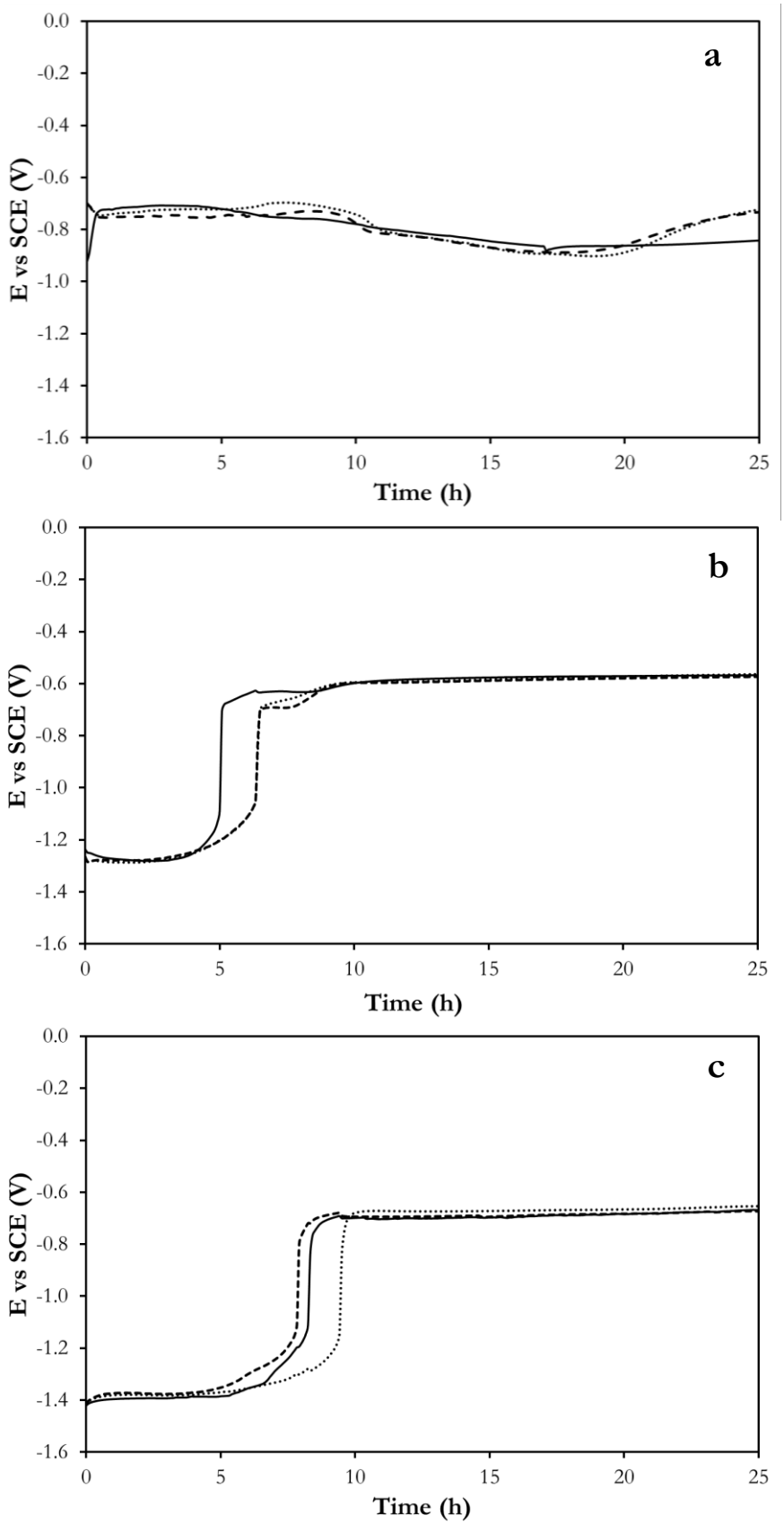


Figure 7-1. Corrosion potential change in time of galvanized bars embedded in concrete specimens manufactured with the following types of cement: *a*) OPC, *b*) OPC with $FeSO_4$ admixture, *c*) WOPC

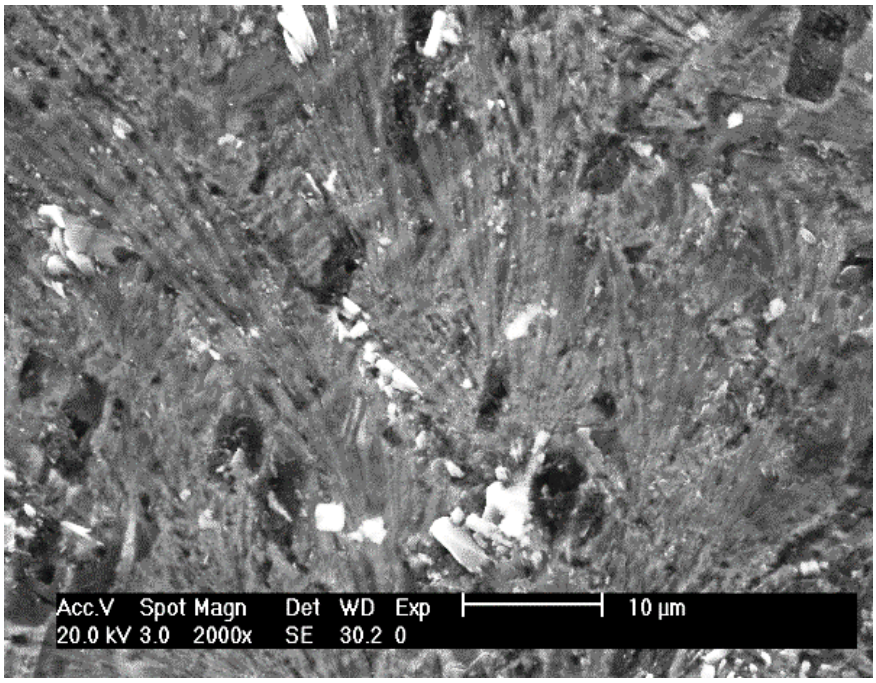


Figure 7-3. SEM image of the galvanized steel surface after 24 hours of immersion in grey concrete with reduced Cr VI

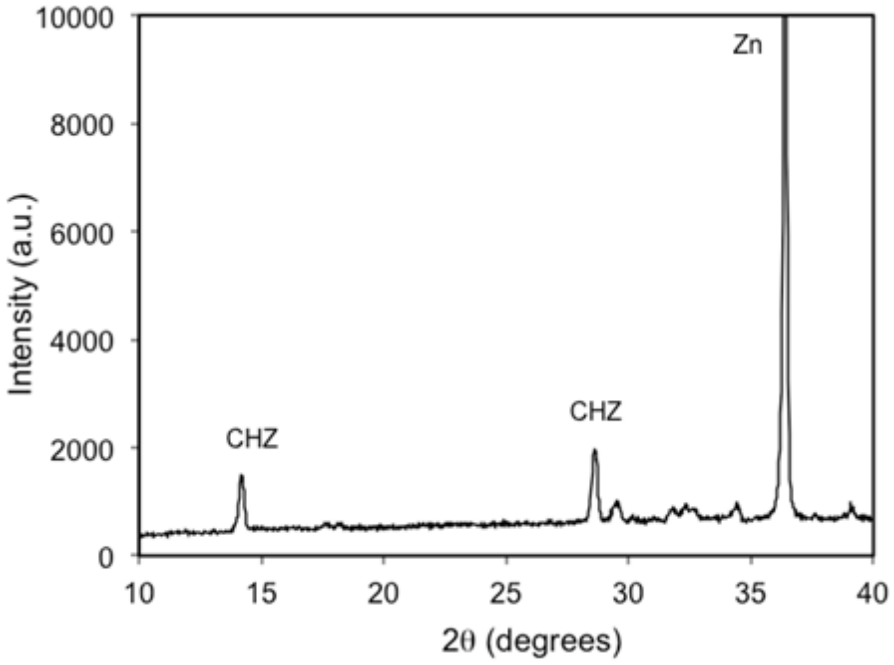


Figure 7-2. X-ray patterns of the galvanized steel surface after 24 hours of immersion in grey concrete with reduced Cr VI

### *7.1.2 Tests with galvanized steel in white concrete with additions of chromium VI*

Corrosion potential of galvanized bars was measured continuously during 48 hours. Figures 7-4 and 7-5 show corrosion potentials change in time during the immersion of bars in concrete specimens made with cements containing different Cr VI concentrations.

Corrosion potential of the galvanized steel just after the embedding in concrete without Cr VI is about -1400 mV vs SCE (Fig. 7-4a); after 8 hours it rapidly grows up to about -700 mV indicating the passivation of zinc. On adding 3 ppm Cr VI to the cement, similar results have been obtained (Fig. 7-4b). With 6 ppm Cr VI in the cement, the passivation of the galvanized steel occurs after about 2 hours (Fig. 7-4c). With 9-12 ppm the passivation occurs after about half an hour only (Fig. 7-5a and 7-5b). Cr VI concentration of 15 ppm determines the immediate passivation of galvanized steel rebars just embedded in concrete mix (Fig. 7-5c).

With Cr VI concentrations ≥ 6 ppm, after 6-7 hours of immersion a reactivation of zinc was always observed, followed by a new passivation after 11-18 hours. Table 7-1 summarizes the passivation and activation average times of the bars. It is noteworthy that the delayed active corrosion of zinc ("reactivation") is not dangerous because the associated hydrogen development occurs when the concrete is partially hardened and cannot lead to the adhesion loss between the rebars and the concrete. It is also noteworthy that high Cr VI concentration favours the first passivation, but delays the second one, indicating that they occur with different mechanisms. The reactivation time is almost constant and does not depend on Cr VI concentration (Tab. 7-1); the most probable explanation is that it is related to the aging of the concrete.

Table 7-1. Passivation and reactivation average times of galvanized steel rebars embedded in concrete specimens containing different concentrations of Cr VI

| Cr VI concentration ppm in the cement | First passivation time h | Reactivation time h | Second passivation time h |
|---|---|---|---|
| 0 | 8.6 | - | - |
| 3 | 7.8 | - | - |
| 6 | 2.7 | 5.8 | 11.2 |
| 9 | 0.6 | 6.5 | 14.1 |
| 12 | 0.5 | 7.0 | 16.7 |
| 15 | 0 | 6.1 | 18.1 |

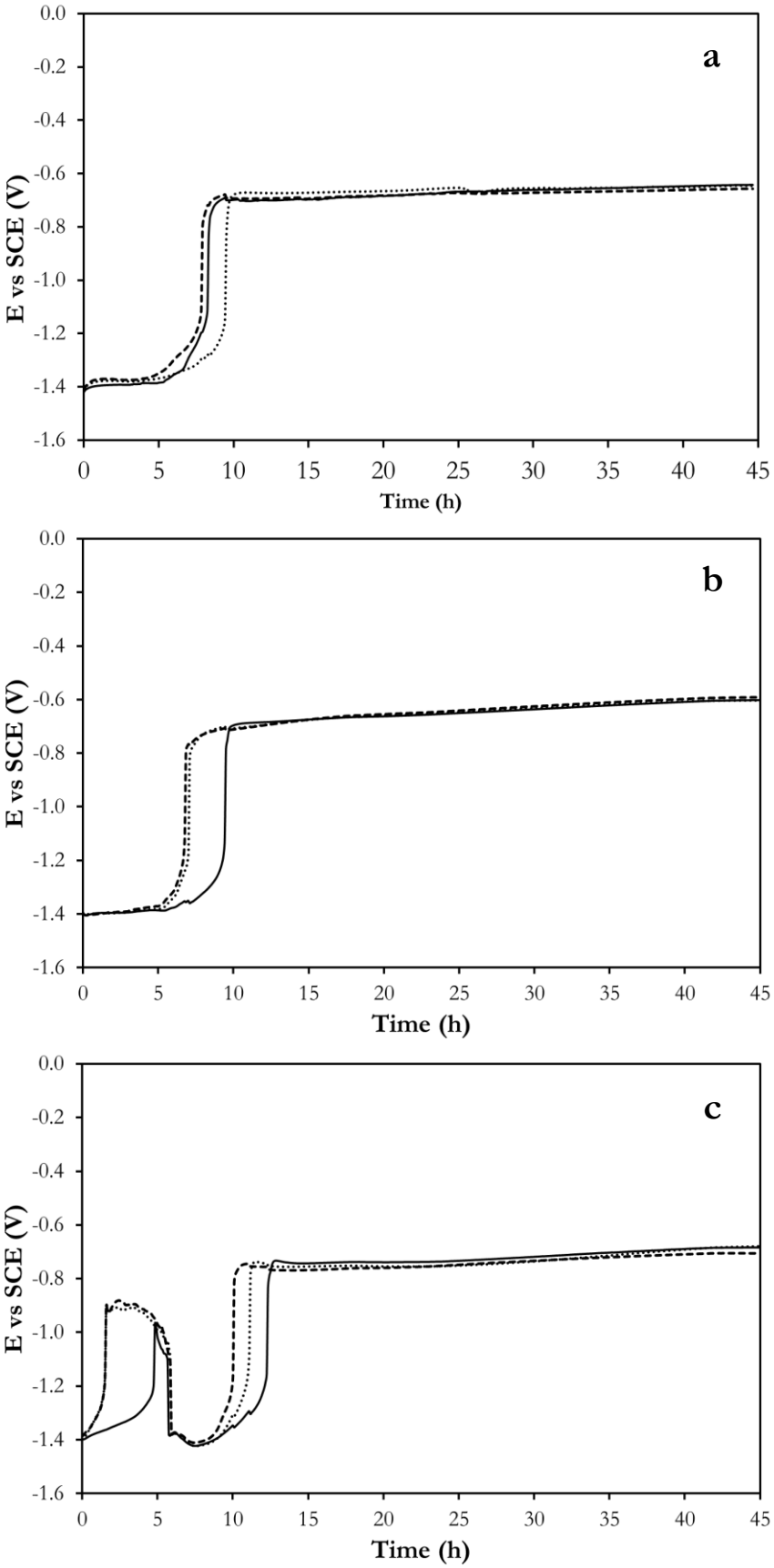


Figure 7-4. Potential change in time of bars embedded in concrete specimens, made with cements containing 0 ppm (a), 3 ppm (b) and 6 ppm (c) Cr VI

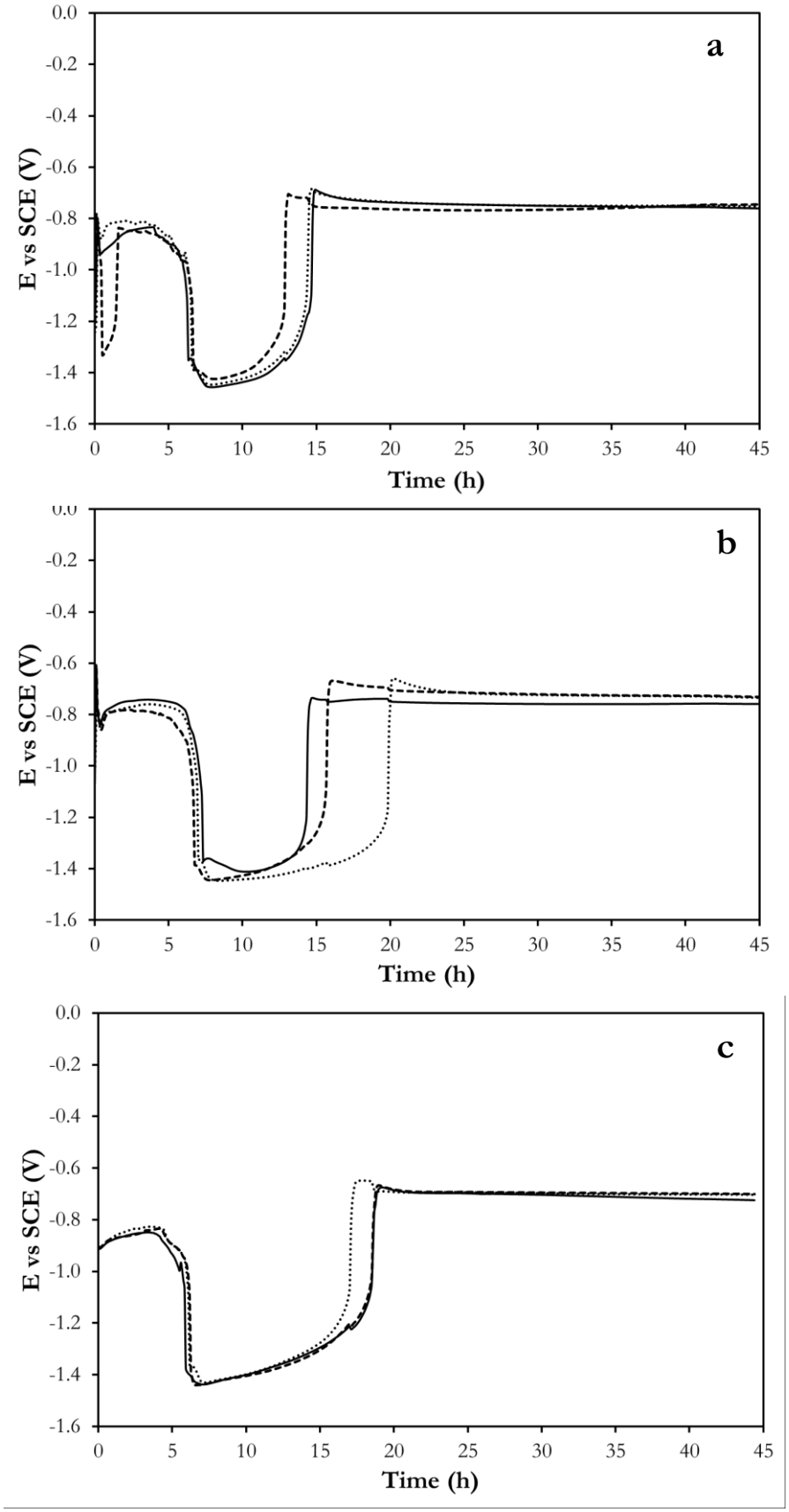


Figure 7-5. Potential change in time of bars embedded in concrete specimens made with cements containing 9 ppm (a), 12 ppm (b) and 15 ppm (c) Cr VI

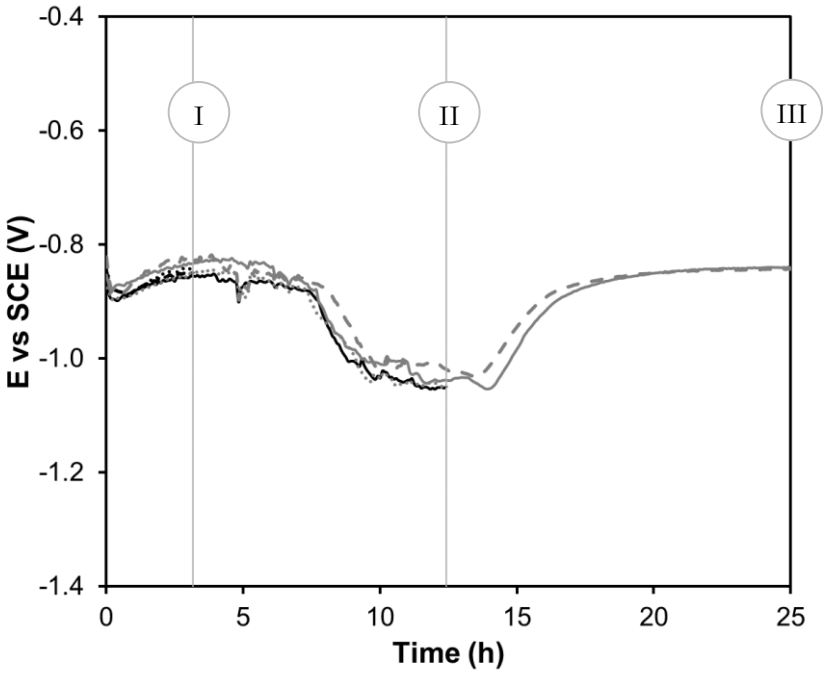


Figure 7-6. Potential change in time of galvanized steel sheets embedded in concrete specimens, manufactured with cement containing 15 ppm Cr VI, with indication of time points, when sheets were removed for SEM and EDX analysis: specimen *I* – after 3 h, specimen *II*– after 12 h and specimen *III* – after 25 h of embedding

Figure 7-6 shows potential change in time of galvanized steel sheets embedded in white concrete specimens manufactured with cement containing 15 ppm Cr VI; sings (I), (II) and (III) indicate the time of the specimens' demolition and removal of galvanized samples for SEM, EDX and RDX analysis. Figures 7-7 and 7-8 show SEM images and X-ray patterns of galvanized steel sheets, respectively. Figure 7-9 reports the results of EDX analysis performed on the zones of galvanized steel sheets marked in Figure 7-7.

SEM image of the sheet removed from the concrete after 3 h of immersion (Fig. 7-7a), corresponding to the first passive state (Fig.7-6), shows a not corroded surface covered by different products; EDX analysis indicated that they are due to the cement paste not yet hardened. X-ray diffraction pattern performed on the same sample (Fig. 7-8a) does not show any peak related to zinc corrosion products, but only two small peaks at 15.6 and 29.3 degrees, which are due to the cement paste. SEM image of the sheet removed from the concrete after 12 h of immersion (Fig. 7-7b), corresponding to the active corrosion (Fig. 7-8b), shows a corroded surface with small white crystals; EDX analysis indicated that also these products are due to the cement paste (Fig.7-9b). As found for the previous galvanized steel sheet, X-ray diffraction pattern does not show any peak related to zinc corrosion products (Fig. 7-8b). SEM image of the sheet removed from the concrete after 25 h of immersion (Fig. 7-7c), corresponding to the second passivation (Fig. 7-6), shows a corroded surface with small white crystals which are prevalently localized inside or next to the most corroded areas. Both EDX analysis and X-ray diffraction pattern indicate that they are calcium hydroxyzincate.

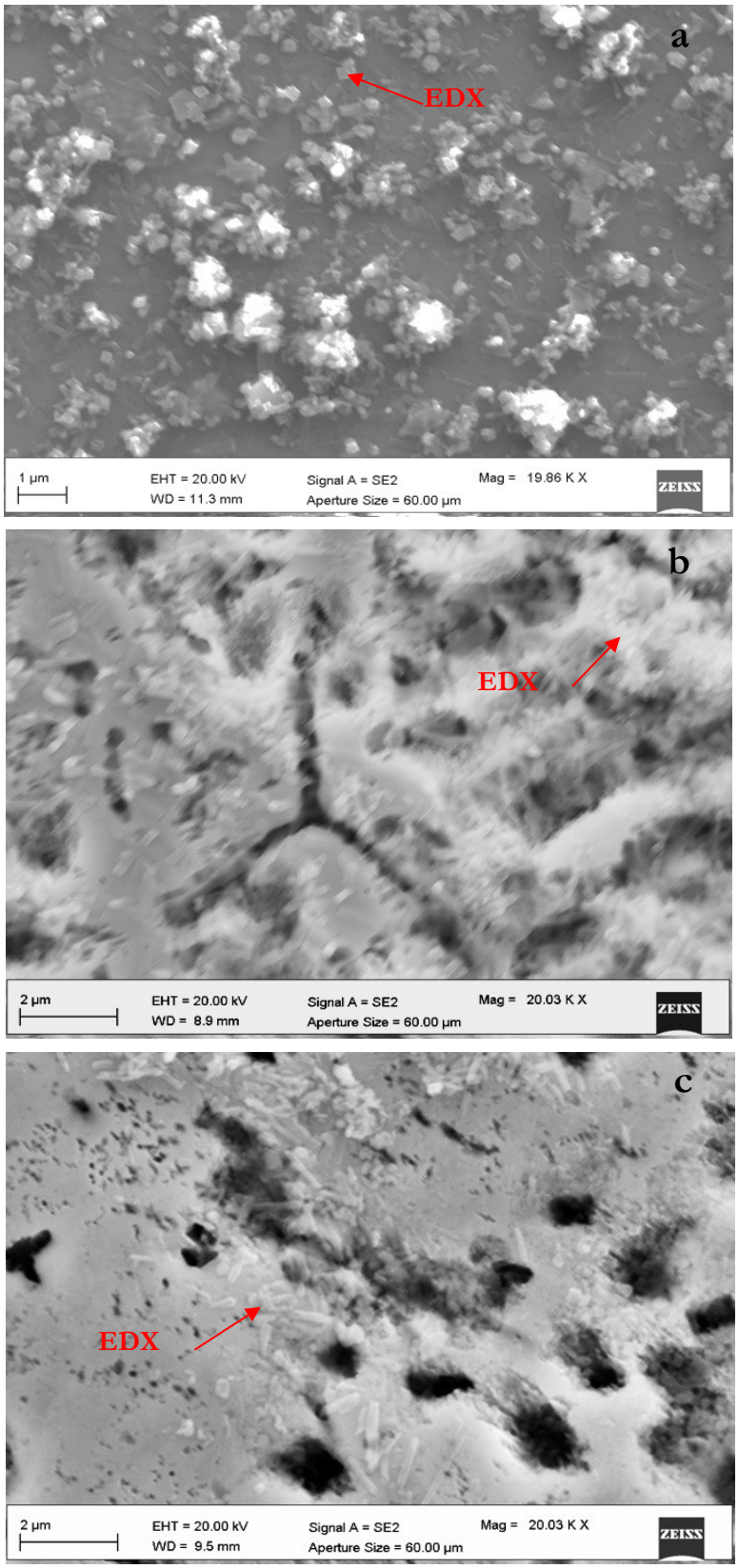


Figure 7-7. SEM images of galvanized steel sheets surface after the immersion in concrete made with cement containing 15 ppm Cr VI for: 3 h (a), 12 h (b) and 25 h (c)

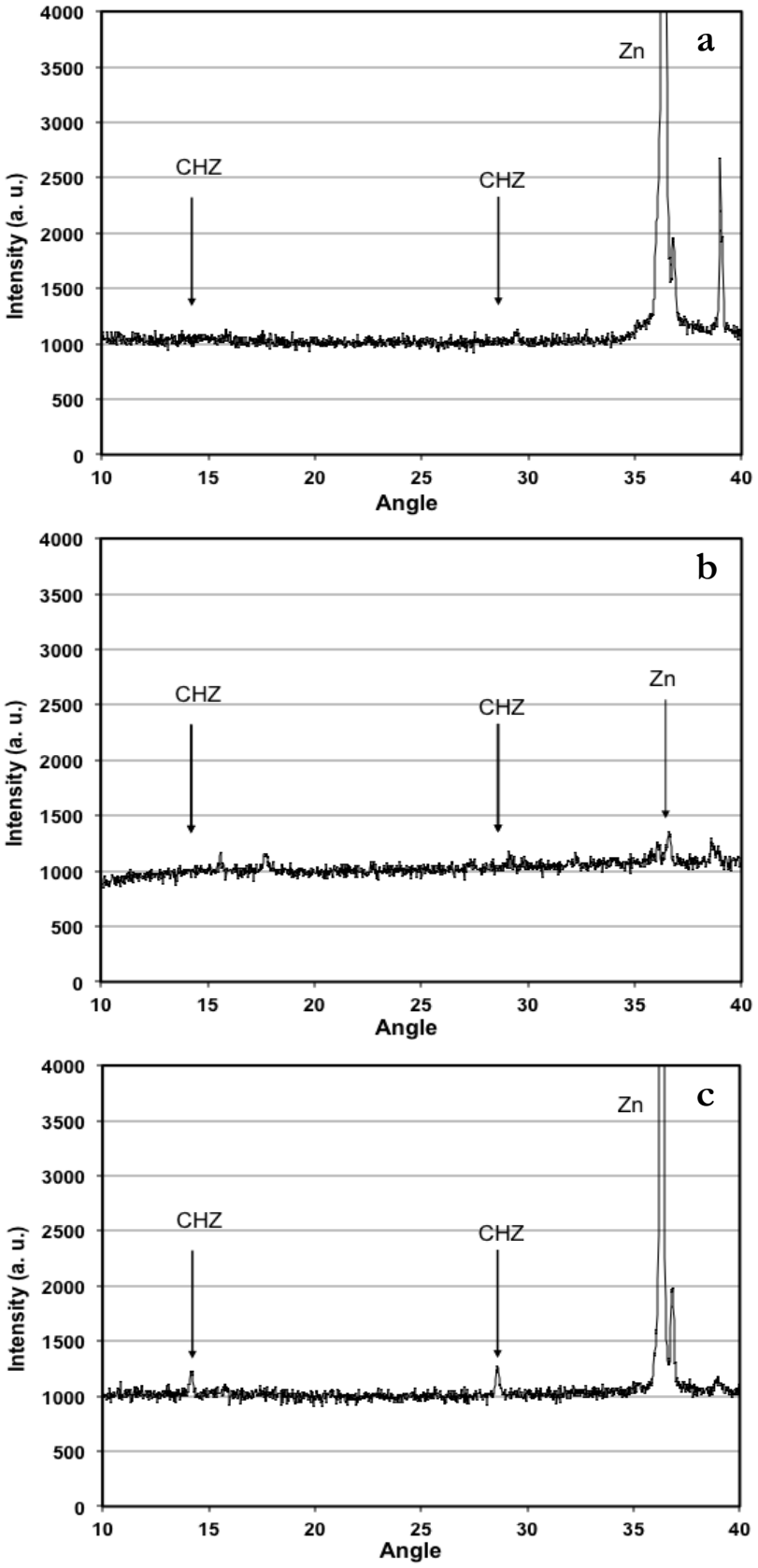


Figure 7-8. X-ray patterns of galvanized steel sheets after the immersion in concrete specimens made with cement containing 15 ppm Cr VI for: 3 h (a), 12 h (b) and 25 h (c)

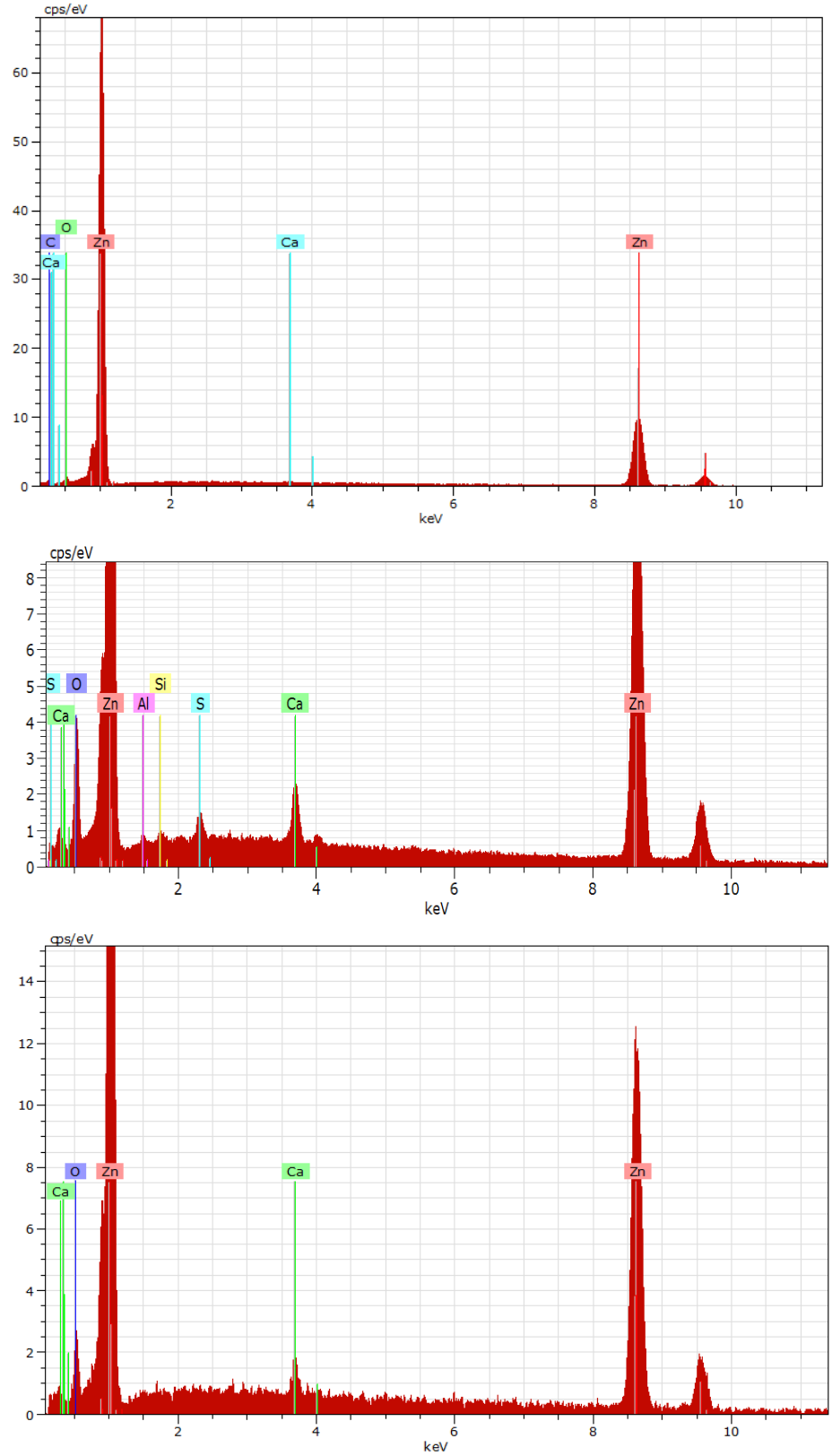


Figure 7-9. EDX analysis performed on zones of galvanized steel sheets marked in Figure 8: a) 3h, b) 12 h and c) 25 hours of immersion

The present results indicate that the two passivations occur with different mechanism, because only the second is due to the formation of calcium hydroxyzincate. Instead, a metastable passivation film determines the first passivation, related to the presence of Cr VI. It seems that an active corrosion period is necessary to produce the amount of zinc ions required for the formation of a calcium hydroxyzincate protective layer.

### *7.1.3 Tests performed in $Ca(OH)_2$ saturated solution with addition of chromium VI*

A preliminary test was performed in order to select the Cr VI concentration able to passivate zinc. Figure 7-10 shows the potential changes in time for pure zinc sample immersed in 3oo mL $Ca(OH)_2$ saturated solution. After one hour of immersion 70 µl of 0,05M $K_2Cr_2O_7$ solution were added to a working cell every 5 minutes until the passivation occurred. The small picks on the plot line are related to the additions of chromate solution, the last addition is accompanied with a sharp increase of potential from about -1400 mV vs SCE to about -700 mV vs SCE, corresponding to the passive state. The passive potential of zinc stayed stable after 24 hours of immersion. The test was repeated five times and the average amount of additions was calculated. e total amount of chromate added in the test, 350 µl of 0.05M $K_2Cr_2O_7$ solution in 300 mL $Ca(OH)_2$ saturated solution, corresponds to 6.07 ppm Cr VI.

The test was repeated in $Ca(OH)_2$ saturated solution with the addition of 6.07 ppm Cr VI immediately after immersion of the pure zinc sample to a working cell. The result of potential monitoring is given in Figure 7-11. The initial potential of zinc immersed in $Ca(OH)_2$ saturated solution is about -1200 mV vs SCE and it rises rapidly up to about -700 mV vs SCE. Figures 7-12 and 7-13 show results of SEM and EDX analysis performed on zinc sample after 20 hours of immersion indicating the presence of some calcium hydroxyzincate crystals, which do not cover the entire surface; no chromium peaks appears on the EDX pattern.

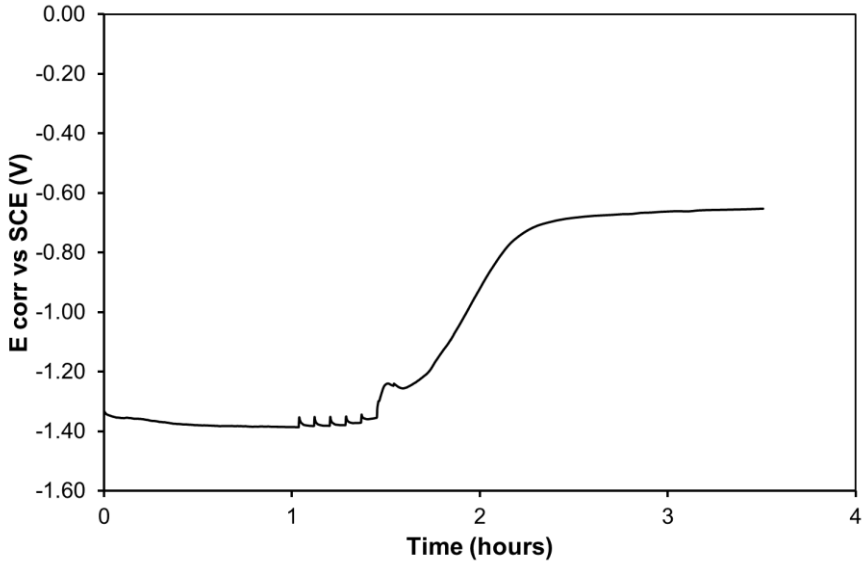


Figure 7-10. Corrosion potential change in time of pure zinc sample immersed in $Ca(OH)_2$ saturated solution with additions of 0.05M $K_2Cr_2O_7$ solution

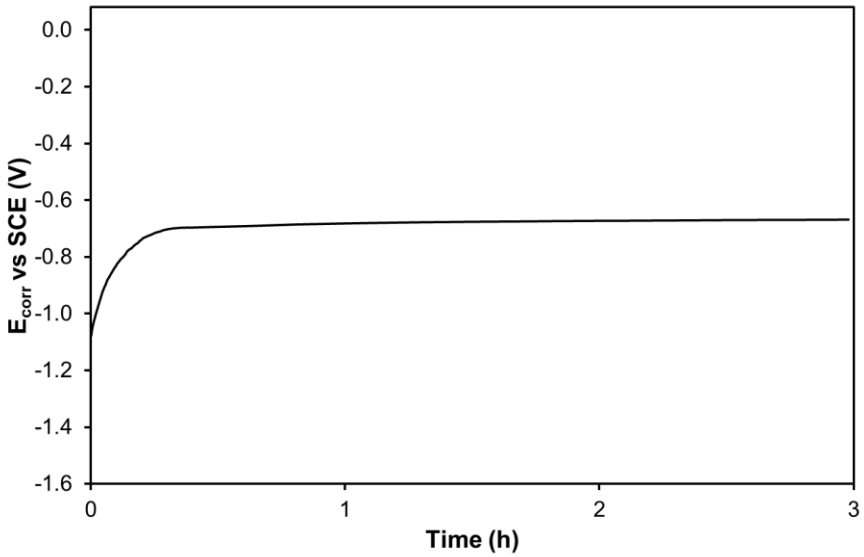


Figure 7-11. Corrosion potential change in time of pure zinc sample immersed in $Ca(OH)_2$ saturated solution with one-time addition of chromate

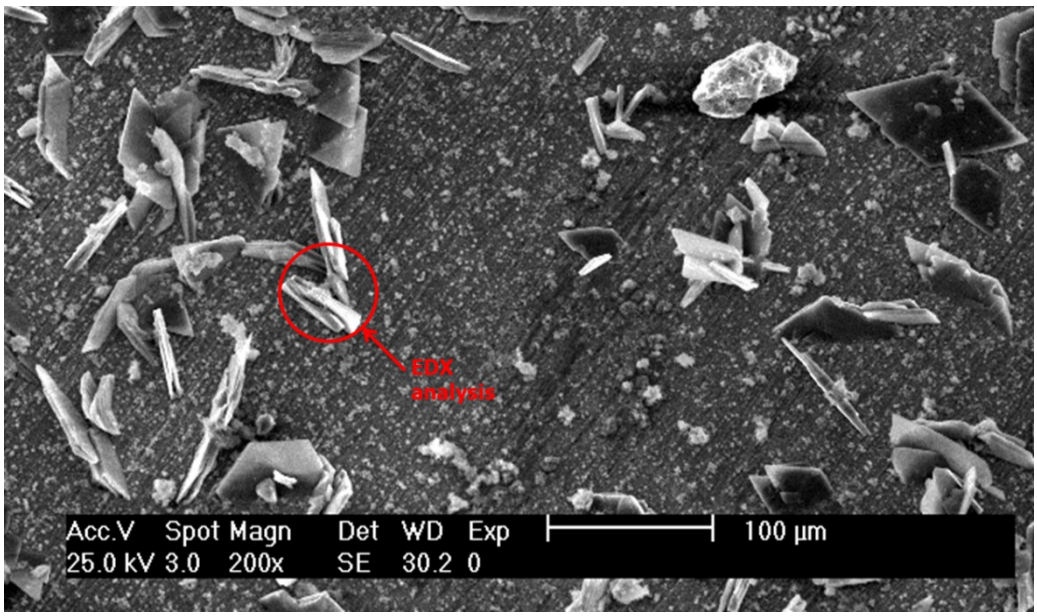


Figure 7-12. SEM image of zinc sample surface after 20 hours of immersion in $Ca(OH)_2$ saturated solution with addition of 6.07 ppm Cr VI

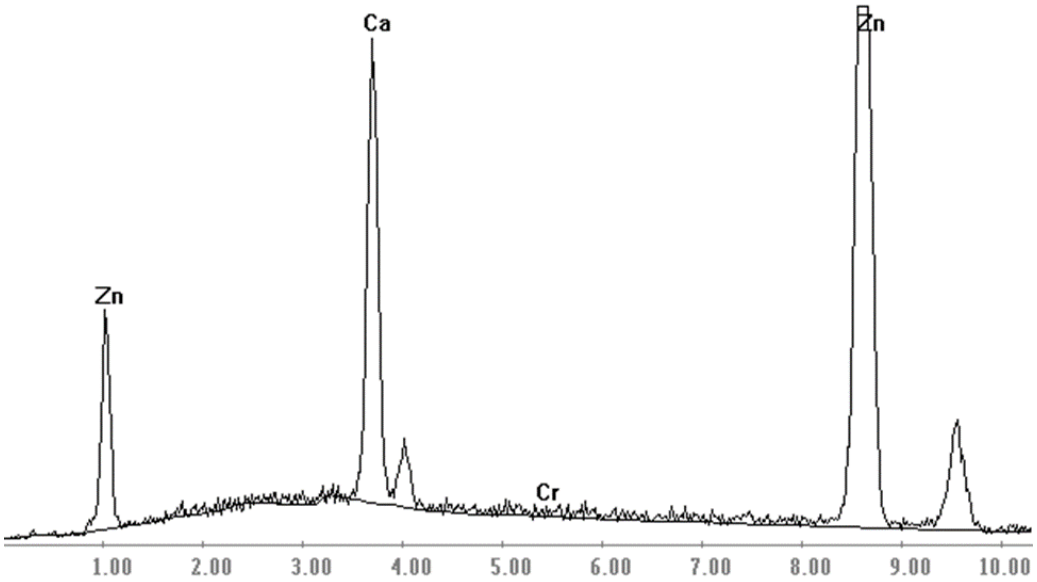


Figure 7-13. EDX patterns of zinc sample after 20 h the immersion in $Ca(OH)_2$ saturated solution with addition of 6.07 ppm Cr VI

To better understand mechanism of Cr VI effect on galvanized steel passivation in concrete, corrosion potentials of pure zinc samples were monitored in $Ca(OH)_2$ saturated solution. Fig. 7-14 shows potential change in time for zinc sample immersed in $Ca(OH)_2$ saturated solutions with different content of Cr VI. Table 7-2 demonstrates that zinc becomes immediately passive after the immersion for Cr VI concentration ≥ 5.0 ppm. Contrarily to what occurred for galvanized steel in concrete, zinc reactivation was not observed in $Ca(OH)_2$ solution.

Table 7-2. Passivation times of zinc in $Ca(OH)_2$ saturated solution containing different Cr VI concentrations

| Cr VI ppm | Passivation time h |
|---|---|
| 0 | 28.0 |
| 1.2 | 16.5 |
| 2.5 | 1.4 |
| 3.7 | 0.2 |
| 5.0 | 0 |
| 6.2 | 0 |

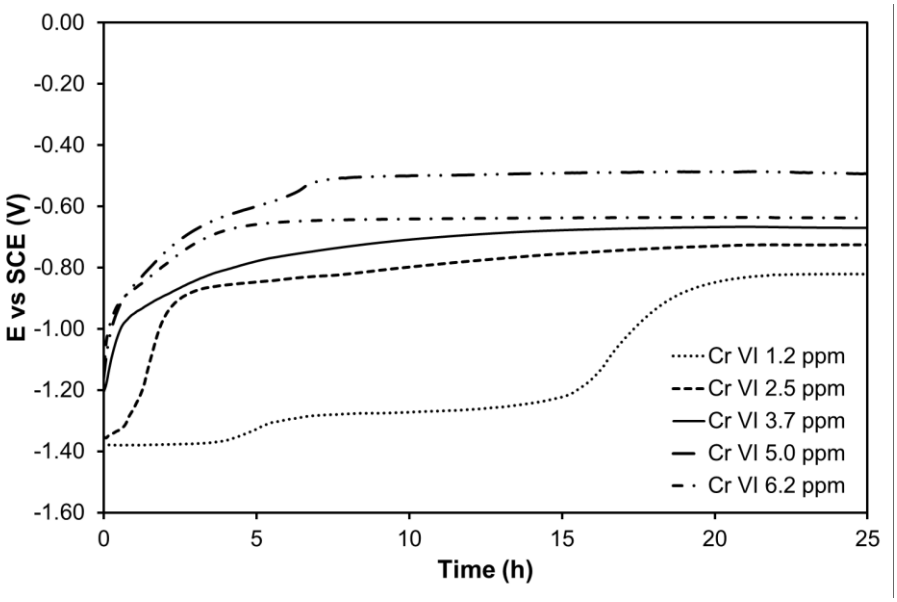


Figure 7-14. Corrosion potential of pure zinc samples in $Ca(OH)_2$ saturated solution containing different Cr VI concentrations

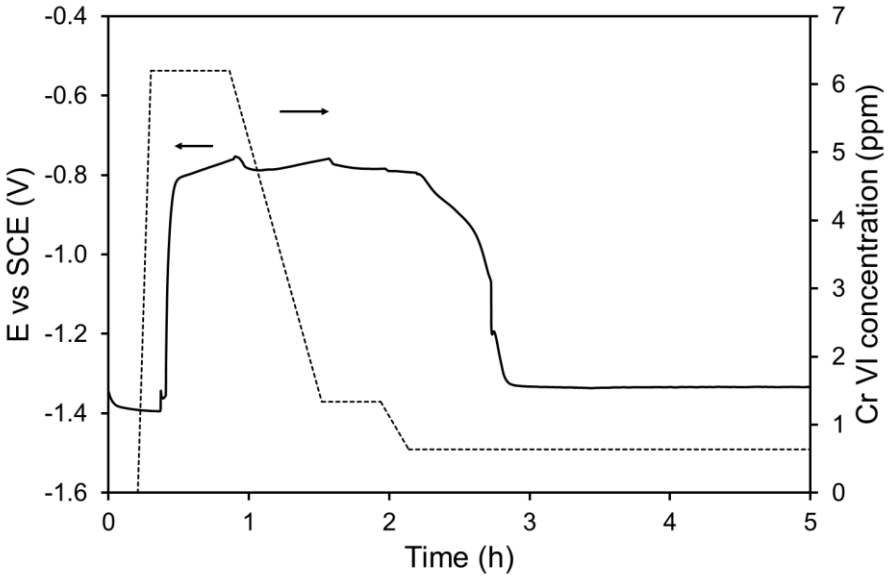


Figure 7-15. Corrosion potentials of galvanized steel sheet in $Ca(OH)_2$ saturated solution containing the Cr VI concentrations indicated by the dotted line

Corrosion potential of galvanized steel was measured then in $Ca(OH)_2$ saturated solution on changing Cr VI concentration (Fig. 7-15). Galvanized steel immersed in Cr VI free solution corrodes actively; when 6.2 ppm Cr VI is added, it immediately becomes passive. On decreasing Cr VI concentration down to 1.3 ppm, by diluting the solution, galvanized steel remains passive, but when the Cr VI concentration is further decreased down to 0.6 ppm corrosion potential starts to decrease and the values typical of the active state are reached. Impedance measurements performed on different stages of dilution confirm the presence of activation and reactivation processes with the changing Cr VI concentration (Fig. 7-16). The present results indicate that the reactivation process is determined by the depletion of Cr VI on the galvanized steel surface.

Figure 7-17 shows the change of polarisation resistance in time of pure zinc samples immersed in calcium hydroxide saturated solutions with different concentrations of Cr VI: from 0 to 6.2 ppm. The higher the concentration of Cr VI the higher the maximum impedance value reached for each period of time. Based on the plot observation, it can be assumed that there is a concentration limit of hexavalent chromium, below which the inhibiting protection provided by Cr VI is small. As it is visible from the plot, the polarisation resistance value increases in time for all Cr VI concentration, no reactivation is observed. The sample surfaces, after 24 hours of immersion, had no visual evidence of corrosion or calcium hydroxyzincate crystals growth (Fig. 7-18). Thus EIS analysis of pure zinc indicate that the passivation is determined by the formation of a protective film invisible to the naked eye.

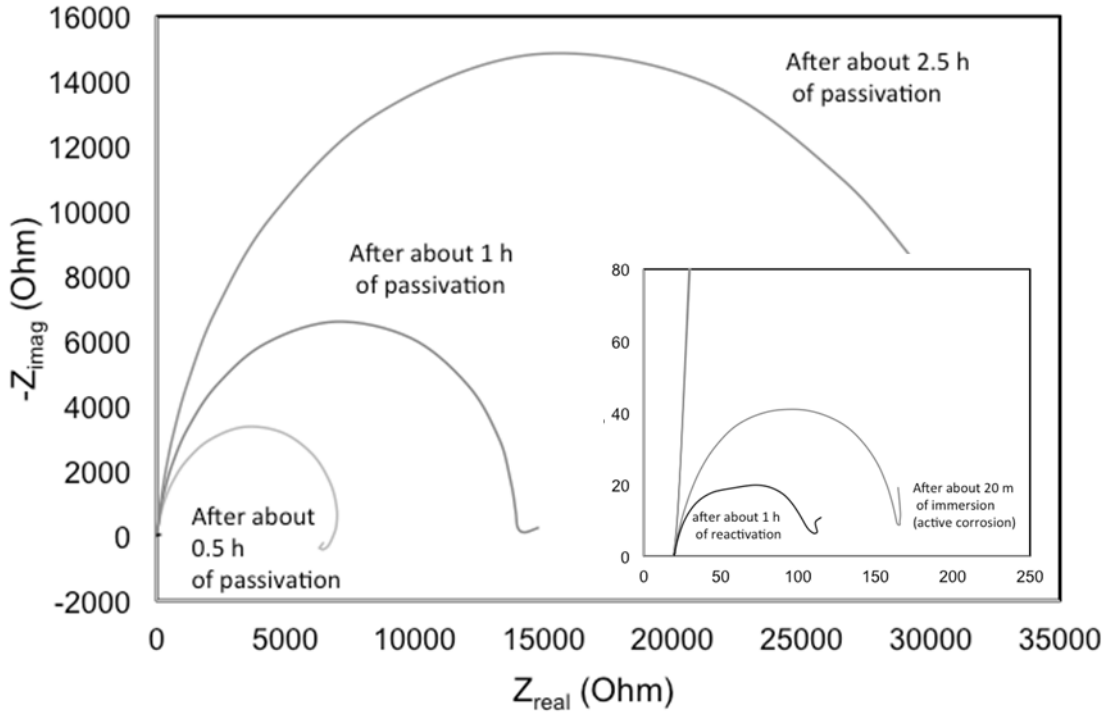


Figure 7-16. Nyquist plots of galvanized steel sheet in $Ca(OH)_2$ saturated solution with changing Cr VI concentration

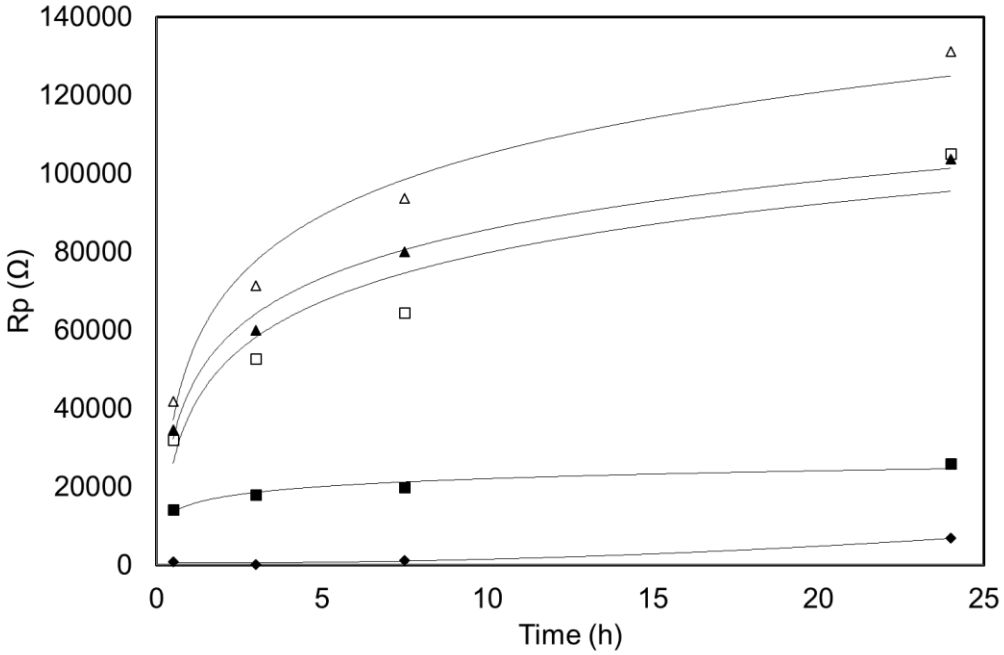


Figure 7-17. Change of polarization resistance in time for pure zinc samples immersed in $Ca(OH)_2$ saturated solutions without addition of Cr VI (♦) and with different Cr VI concentrations: ■ – 1.6 ppm, □ – 2.3 ppm, ▲ – 3.1 ppm, Δ – 6.2 ppm

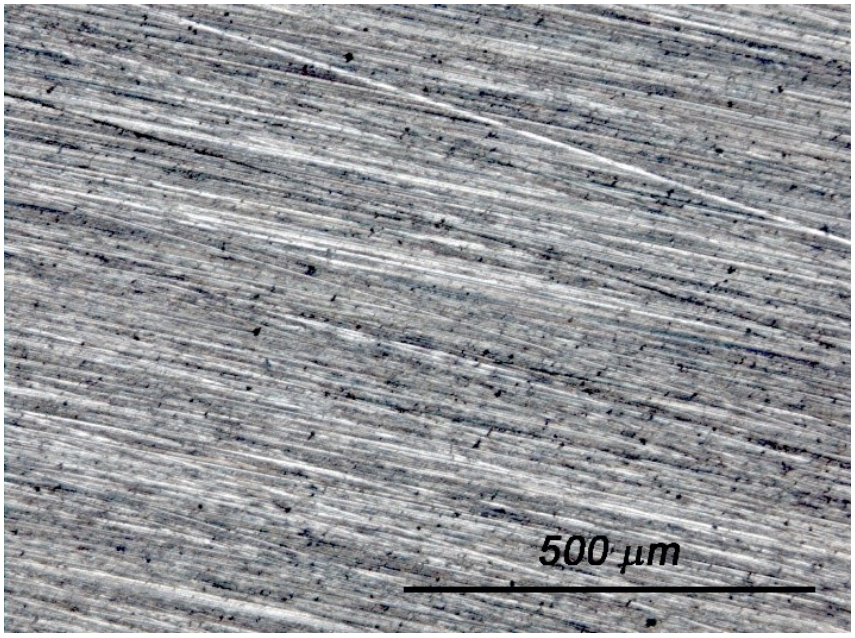


Figure 7-18. Microscope observation of pure zinc sample after 24 hours of immersion in $Ca(OH)_2$ saturated solution with 6.2 ppm Cr VI, original magnification x 100

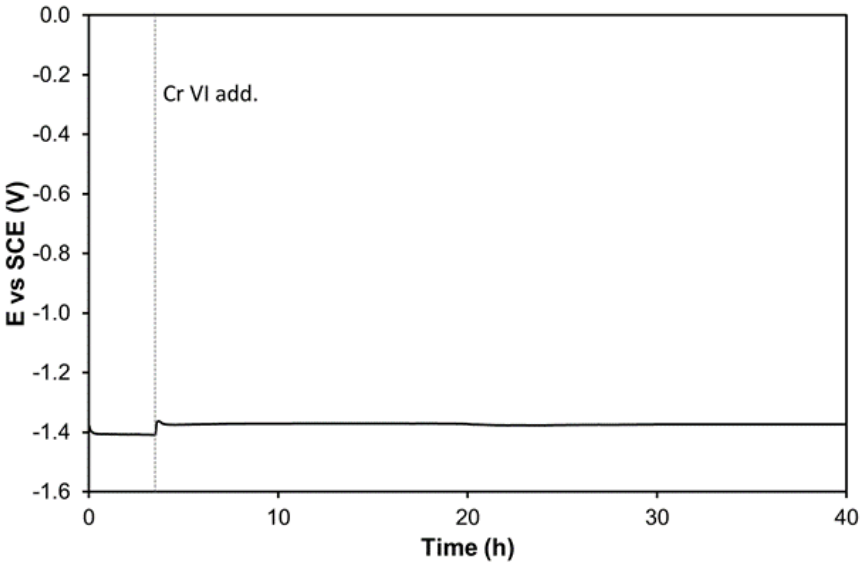


Figure 7-19. Potential change in time of zinc sample in deaerated $Ca(OH)_2$ saturated solution

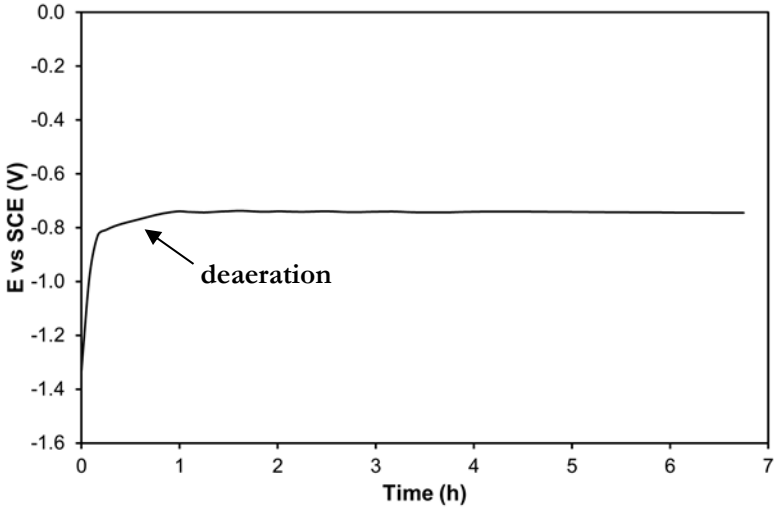


Figure 7-20. Potential change in time of galvanized steel sample with progressive deaeration of $Ca(OH)_2$ saturated solution

Figures 7-19 and 7-20 show the potential change in time for zinc and galvanized steel samples immersed in $Ca(OH)_2$ saturated solution and the effect of dissolved oxygen concentration on the passivation process. In the first test, zinc sample was immersed in $Ca(OH)_2$ saturated solution deaerated through $N_2$ bubbling, then $K_2Cr_2O_7$ solution was added to obtain 6.2 ppm concentration of Cr VI (Fig. 7-16). The initial corrosion potential of zinc sample was about -1400 mV and it changed slightly after oxidant addition. In the second test, galvanized steel sample was immersed in aerated $Ca(OH)_2$ saturated solution and had corrosion potential about -1400 mV after immersion; after addition of $K_2Cr_2O_7$ solution and achieving 6.2 ppm

concentration of Cr VI, potential abruptly rose to about -800 mV and passive state was obtained. With decreasing the oxygen present in the solution through $N_2$ bubbling, but maintaining Cr VI concentration at 6.2 ppm, the passive state was maintained. The addition of chromium VI with concentration 6.2 ppm, which gave the best and fastest inhibiting effect during previous experiments both in concrete and in $Ca(OH)_2$ saturated solution, without oxygen was not sufficient to achieve passive state and to provide appropriate protection of zinc in alkaline medium. Though when the passive state is already obtained, the decreasing of oxygen does not cause reactivation of zinc. Presents results reveal the important role of dissolved oxygen in initiation of passivation in $Ca(OH)_2$ saturated solution in presence of oxidizing inhibitors.

## 7.2 Tests performed with additions of other inhibitors

### *7.2.1 Tests performed in $Ca(OH)_2$ saturated solution*

Figure 7-21 shows the trends of open circuit potential in time of galvanized steel sheets immersed in $Ca(OH)_2$ saturated solution with additions of diethanolamine, sodium molybdate or sodium nitrite in concentrations given in Table 6-1. To highlight and compare inhibiting efficiency of the different substances, the trends of galvanized steel immersed in $Ca(OH)_2$ saturated solution without inhibitors and with addition of 6.2 ppm chromium VI were also added to the plot. As visible in the plot, among the three tested inhibitors, nitrite shows the most promising result; in fact, it causes a sharp increase of potential from -1340 mV to about -1100 mV vs SCE already after 30 min of immersion, with the maximum potential of -970 mV vs SCE reached in 24 hours. Although the inhibiting effect provided by nitrite is less than the effect of chromium VI with 6.2 ppm concentration, it can be considered enough to decrease negative corrosion effects during the early periods of immersion.

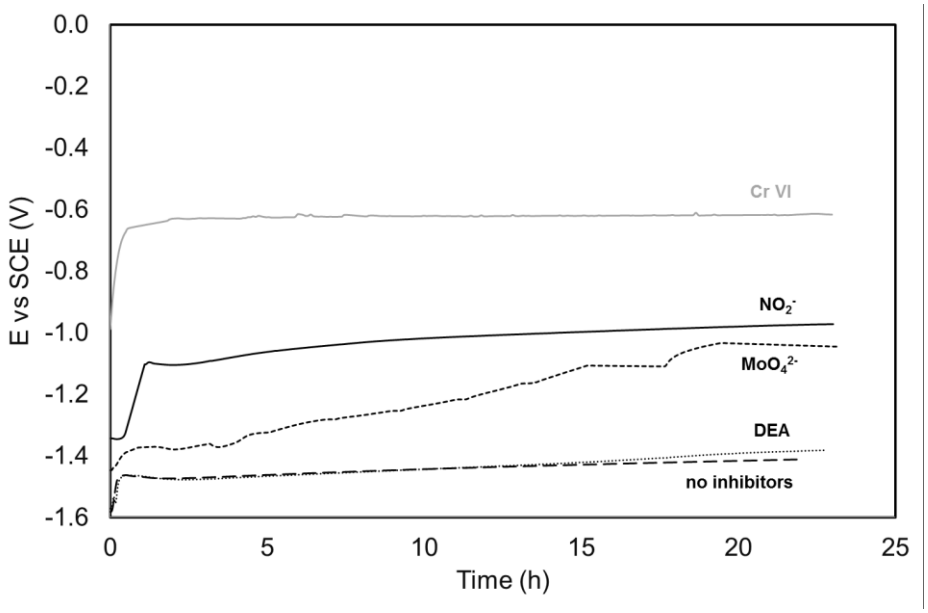


Figure 7-21. Open circuit potential change in time of galvanized steel sheets immersed in $Ca(OH)_2$ saturated solution without inhibitors and with addition of inhibitors: 3 wt% $NO_2^-$, 0.01M $MoO_4^{2-}$, 3.5 L/m$^3$ DEA and 6.2 ppm Cr VI

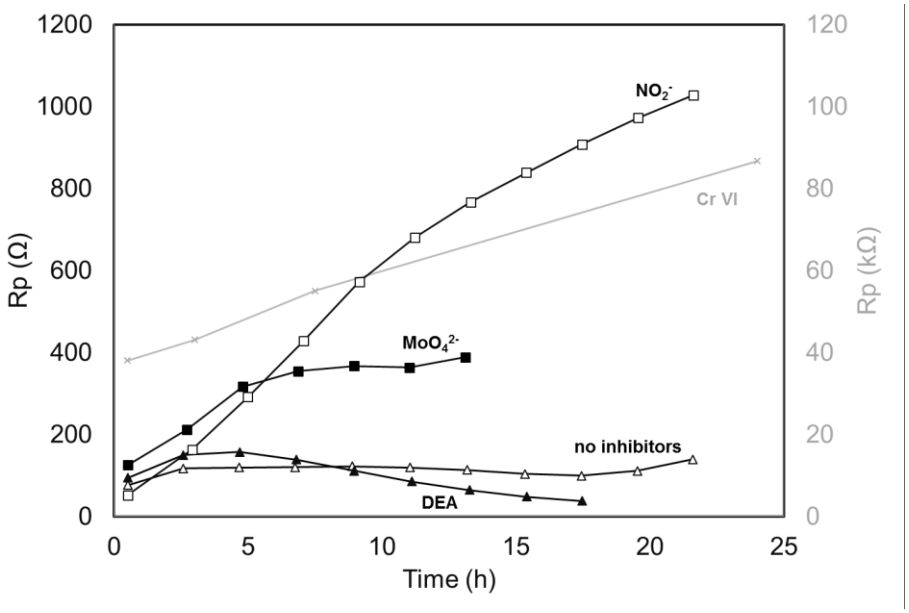


Figure 7-22. Polarization resistance change in time of galvanized steel sheets immersed in $Ca(OH)_2$ saturated solution without inhibitors (Δ) and with addition of inhibitors: □ – 3 wt% $NO_2^-$, ■ – 0.01M $MoO_4^{2-}$, ▲ – 3.5 L/m3 DEA. Secondary vertical axis: x – 6.2 ppm Cr VI

Galvanized steel immersed in $Ca(OH)_2$ saturated solution with molybdate demonstrates the lower initial potential (about -1450 mV) compared to that of galvanized steel immersed in same solution but with nitrides addition and the smooth growth of potential in time up to about -1050 mV vs SCE.

Diethanolamine shows no inhibiting effect, in fact the curve related to DEA overlaps that obtained without inhibitor. In both cases, the initial potential of galvanized steel is very low and it remains stable active during all the experiment.

Figure 7-22 displays polarization resistance change in time of the same samples received as a result of impedance measurements made contemporarily with potential monitoring. *Rp* was calculated as difference between the magnitude of impedance modulus at low frequencies and the solution resistance *Rsol* at high frequencies: $R_p = |Z|_{max} - Rsol$, knowing that the surface of all tested samples was equal. The plot confirms the trends obtained for inhibitors during potential monitoring. Nitrite demonstrates the highest values of polarization resistance among three tasted inhibitors – about 1 kΩ – that is however by two order smaller than the polarization resistance for galvanized steel immersed in $Ca(OH)_2$ saturated solution with addition of 6.2 ppm chromium VI (Fig 7-22, grey line, secondary vertical axis).

### *7.2.2 Tests performed in concrete with additions of hydrogen peroxide*

Tests in concrete with additions of hydrogen peroxide were performed to demonstrate the chemical transformation in different cement pastes that can be caused by some oxidants.

Figure 7-23 shows potential change in time of galvanized steel bars and pure zinc rods embedded in white concrete specimens manufactured with cements containing 1.2 % and 2.4 % of $H_2O_2$. In both cases, corrosion potential of the galvanized steel bars and zinc rods just after the embedding in concrete is about -1400 mV vs SCE. After 5 hours potential quickly increases up to about -800 mV vs SCE for the concrete with 1.2 % of $H_2O_2$ and -

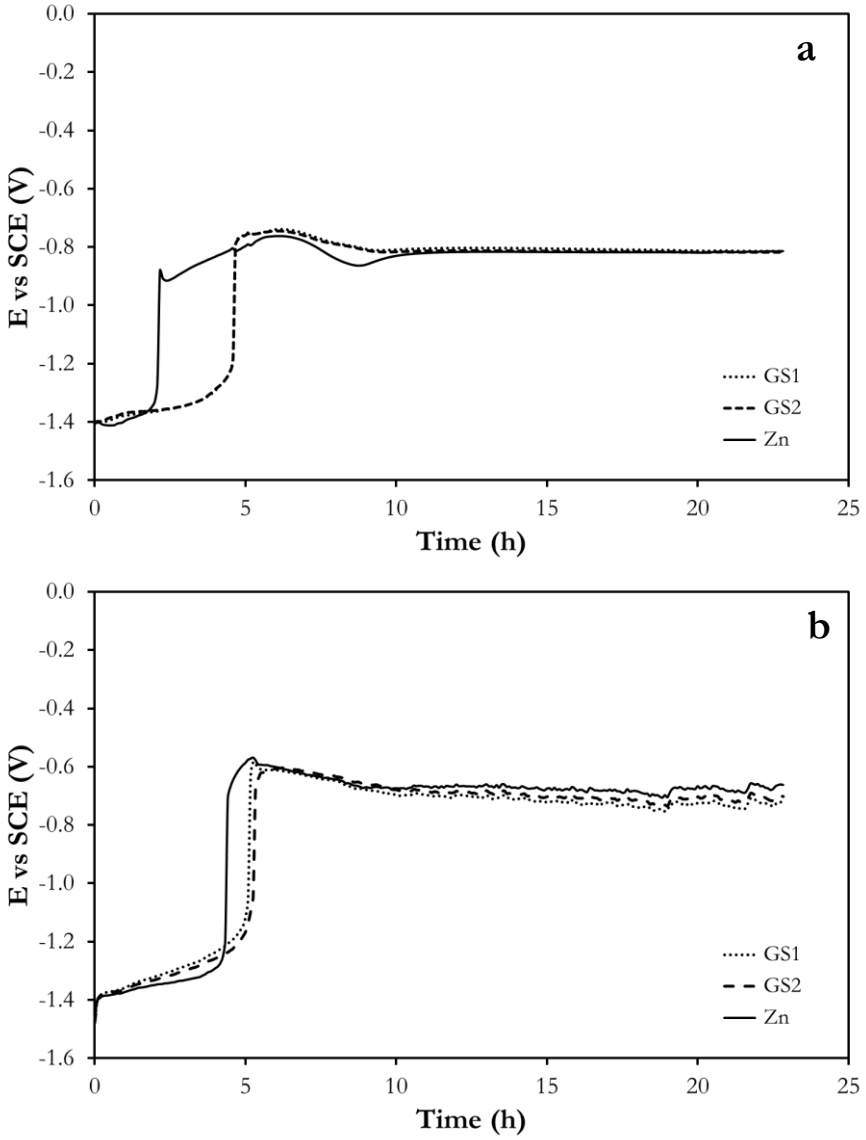


Figure 7-23. Corrosion potential change in time of galvanized steel bars (*GS*) and pure zinc rod (*Zn*) embedded in concrete specimens made with white cements, containing 1.2 % (*a*) and 2.4 % (*b*) $H_2O_2$

700 mV for the concrete with 2.4 % of $H_2O_2$. There is a quite good similarity in corrosion behavior of galvanized steel and pure zinc. The only noticeable difference is in the speed of passivation: with 1.2 % the passivation of zinc occurs after about 2 hours, means 3 hours earlier than that of galvanized steel; with 2.4 % the difference in passivation speed is not significant.

According to the present results, $H_2O_2$ in a concentration 2.4 % or less has no inhibiting effect on galvanized steel in concrete produced with white Portland cement and cannot be used for prevention of hydrogen evolution on the zinc-concrete interface at the early stage of concrete setting.

Figure 7-24 shows potential change in time of galvanized steel bars and pure zinc rods embedded in concrete specimens made with grey cement (with $FeSO_4$ admixture) containing

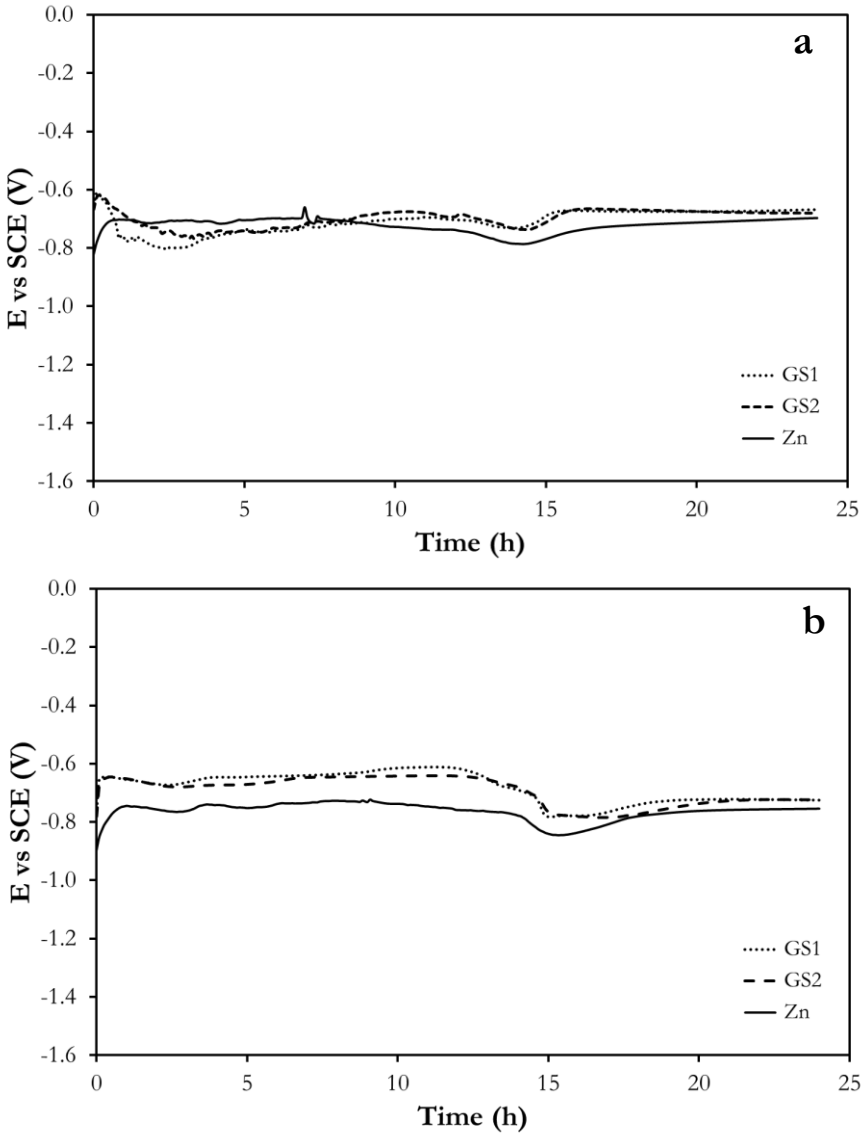


Figure 7-24. Corrosion potential change in time of galvanized steel bars (*GS*) and pure zinc rod (*Zn*) embedded in concrete specimens made with grey cements, containing 1.2 % (*a*) and 2.4 % (*b*) $H_2O_2$

1.2 % and 2.4 % of $H_2O_2$. As can be seen in the graphs, the data obtained in grey and white concrete with the same amount of $H_2O_2$ are completely different: with grey cement the immediate passivation of all sample occurs just after embedding. Initially corrosion potential of all six samples is higher than -900 mV vs SCE and it does not drop below -850 mV throughout the experiment, staying at about -700 mV vs SCE on the average.

The explanation of this discrepancy in peroxide effect on corrosion behaviour of galvanized steel and zinc in concrete produced with different types of cement may be as follows.

Grey Portland cement used in the experiment contains as additive the reducing agent $FeSO_4$, which can convert water-soluble chromate into hardly soluble, trivalent form by the following reaction:

$$CrO_4^{2-} + 3Fe^{2+} + 4OH^- + 4H_2O \rightarrow Cr(OH)_3 + 3Fe(OH)_3 \quad (7.1)$$

The chemical reaction (7.1) does not start immediately after mixing cement with water. Owing the highly alkaline environment, the iron is subject to competing reaction, such as oxidation. Addition of hydrogen peroxide in grey cement causes the reactivation of ferrous sulphate due to following reactions:

$$2Fe^{2+} + 4OH^- + H_2O_2 \rightarrow 2Fe(OH)_3 \quad (7.2)$$

$$2Cr(OH)_3 + 4OH^- + 3H_2O_2 \rightarrow 2CrO_4^{2-} + 8H_2O \quad (7.3)$$

Released in such way Cr VI inhibits the corrosion of galvanized steel and zinc (Fig. 7-24). Thus, $H_2O_2$ has no direct inhibitory effect, but acts as a neutralizer of the reducing agent. White Portland cement originally contains very low amount of Cr VI (below 2 ppm). Therefore, $H_2O_2$ added in white concrete does not show the same result (Fig. 7-23). This fact reveals impossibility of using hydrogen peroxide for corrosion protection of galvanized steel in concrete.

### *7.2.3 Tests performed in concrete with additions of nitrite*

Figure 7-25 shows potential change in time of galvanized steel bars and pure zinc rods embedded in white concrete specimens containing different amounts of $NaNO_2$. Corrosion potential of the galvanized steel and zinc just after the embedding in concrete made with the cement containing 3% of $NO_2^-$ is about -1400 mV vs SCE; within 6 hours, it slowly increases up to about -850 mV for galvanized steel; it takes more time for pure zinc sample to arrive at the same potential level (about 11 hours) (Fig. 7-25a). On adding 6 % of $NO_2^-$ to the white cement, initial corrosion potential is similarly about -1400 mV vs SCE for both galvanized steel and pure zinc; then it grows stepwise: after 1 hour it quickly increases up to -1200 mV and in subsequent 5 hours it slowly rises to about -800 mV vs SCE (Fig. 7-25b). With 10 % of $NO_2^-$, initial potential is about -1100 mV vs SCE; it also grows stepwise: first rapidly after half an hour up to -950 mV (after 1.5 hour up to -1000 mV for the zinc rod), then after next 6 hours again rapidly up to about -700 mV (Fig. 7-25c).

Figure 7-26 shows potential change in time of galvanized steel bars and pure zinc rods embedded in grey concrete specimens (with $FeSO_4$ admixture) containing different amounts of $NaNO_2$. Corrosion potential of the galvanized steel and zinc just after the embedding in concrete made with cement containing 3% of $NO_2^-$ is about -1200 mV vs SCE; within 6 hours, it slowly increases up to about -800 mV that indicates the passivation (Fig. 7-26a). On adding 6 % of $NO_2^-$ to the grey cement, initial corrosion potential is similarly about -1200 mV vs SCE for both galvanized steel and pure zinc; potential grows stepwise: after 30 minutes it quickly increases up to -1050 mV (after 1 hour for the zinc rod), then it slowly rises up to about -700 mV vs SCE (Fig. 7-26b). With 10 % of $NO_2^-$, initial potential is about -1100 mV vs SCE; it increases gradually up to about -700 mV vs SCE within 8 hours (Fig. 7-26c).

Corrosion behaviour of galvanized steel and pure zinc has small differences: in active state zinc has a slightly low corrosion potential and a less tendency to passivation with respect to galvanized steel, though, when the passive state is reached, zinc leads to more positive potentials than galvanized steel. However, discrepancies are insignificant and can be neglected within experimentation.

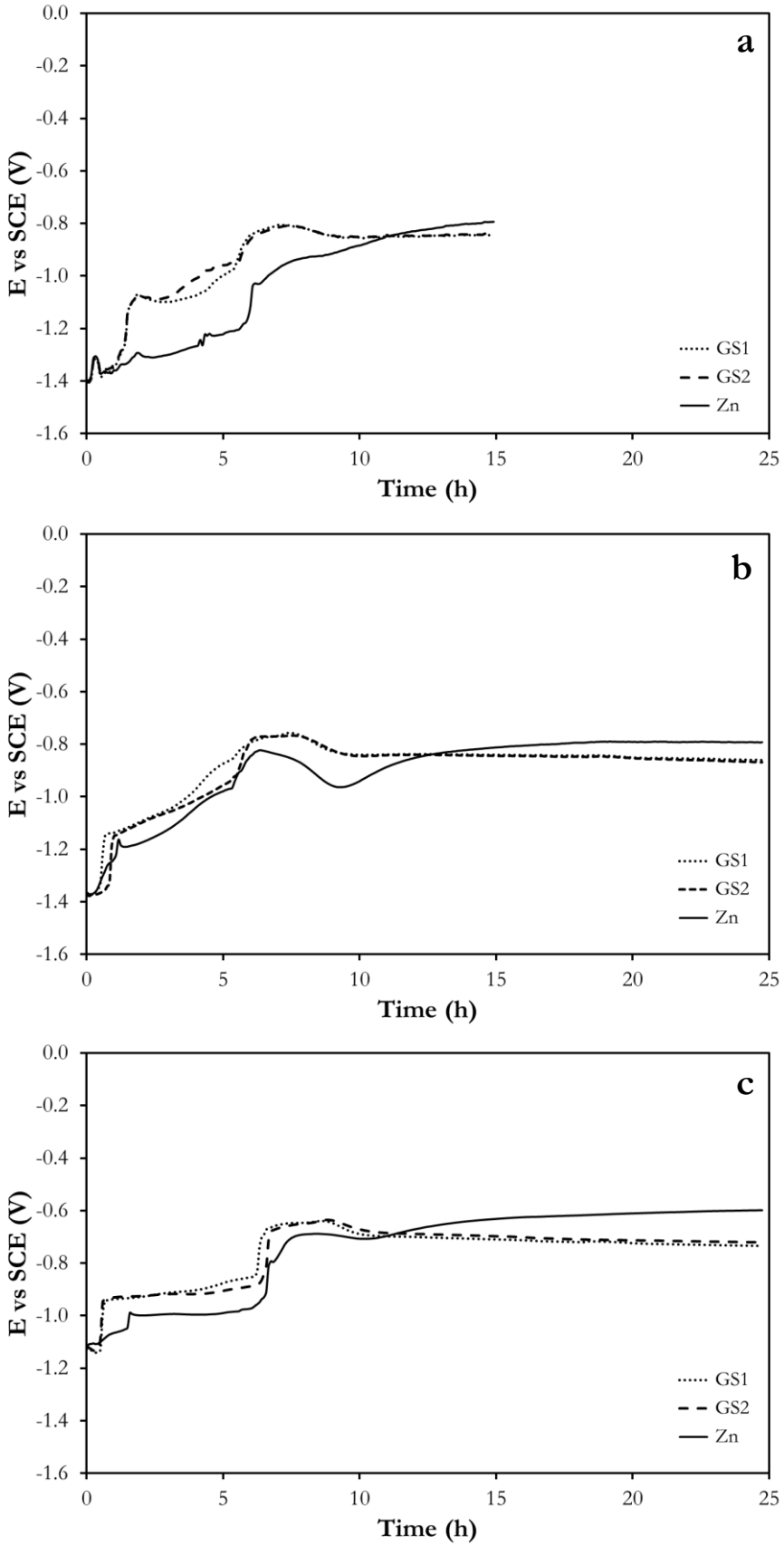


Figure 7-25. Corrosion potential change in time of galvanized steel bars (*GS*) and pure zinc rod (*Zn*) embedded in concrete specimens made with white cement, containing 3 % (*a*), 6 % (*b*) and 10 % (*c*) of $NO_2^-$

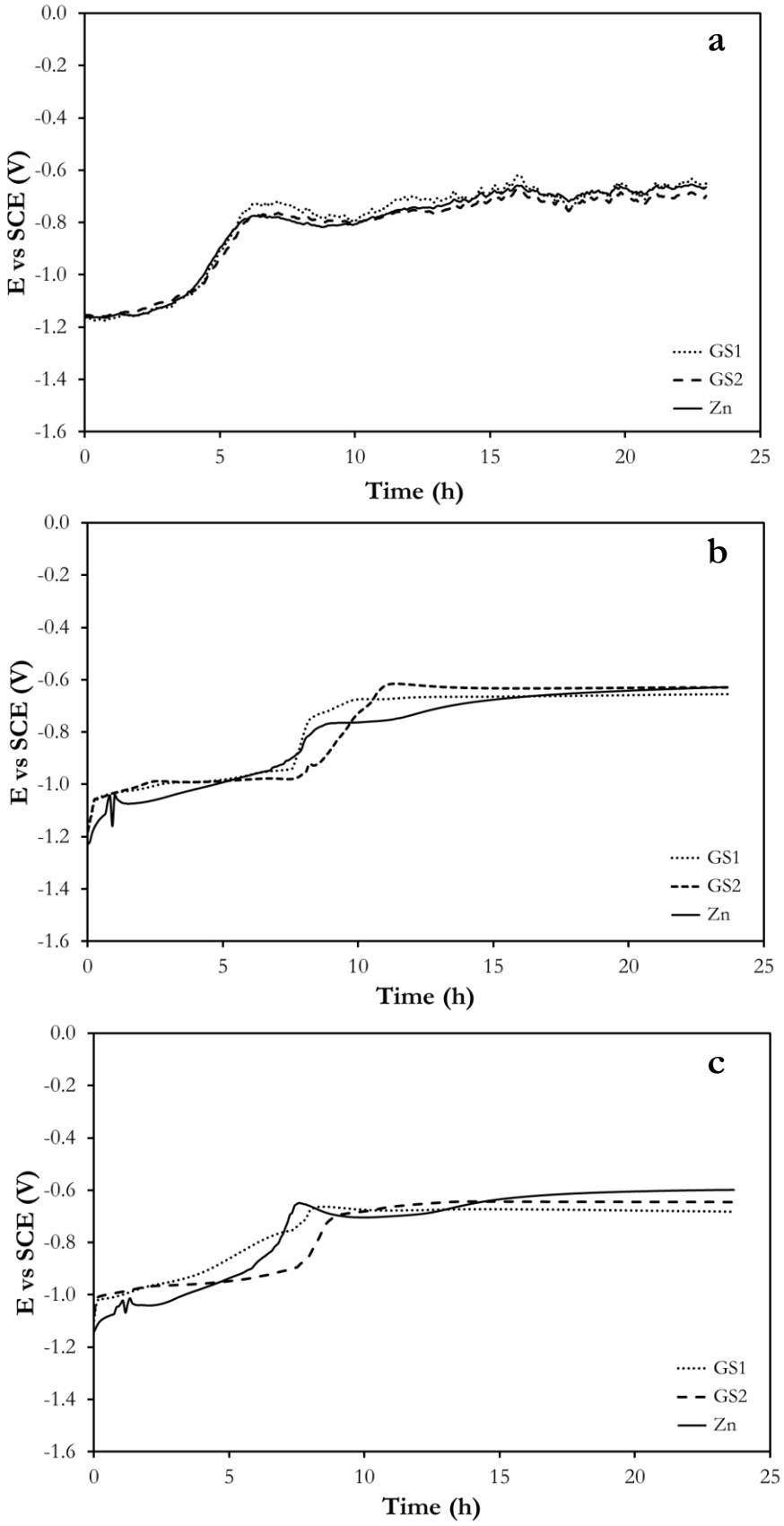


Figure 7-26. Corrosion potential change in time of galvanized steel bars (*GS*) and pure zinc rod (*Zn*) embedded in concrete specimens made with grey cement, containing 3 % (*a*), 6 % (*b*) and 10 % (*c*) of $NO_2^-$

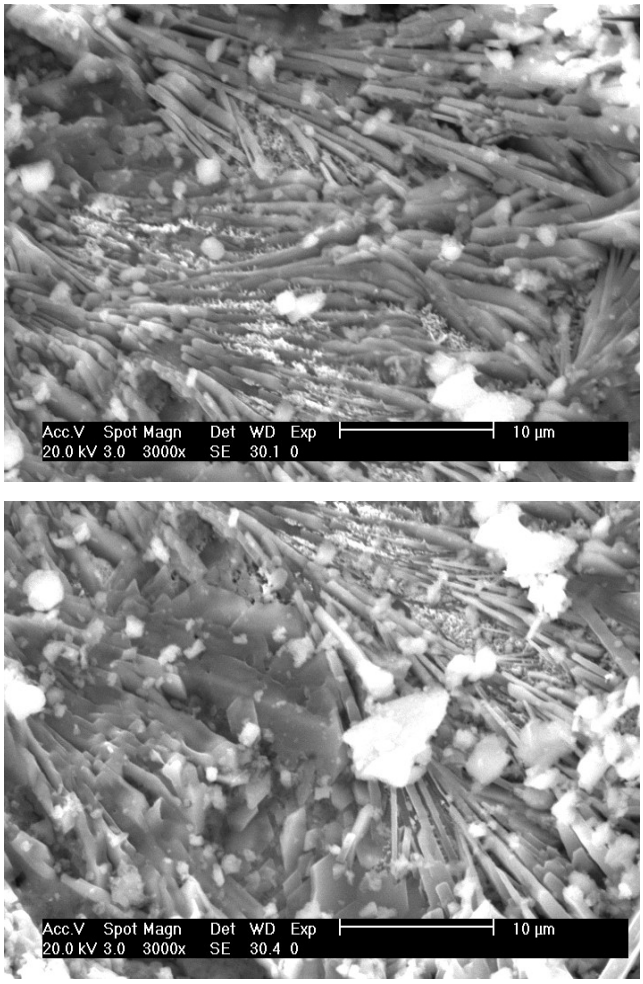


Figure 7-27. SEM images of galvanized steel surface after the test performed in grey cement containing 3 % $NO_2^-$

The difference in oxidant activity, previously observed for hydrogen peroxide in experiments with white and grey concrete, does not appear in the case of nitrite additive. Corrosion behaviour of galvanized steel and pure zinc is similar in grey and white concretes in presence of nitrite, indicating that it does not react with $FeSO_4$ additive.

Nitrite exhibits a weaker inhibitory effect compared to chromate (Fig. 7-5). Nevertheless, galvanized steel potential reaches -950 mV vs SCE in about 40 minutes, which lowers the risk of hydrogen gas evolution, although does not prevent it completely as the effect is not immediate. The SEM observation and X-ray patterns shown on Figures 7-27 – 7-28 reveal that the passivation of galvanized steel in presence of nitrite is stable because it is due to the formation of a thick calcium hydroxyzincate layer. EDX analysis reveals the high content of Ca – about 5.5 %. It seems that the nitrite somehow promotes the formation of calcium hydroxyzincate layer and, thus, the mechanism of inhibition significantly differs from that one of chromate.

Visual observation of the cross-section of grey concrete specimens after break indicates a reduction of number and size of the pores in concrete made with addition of 3 % $NO_2^-$ compared to grey concrete with reduced chromium VI without additions of inhibitors that furthermore validates the protective capacity of nitrite due to diminution of hydrogen evolution on the early stage of concrete cast (Fig. 7-29).

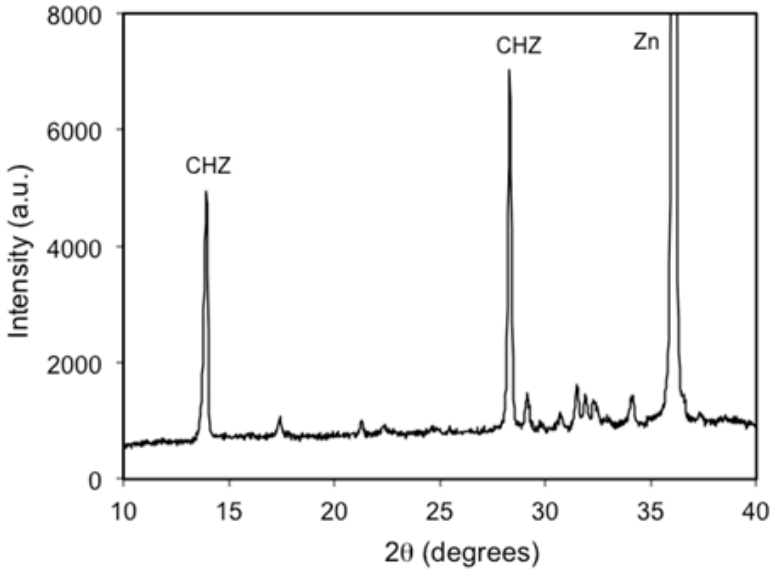


Figure 7-28. X-ray pattern of galvanized steel surface after the test performed in grey cement containing 3 % $NO_2^-$

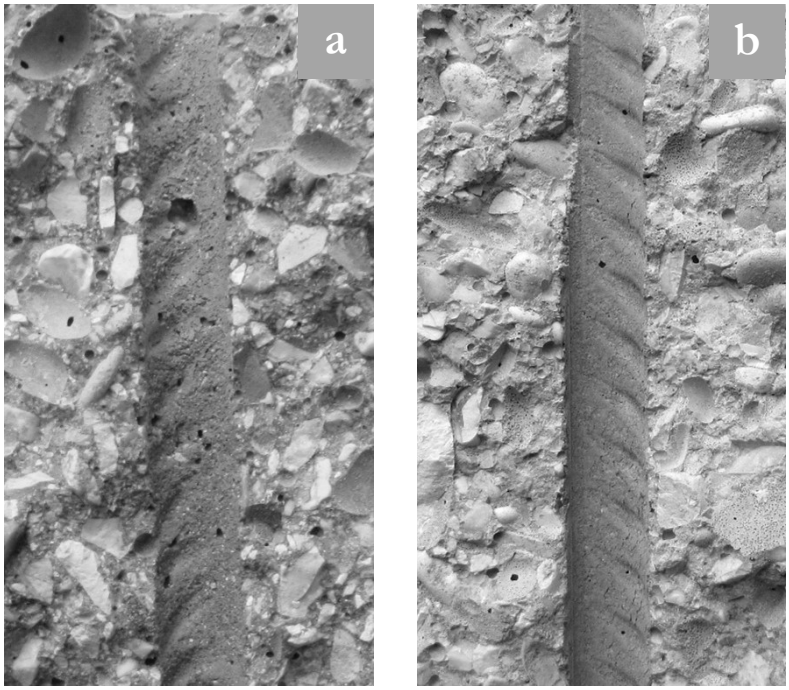


Figure 7-29. Cross-section through separated test specimens made of grey concrete without inhibitor (*a*) and with 3 % $NO_2^-$ (b) after removal of the galvanized steel bars

### *7.2.4 Tests performed in concrete with diethanolamine*

Figure 7-30 shows potential change in time of galvanized steel bars embedded in white and grey concrete specimens containing diethanolamine (DEA). Indications on the plots correspond to those given in Table 5-6.

Corrosion potential for galvanized steel bars just after the embedding in concrete is about -1400 mV vs SCE in all cases, regardless concrete type or inhibitor addition. After 7-9 hours, potential quickly rises up to about -800 mV vs SCE for white concrete specimen. The increase in corrosion potential in grey concrete occurs about 3-4 hours early for specimens with addition of DEA (Fig. 7-30).

DEA is an adsorption type inhibitor. DEA concentration (3.5 L/m$^3$) was chosen on the base of literature data. The tests performed in concrete (Fig. 7-30) do not demonstrate the acceleration of the passivation of galvanized steel due to DEA presence (compare Fig. 7-30 with Fig. 7-1). The only observed effect is a slight reduction of the passivation time in grey cement.

SEM image and X-ray pattern obtained on the galvanized steel surface after the test performed in grey cement containing DEA (Fig. 7-31, 7-32) indicate that the galvanized steel passivation cannot be related to the formation of calcium hydroxyzincate; in particular, SEM image shows a corroded surface, without the characteristic calcium hydroxyzincate crystals.

Other authors reported that the corrosion behaviour of galvanized steel in reinforced mortar specimens is greatly improved by the addition of DEA, which acted as an efficient corrosion inhibitor in chloride environment by influencing the microstructure of the mortar [17].

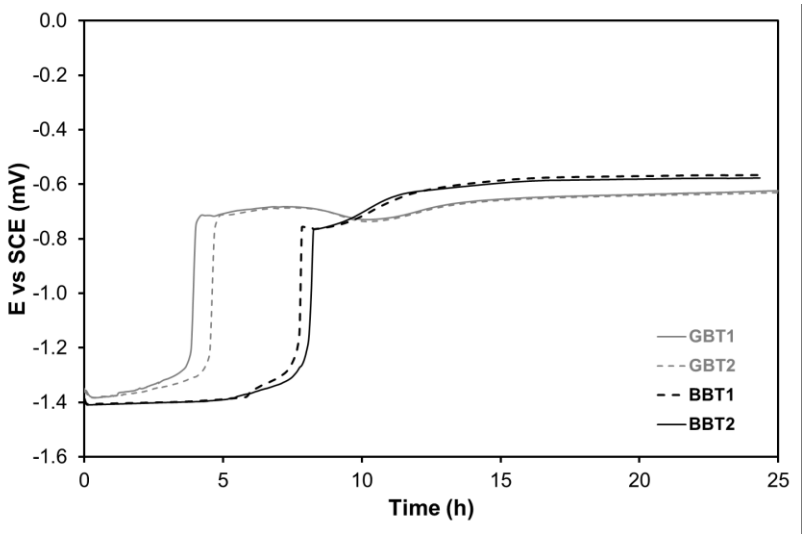


Figure 7-30. Corrosion potential change in time of galvanized steel bars embedded in white (*B*) and grey (*G*) concrete specimens with addition of DEA, 3.5 L/m$^3$

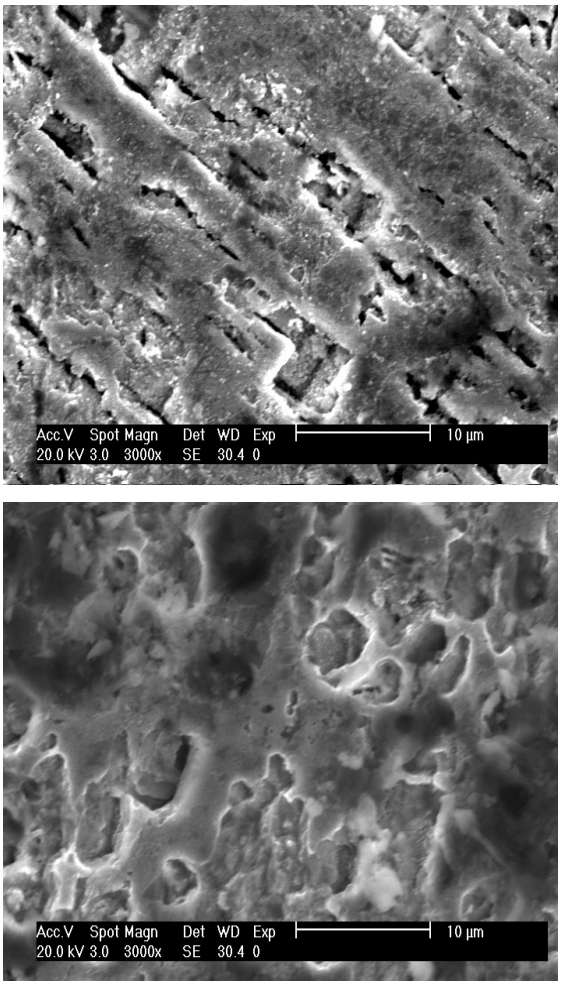


Figure 7-32. SEM image of galvanized steel surface after the test performed in grey cement containing DEA

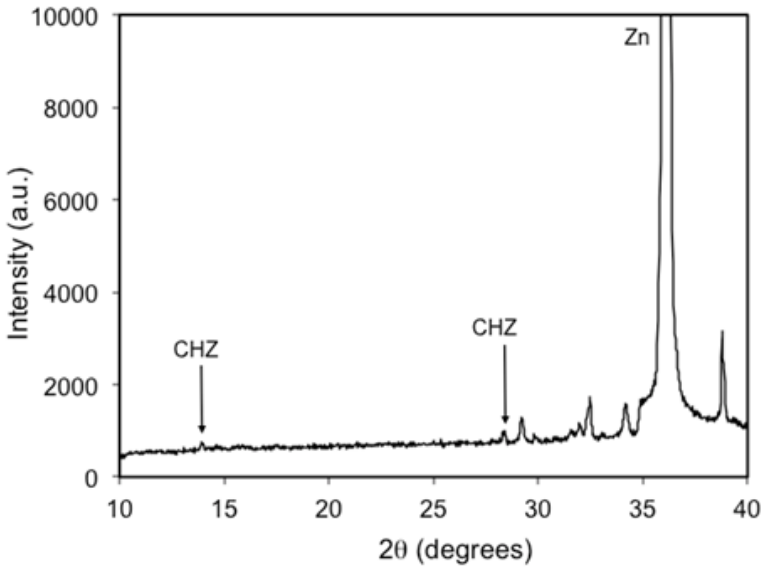


Figure 7-31. X-ray pattern of galvanized steel surface after the test performed in grey cement containing DEA

The effect of the DEA as a corrosion inhibitor for steel in concrete is twofold: direct and indirect. The direct action concerns the faradaic process that is hindered in presence of the amine, as the polarization results reveal. The indirect action concerns the barrier-forming effect because it decreases the porosity of the concrete and increases resistivity. Present results indicate that the the effect of DEA on the concrete microstructure is not significative during the early period of aging.

### *7.2.5 Tests performed in concrete with molybdate*

The corrosion potential curves of galvanized steel imbedded in grey concrete with ferrous phosphate in presence of molybdate, 0.1 mM, are given in Figure 7-33. The trends of potential change in time of galvanized steel sheets in grey concrete with reduced chromium VI without inhibitors were added to show the lack of molybdate effects on the passivation process. The corrosion behaviour of galvanized steel in grey concrete with and without addition of molybdate is equal: the passivation occurs in about 7 hours from immersion and it is characterized by a sharp increase in potential up to about -800 mV vs SCE, which indicates the absence of inhibition efficiency of molybdate, at the studied concentration, on galvanized steel corrosion in concrete.

Even if other researchers found that $MoO_4^{2-}$ inhibit hot-dip galvanized steel corrosion, the tests performed in the present research indicate that they do not have any significant inhibition effect during the first period of embedding in concrete [32]. SEM images and X-ray patterns indicate that the passivation is due to the formation of calcium hydroxyzincate (Fig. 7-34 and 7-35). However, the comparison between Fig. 7-34 and Fig. 7-27 indicates that the formation of calcium hydroxyzincate is more difficult in presence of molybdate than in presence of nitrite; in fact in the first case only a thin layer of this compound was observed.

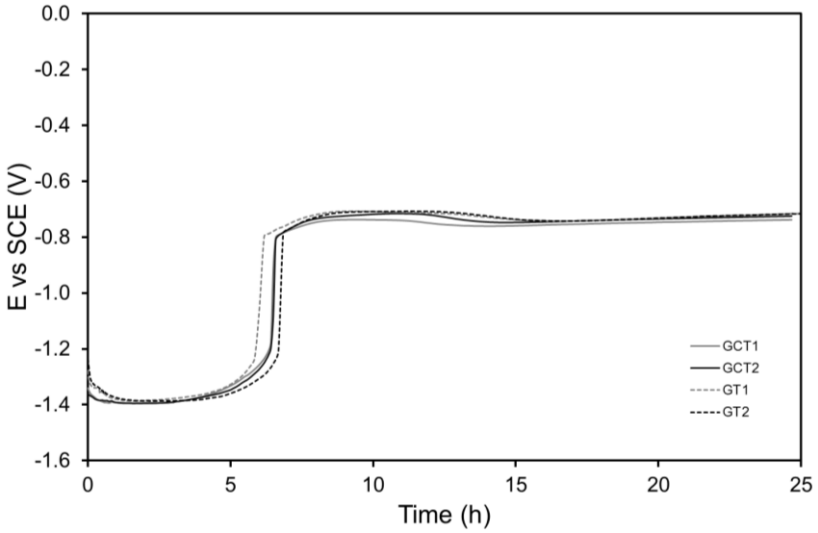


Figure 7-33. Corrosion potential change in time of galvanized steel bars embedded in grey concrete specimens without inhibitor (*G*) and with addition of $MoO_4^{2-}$, 0.1 mM (*GC*)

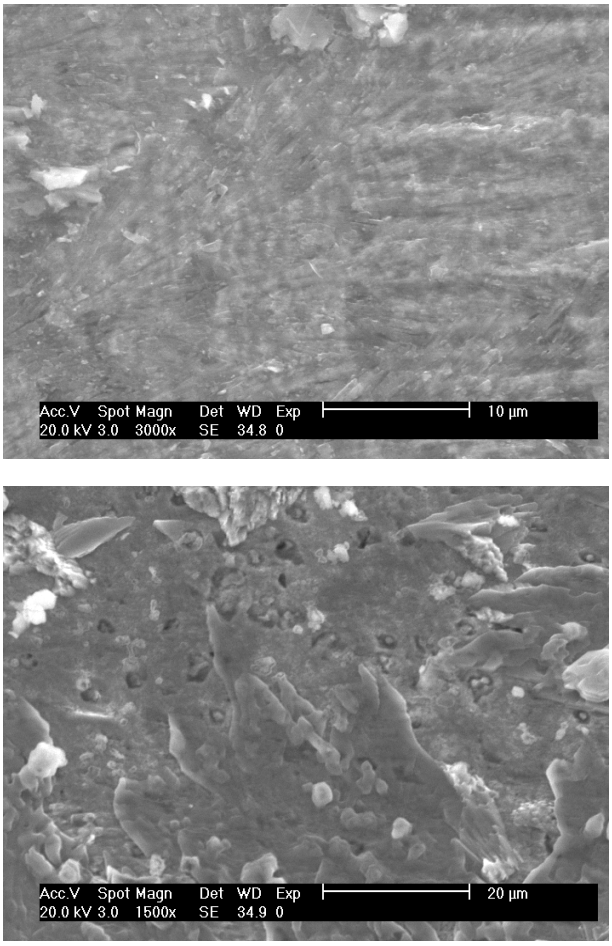


Figure 7-34. SEM images of galvanized steel sheets after the immersion in concrete specimens obtained by adding to the grey cement 0.1 mM $Na_2MoO_4 \cdot 2H_2O$

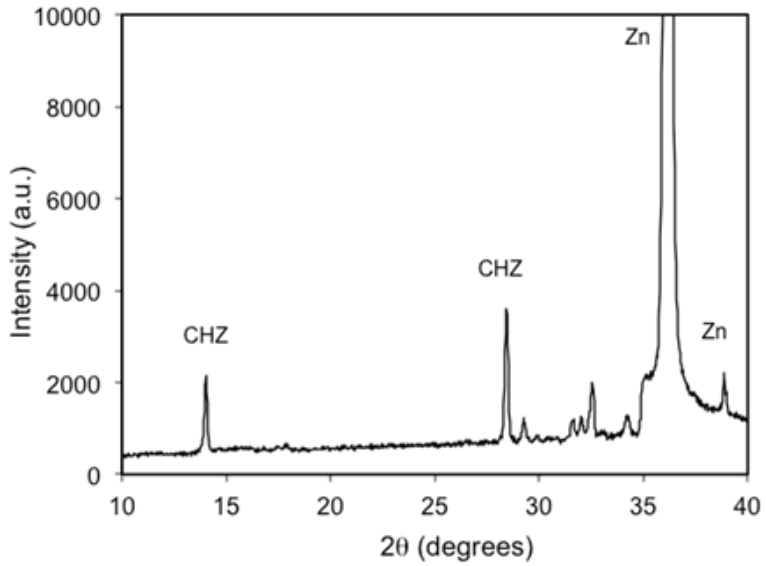


Figure 7-35. X-ray patterns of galvanized steel sheets after the immersion in concrete specimens obtained by adding to the grey cement 0.1 mM $Na_2MoO_4 \cdot 2H_2O$

# 8 Conclusions

The effect of the presence of several inhibitors on the corrosion behaviour of galvanized steel was studied both in concrete and in $Ca(OH)_2$ saturated solution.

The inhibiting mechanism of hexavalent chromium on galvanized steel and zinc in alkaline environment was studied. Chromium VI promotes the passivation of zinc and galvanized steel both in concrete and in $Ca(OH)_2$ saturated solution due to its inhibitor effect on the zinc corrosion.

The higher is the concentration of Cr VI, the shorter is the time required for the passivation of zinc. To passivate galvanized steel immediately after the embedding in concrete and to avoid the hydrogen development, which causes the adhesion loss between the rebars and the concrete, 15 ppm Cr VI with respect to the cement weight are necessary.

Passivation of galvanized steel in concrete occurs in three steps: first passivation, reactivation and second passivation.

The first passivation of GS in concrete is related to the presence of chromium VI and is determined by a metastable passivation film.

Reactivation of galvanized steel, followed by a new passivation, was observed for concentrations of Cr VI $\geq$ 6 ppm in the cement; this behaviour does not occur in $Ca(OH)_2$ saturated solution. The reactivation process is due to the depletion of Cr VI on the galvanized steel surface, caused probably by the aging of concrete, which consumes the pore solution.

The second passivation is stable and is due to the formation of calcium hydroxyzincate.

The maximum content of Cr VI in cement allowed by EU directive 53/2003/EEC (2 ppm) is not sufficient for accelerating the passivation of galvanized steel.

The study of oxygen effect on the process of zinc and galvanized steel passivation revealed the importance of dissolved oxygen concentration in the initiation of passivation process.

Among generic oxidants and non-oxidizing inhibitors studied in present work, nitrite showed satisfactory results, even if its inhibiting effect is less efficient than that of chromate. Therefore, further research on the prevention of corrosion of galvanized steel in concrete at the early casting stage can proceed along two parallel tracks; namely, a depth study of the nitrite effect, and a search for alternative "green" inhibitors.

## References

[1] S.R Yeomans (Ed.), *Galvanized Steel Reinforcement in Concrete: an Overview* Elsevier Science Ltd, Oxford, 2004.

[2] D. Darwin, J. Browning, M. O'Reilly, L. Xing, J. Ji, *Critical chloride corrosion threshold of galvanized reinforcing bars.* ACI Mater. J. 106 (2009) 176-183.

[3] G. Roventi, T. Bellezze, G. Giuliani, C. Conti, *Corrosion resistance of galvanized steel reinforcements in carbonated concrete: effect of wet–dry cycles in tap water and in chloride solution on the passivating layer.* Cem. Conc. Res. 65 (2014) 76-84.

[4] M.C. Andrade, A. Macias, *Galvanized reinforcements in concrete, in Surface Coatings-2,* Wilson A.D., Nichols J.W., Prosser H.J., editors. Elsevier Applied Science, New York 1988: pp. 137-182.

[5] G. Arliguie, F. Belaïd, R. François*, Effect of galvanized coating and bars properties on bond strength of reinforcements,* COST 521 Workshop, Belfast, 28-31 August 2000: pp. 37-43.

[6] R. Fratesi, G. Moriconi, L. Coppola, *The influence of steel galvanization on rebars behaviour in concrete, in Corrosion of Reinforcement in Concrete Costruction*, The Royal Society of Chemistry, 1996: pp. 630-641.

[7] M.F. Montemor, A.M.Simões, M.G.S. Ferreira, *Composition and corrosion behaviour of galvanised steel treated with rare-earth salts: the effect of the cation*. Prog Org Coat 44 (2002)111–120.

[8] M.G.S. Ferreira, R.G. Duarte, M.F. Montemor, A.M.P. Simões. *Silanes and rare earth salts as chromate replacers for pre-treatments on galvanised steel*. Electrochim. Acta 49 (2004) 2927–2935.

[9] W. Trabelsi, P. Cecilio, M.G.S. Ferreira, M.F. Montemor. *Electrochemical assessment of the self-healing properties of Ce- doped silane solutions for the pre-treatment of galvanised steel substrates.* Prog. Org. Coat. 54 (2005) 276–284.

[10] M. Sánchez, M.C. Alonso, P. Cecílio, M.F. Montemor, C. Andrade. *Electrochemical and analytical assessment of galvanized steel reinforcement pre-treated with Ce and La salts under alkaline media.* Cem. Concr. Compos. 28 (2006) 256–266.

[11] D.J.H. Corderoy, H. Herzog, *Passivation of Galvanized Reinforcement by Inhibitor Anions. Corrosion of Reinforcing Steel in Concrete*, ASTM STP 713, D.E: Tonini and J.M: Gaidis, Eds., Americam Society for testing and Materials, 1980, pp. 142-159.

[12] E. Ramirez, J.A. Gonzalez, A. Bautista, *The protective efficiency of galvanizing against corrosion of steel in mortar and in $Ca(OH)_2$ saturated solutions containing chlorides*. Cem. Concr. Res. 26 (1996)1525–1536.

[13] Linda Hills and Vagn C. Johansen *Hexavalent Chromium in Cement Manufacturing: Literature Review* Portland Cement Association 2007.

[14] C.E. Bird, Corrosion, Prevention and Control, 11 (1964) 17-19.

[15] G. Ebell, A. Burkert, J. Lehmann, J. Mietz, *Electrochemical investigations on the corrosion behaviour of galvanized reinforcing steels in concrete with chromate-reduced cements*, Mater. Corros., 63 (2012) 791-802.

[16] Konstantin Salnikow and Anatoly Zhitkovich *Genetic and Epigenetic Mechanisms in Metal Carcinogenesis and Cocarcinogenesis: Nickel, Arsenic, and Chromium* Chem. Res. Toxicol., 2008, 21 (1), pp 28–44.

[17] I. Fayala, L. Dhouibi, X.R. Nóvoa, M. Ben Ouezdou, *Effect of inhibitors on the corrosion of galvanized steel and on mortar properties*. Cem. Conc. Comp. 35 (2013)181-189.

[18] R. Berger, U. Bexell, T.M. Grehk, S.E. Hörnström, *A comparative study of the corrosion protective properties of chromium and chromium free passivation methods*. Surf. Coat. Technol. 202 (2007) 391-397.

[19] Shiyuan Qian, Daniel Cusson *Electrochemical evaluation of the performance of corrosion-inhibiting systems in concrete bridges* Cement & Concrete Composites 26 (2004) 217–233.

[20] Fei-long Fei, Jie Hu, Jiang-xiong Wei, Qi-jun Yu, Zheng-shan Chen *Corrosion performance of steel reinforcement in simulated concrete pore solutions in the presence of imidazoline quaternary ammonium salt corrosion inhibitor* Construction and Building Materials 70 (2014) 43–53.

[21] L. Benzina Mechmeche, L. Dhouibi, M. Ben Ouezdou, E. Triki, F. Zucchi *Investigation of the early effectiveness of an amino-alcohol based corrosion inhibitor using simulated pore solutions and mortar specimens*

Cement & Concrete Composites 30 (2008) 167–173.
[22] M. Cabrini, S. Lorenzi, T. Pastore *Cyclic voltammetry evaluation of inhibitors for localised corrosion in alkaline solutions* Electrochimica Acta 124 (2014) 156–164.
[23] Charles K. Nmai *Multi-functional organic corrosion inhibitor* Cement & Concrete Composites 26 (2004) 199–207.
[24] K.K. Sideris, A.E. Savva *Durability of mixtures containing calcium nitrite based corrosion inhibitor* Cement & Concrete Composites 27 (2005) 277–287.
[25] Neal S. Berke, Maria C. Hicks *Predicting long-term durability of steel reinforced concrete with calcium nitrite corrosion inhibitor* Cement & Concrete Composites 26 (2004) 191–198
[26] F. Wombacher, U. Maeder, B. Marazzani *Aminoalcohol based mixed corrosion inhibitors* Cement & Concrete Composites 26 (2004) 209–216.
[27] K.Y. Ann, H.S. Jung, H.S. Kim, S.S. Kim, H.Y. Moon *Effect of calcium nitrite-based corrosion inhibitor in preventing corrosion of embedded steel in concrete* Cement and Concrete Research 36 (2006) 530 – 535.
[28] H.E. Jamil, A. Shriri, R. Boulif, M.F. Montemor, M.G.S. *Ferreira Corrosion behaviour of reinforcing steel exposed to an amino alcohol based corrosion inhibitor* Cement & Concrete Composites 27 (2005) 671–678.
[29] Hilke Verbruggen, Herman Terryn, Iris De Graeve *Inhibitor evaluation in different simulated concrete pore solution for the protection of steel rebars* Construction and Building Materials 124 (2016) 887–896.
[30] Kunitsugu Aramaki *Cerium(III) chloride and sodium octylthiopropionate as an effective inhibitor mixture for zinc corrosion in 0.5 M NaCl* Corrosion Science 44 (2002) 1361–1374
[31] Kunitsugu Aramaki *The inhibition effects of chromate-free, anion inhibitors on corrosion of zinc in aerated 0.5 M NaCl* Corrosion Science 43 (2001) 591-604.
[32] Ioannis A. Kartsonakis, Stefan G. Stanciu, Alecs A. Matei, Radu Hristu, Antonis Karantonis, Costas A. Charitidis *A comparative study of corrosion inhibitors on hot-dip galvanized steel* Corrosion Science 112 (2016) 289–307.
[33] C.N. Panagopoulos, E.P. Georgiou, C. Markopoulos Corrosion and wear of zinc in various aqueous based environments Corrosion Science 70 (2013) 62–67.
[34] Haji Sheik Mohammed, M.S., Samuel Knight, G.M., Raghavan, R.S. *Performance of galvanized rebars in inhibitor admixed concrete under accelerated corrosion conditions* (2012) Journal of Structural Engineering (India), 39 (1), pp. 48-55.
[35] Herrera, M.J., Torres, A.A., Pĭrez, J.T., Martнnez, M. *Electrochemical evaluation of galvanized rebars in alkaline solutions with an inhibitor* (2007) ECS Transactions, 3 (13), pp. 139-144.
[36] Nuernberger, U., Beul, W. *Influence of galvanizing and PVC-coating of reinforcing steels and of inhibitors on steel corrosion in cracked concrete* [Einfluss einer Feuerverzinkung und PVC-Beschichtung von Bewehrungsstaehlen und von inhibitoren auf die Korrosion von Stahl in gerissenem Beton] (1991) Werkstoffe und Korrosion, 42 (10), pp. 537-546.
[37] Haran, B.S., Popov, B.N., Petrou, M.F., White, R.E. Studies on galvanized carbon steel in Ca(OH)2 solutions (2000) ACI Structural Journal, 97 (4), pp. 425-431.
[38] U.S. Geological Survey 2016. *Mineral commodity summaries 2016*. U.S. Government Publishing Office, pp. 44-45, 2016.
[39] ASTM C125-15b. *Standard Terminology Relating to Concrete and Concrete Aggregates.* Annual Book of ASTM Standards, vol. 04.02, Concrete and Aggregates, 2016.
[40] EN 197-1. *Cement - Part 1: Composition, specifications and conformity criteria for common cements*, 2000.
[41] L. Bertolini, B. Elsener, P. Pedeferri and R. Polder. *Corrosion of steel in concrete: Prevention, Diagnosis, Repair*. WILEY-VCH, 2004.
[42] P. C. Hewlett. *Lea's Chemistry of Cement and Concrete.* Butterworth-Heinemann, 4th Edition, 2003.
[43] ASTM C28 / C28M - 10(2015). *Standard Specification for Gypsum Plasters.* Annual Book of ASTM Standards, vol. 04.01, Cement; Lime; Gypsum, 2016.
[44] J. Davidovits. *Geopolymer Chemistry and Applications*. Institut Géopolymère, 2008.
[45] P. Duxson, A. Fernández-Jiménez, J.L. Provis, G.C. Lukey, A. Palomo, J.S.J. van Deventer.

*Geopolymer technology: The current state of the art.* Journal of Materials Science, vol. 42(9), pp. 2917-2933, 2007.
[46] B. Singh, G. Ishwarya, M. Gupta, S.K. Bhattacharyya. *Geopolymer concrete: A review of some recent developments.* Construction and Building Materials, vol. 85, pp. 78-90, 2015.
[47] W. K. Part, M. Ramli, C. B. Cheah. *An overview on the influence of various factors on the properties of geopolymer concrete derived from industrial by-products.* Construction and Building Materials, vol. 77, pp. 370-395, 2015.
[48] S. Onutaia, S. Jiemsirilersb, P. Thavornitic, T. Kobayashia. *Aluminium hydroxide waste based geopolymer composed of fly ash for sustainable cement materials.* Construction and Building Materials, vol. 101, part 1, pp. 298-308, 2015.
[49] C. Monticelli, M.E. Natali, A. Balbo, C. Chiavari, F. Zanotto, S. Manzi, M.C. Bignozzi. *A study on the corrosion of reinforcing bars in alkali-activated fly ash mortars under wet and dry exposures to chloride solutions.* Cement and Concrete Research, vol. 87, pp. 53-63, 2016.
[50] A. Mobili, A. Belli, C. Giosuè, T. Bellezze, F. Tittarelli. *Metakaolin and fly ash alkali-activated mortars compared with cementitious mortars at the same strength class*. Cement and Concrete Research, vol. 88, pp. 198-210, 2016.
[51] X. Yaoa, Z. Zhanga, H. Zhua, Y. Chena. *Geopolymerization process of alkali–metakaolinite characterized by isothermal calorimetry.* Thermochimica Acta, vol. 493(1-2), pp. 49-54, 2009.
[52] H.F.V. Taylor. *Cement Chemistry.* Thomas Telford, 2nd Edition, 1997.
[53] S.W. Chang, W.J. Shon, W.C. Lee, K.Y. Kum, S.H. Baek, K.S. Bae. *Analysis of heavy metal contents in gray and white MTA and 2 kinds of Portland cement: a preliminary study*. Journal of Oral Surgery, Oral Medicine, Oral Pathology, Oral Radiology, and Endodontics, Vol. 109, No. 4, pp. 642-646.
[54] http://iti.northwestern.edu/cement/monograph/Monograph5_1.html
[55] http://www.concretecountertopinstitute.com/the-importance-of-watercement-ratio/
[56] D. Koh, Yung Hian Leowb, Chee Leok Goh. *Occupational allergic contact dermatitis in Singapore.* The Science of the Total Environment, vol. 270, pp. 97-101, 2001.
[57] M. Schembri, G. Peplow, J. Camilleri. *Analyses of heavy metals in mineral trioxide aggregate and Portland cement*. Journal of Endodontics, vol. 36, part 7, pp. 1210-1215, 2010.
[58] M. Sumner, C. Porteneuve, L. Jardine, M. Macklin. *Advances in Chromium Reduction.* World Cement, vol. 37, part 3, pp. 33-36, 2006
[59] S. Baetzner, J. Glöckler, D. Israel, M. Paul. *Long-term effectiveness of tin (II) sulphate as a chromate reducer.* Cement International 8, vol. 5, pp. 68-76, 2010.
[60] T. Ilvana, C. Amira, M. Snezana. *Effect of raw materials and reduction agents on hexavalent chromium levels in Portland cement.* Proceedings of 15th International Conference on Trends in the Development of Machinery and Associated Technology; Czech Republic, pp. 717-720, 2011.
[61] Devesh K. Sharma, Rekha Sharma. *Reduction of water soluble hexavalent chromium in hydrated Portland cement.* Indian Journal of Science and Technology, vol. 8, part 11, 2015.
[62] http://www.cement.org/cement-concrete-basics/concrete-materials/aggregates
[63] http://iti.northwestern.edu/cement/monograph/Monograph7_2.html
[64] http://www.cement.org/docs/default-source/fc_concrete_technology/durability/is536-types-and-causes-of-concrete-deterioration.pdf?sfvrsn=4
[65] http://www.cement.org/for-concrete-books-learning/concrete-technology/durability/alkali-aggregate-reaction
[66] http://www.cement.org/for-concrete-books-learning/concrete-technology/durability/corrosion-of-embedded-materials
[67] file:///C:/Users/MTC/Downloads/Lab%204%20Report.pdf
[68] https://ocw.mit.edu/courses/materials-science-and-engineering/3-014-materials-laboratory-fall-2006/labs/w3_b2.pdf
[69] http://chem.libretexts.org/Textbook_Maps/Inorganic_Chemistry_Textbook_Maps/Map%3A_Inorganic_Chemistry_(Wikibook)/Chapter_04%3A_Redox_Stability_and_Redox_Reactions/4.5%3A_Pourbaix_diagrams

[70] D.A. Jones. *Principles and Prevention of Corrosion*. Prentice Hall, Upper Saddle River, NJ, 1996.
[71] X. G. Zhang. *Corrosion and electrochemistry of zinc*. Plenum Press, New York, 1996.
[72] P. Bicao, W. Jianhua, S. Xuping, Li Zhi, Yin Fucheng. *Effects of zinc bath temperature on the coatings of hot-dip galvanizing*. Surface & Coatings Technology, vol. 202, pp. 1785–1788, 2008.
[73] Z.W. Chen, N.F. Kennon, J.B. See, and M.A. Barter. *Technigalva and Other Developments in Batch Hot-Dip Galvanizing*. The Journal of The Minerals, Metals & Materials Society, vol. 44, pp. 22-26, 1992.
[74] S. Skale, V. Dolecek, M. Slemnik. *Electrochemical impedance studies of corrosion protecte surfaces covered by epoxy polyamide coating systems*. Progress in Organic Coatings, vol. 62, pp. 387–392, 2008.
[75] P. A. Sorensen, S. Kiil, K. Dam-Johansen, C. E. Weinell. *Anticorrosive coatings: a review*. Journal of Coatings Technology and Research, vol. 6, pp. 135–176, 2009.
[76] Shi Gang Dong, Bing Zhaoa, ChangJian Lina, RongGui Dua, RongGang Hua, Gregory Xiaoge Zhang. *Corrosion behavior of epoxy/zinc duplex coated rebar embedded in concrete in ocean environment*. Construction and Building Materials, vol. 28, pp. 72–78, 2012.
[77] R.B. Figueira, C.J.R. Silva, E.V. Pereira. *Hot-dip galvanized steel dip-coated with ureasilicate hybrid in simulated concrete pore solution: Assessment of coating morphology and corrosion protection efficiency*. Progress in Organic Coatings, vol. 88, pp. 245–255, 2015.
[78] E. Huttunen-Saarivirta, V.E. Yudinb, L.A. Myagkova, V.M. Svetlichnyi. *Corrosion protection of galvanized steel by polyimide coatings: EIS and SEM investigations*. Progress in Organic Coatings, vol. 72, pp. 269 –278, 2011.
[79] Xuwen Liu, Jinping Xiong, Yongwu Lv, Yu Zuo. *Study on corrosion electrochemical behaviour of several different coating systems by EIS*. Progress in Organic Coatings, vol. 64, pp. 497–503, 2009.
[80] E. D. Schachinger, R. Braidt, B. Strauss, A.W. Hassel. *EIS study of blister formation on coated galvanised steel in oxidising alkaline solutions*. Corrosion Science, vol. 96, pp. 6–13, 2015.
[81] P.R. Seré, C. Deya, C.I. Elsner, A.R. Di Sarli. *Corrosion of painted galvanneal steel*. Procedia Materials Science, vol. 8, pp. 1 – 10, 2015.
[82] Cheng-Yang Tsai, Jen-Shou Liu, Pei-Li Chen, Chao-Sung Lin. *A roll coating tungstate passivation treatment for hot-dip galvanized sheet steel*. Surface & Coatings Technology, vol. 205, pp. 5124–5129, 2011.
[83] R. Ramanauskas, O. Girciene, L. Gudaviciute, A. Selskis. The interaction of phosphate coatings on a carbon steel surface with a sodium nitrite and silicate solution. Applied Surface Science, vol. 327, pp. 131–139, 2015.
[84] M. Hansson, L. Mammoliti, B.B. Hope. *Corrosion inhibitors in concrete—Part 1: The principles*. Cement and Concrete Research, vol. 28, No. 12, pp. 1775–1781, 1998.
[85] G. Wranglen. *An introduction to corrosion and protection of metals*. Butler & Tanner Ltd., London, 1972.
[86] S.F.L. Mertens, E. Temmerman. *Study of zinc passivation in chromium (VI)-containing electrolytes with short-term impedance measurements*. Corrosion Science, vol. 43, pp. 301-316, 2001.
[87] V. Shkirskiya, P. Keilb, H. Hintze-Brueningb, F. Lerouxc, T. Stimpflingc, D. Dragoed, K. Oglea, P. Volovitch. *$MoO_4^{2-}$ as a soluble inhibitor for Zn in neutral and alkaline solutions*. Corrosion Science, vol. 99, pp. 31–41, 2015.
[88] J.M. Gaidis. *Chemistry of corrosion inhibitors*. Cement & Concrete Composites, vol. 26, pp. 181–189, 2004.
[89] V.T. Ngala, C.L. Page, M.M. Page. *Corrosion inhibitor systems for remedial treatment of reinforced concrete. Part 1: calcium nitrite*. Corrosion Science, vol. 44, pp. 2073-2087, 2002.
[90] P. Garcers, P. Saura, A.Mrendez, E. Zornoza, C. Andraded. *Effect of nitrite in corrosion of reinforcing steel in neutral and acid solutions simulating the electrolytic environments of micropores of concrete in the propagation period*. Corrosion Science, vol. 50, pp. 498–509, 2008.
[91] P. Garces, P. Saura, E. Zornoza, C. Andrade. *Influence of pH on the nitrite corrosion inhibition of reinforcing steel in simulated concrete pore solution*, Corrosion Science, vol. 53, pp. 3991–4000, 2011.

[92] J.O. Okeniyi, O.A. Omotosho, O.O. Ajayi, C. A. Loto. *Effect of potassium-chromate and sodium-nitrite on concrete steel-rebar degradation in sulphate and saline media*. Construction and Building Materials, vol. 50, pp. 448-456, 2014.

[93] A.M. Simoes, J.C.S. Fernandes. *Studying phosphate corrosion inhibition at the cut edge of coil coated galvanized steel using the SVET and EIS*. Progress in Organic Coatings, vol. 69, pp. 219–224, 2010.

[94] T. Chaussadent,V. Nobel-Pujol, F. Farcas, I. Mabille, C. Fiaud. *Effectiveness conditions of sodium monofluorophosphate as a corrosion inhibitor for concrete reinforcements*. Cement and Concrete Research, vol. 36, pp. 556 – 561, 2006.

[95] V.T. Ngala, C.L. Page, M.M. Page. *Corrosion inhibitor systems for remedial treatment of reinforced concrete. Part 2: sodium monofluorophosphate*. Corrosion Science, vol. 45, pp. 1523–1537, 2003.

[96] T.A. Soylev, M.G. Richardson. *Corrosion inhibitors for steel in concrete: State-of-the-art report*. Construction and Building Materials, vol. 22, pp. 609–622, 2008.

[97] M. Aliofkhazraei. *Developments in Corrosion Protection*. Intech, 2014.

[98] K. Aramaki. *Effects of organic inhibitors on corrosion of zinc in an aerated 0.5 M NaCl solution*. Corrosion Science, vol. 43, pp. 1985-2000, 2001.

[99] T. Kosec, D. Kek Merl, I. Milošev. *Impedance and XPS study of benzotriazole films formed on copper, copper–zinc alloys and zinc in chloride solution*. Corrosion Science, vol. 50, pp. 1987–1997, 2008.

[100] J.V. Custodio, S.M.L. Agostinho, A.M.P. Simoes. *Electrochemistry and surface analysis of the effect of benzotriazole on the cut edge corrosion of galvanized steel*. Electrochimica Acta, vol. 55, pp. 5523–5531, 2010.

[101] Y. Ein-Eli, M. Auinat, D. Starosvetsky. *Electrochemical and surface studies of zinc in alkaline solutions containing organic corrosion inhibitors*. Journal of Power Sources, vol. 114, pp. 330-337, 2003.